Appendix I. Tree diagram of the MRI•GCM-I

The schematic structure of the program of the MRI•GCM-I is illustrated in Fig. AI.1. Names in the boxes indicate the subroutines. The functions of the subroutines are listed in Table AI. 1.

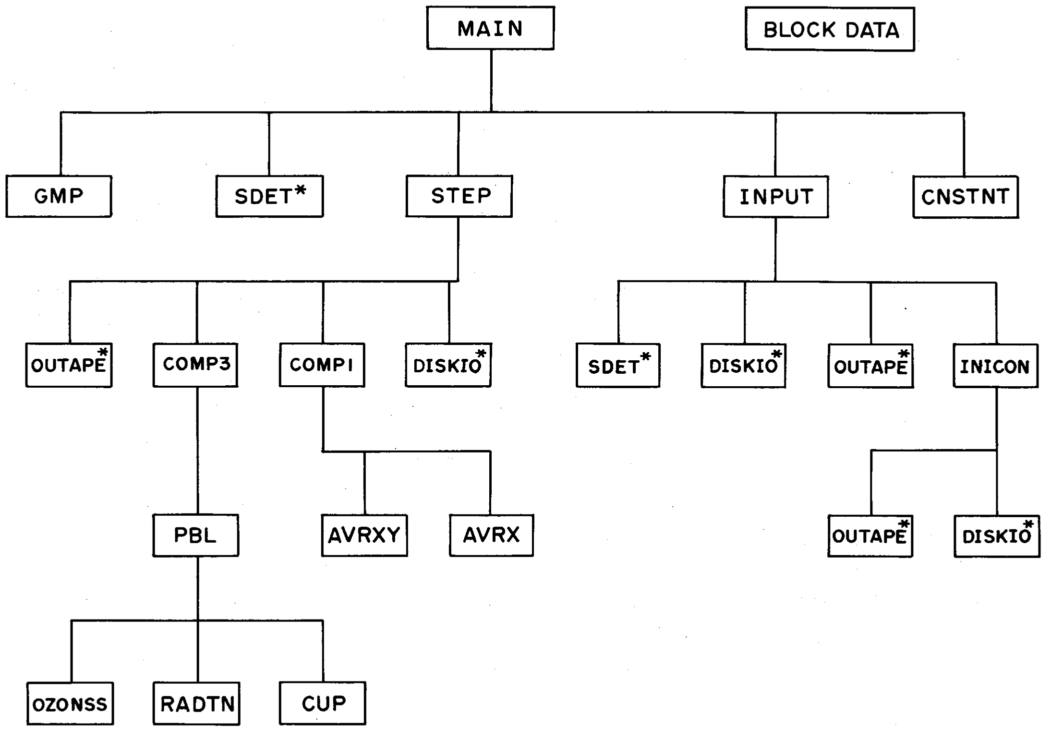

Fig. AI.1 Tree diagram of the MRI • GCM-I. Names in the boxes indicate subroutines. Subroutines with asterisk appear more than once in the diagram.

Table AI.1

subroutine	function
MAIN	Main program.
CNSTNT	Computing constant parameters once for all.
INPUT	Preparing initial data.
STEP	Doing time integration. Controlling data flow and advective and physical processes.
SDET	Computing astronomical parameters. Refer to Chapter 13.
GMP	Adjusting the global average surface pressure to its standard values once every 24 hours.*
INICON	Setting the initial condition when the previous history is not available.
OUTAPE	Dealing with the data exchange between "MSS" (Mass Strage System) and disk.
DISKIO	Dealing with the data exchange between global data and latitude strip data.
COMP1	Calculating the dynamical precesses. Refer to Chapters 1, 3 and 11.
COMP3	Calculating the physical processes. Refer to Chapters 2, 6, 9, 10 and 11.
AVRX	Smoothing the selected terms at Π-and u-points near the poles. Refer to Chapter 4.
AVRXY	Smoothing the selected terms at v-points near the poles. Refer to Chapter 4.
PBL	Computing the PBL processes. Refer to Chapter 8.
CUP	Computing the processes of penetrative cumulus convection. Refer to Chapter 7.
RADTN	Computing the radiation processes. Refer to Chapter 13.
OZONSS	Computing the photochemical processes of ozone. Refer to Chapter 12.

* Although the mass continuity equation in the finite difference form guarantees the conservation of mass in both the horizontal and vertical differencing, the globally integrated mass continues to decrease with time. This is related with the fact that the computer has the limit of at most 7 decimal digits in the single-precision calculation. This gives rise to a small loss of mass at each time step.

Appendix II. Surface boundary conditions and numerical constants used in the MRI•GCM-I

II.1 Surface boundary conditions.

Topography used in the MRI•GCM-I is shown in Fig. AII.1. Also shown are prescribed sea surface temperature and sea-ice distributions for January, April, July and October.

(a)

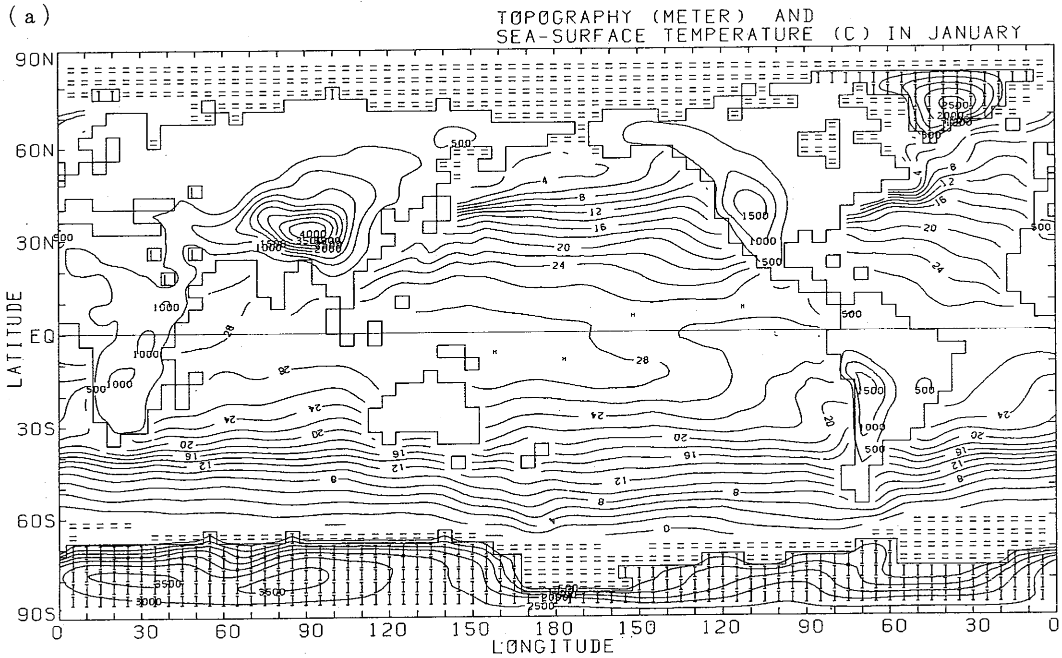

(b)

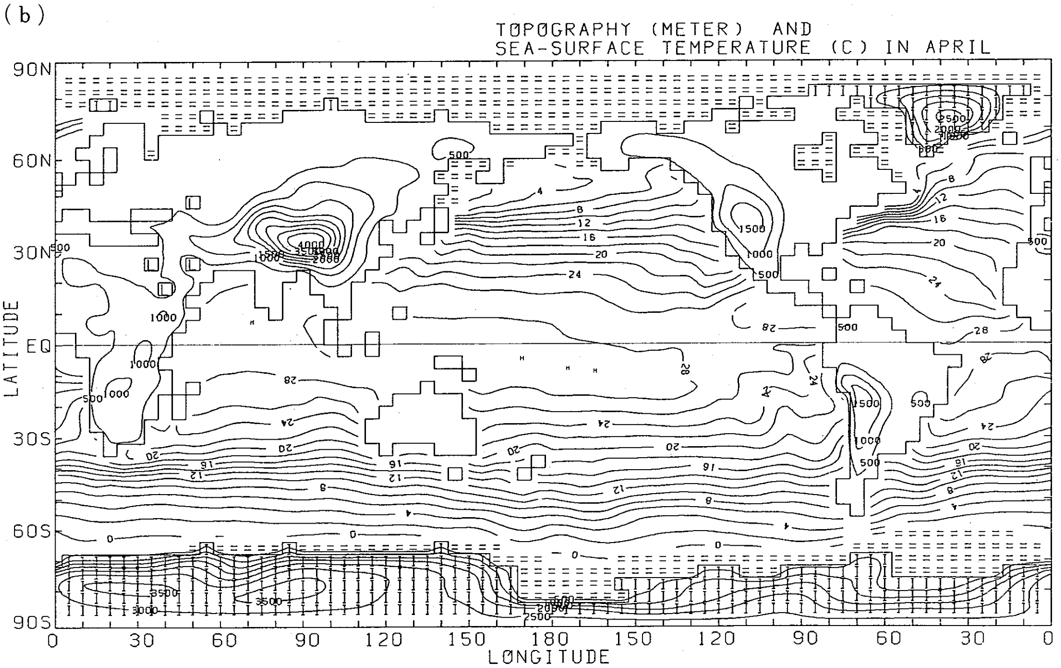

Fig. AII.1 Topography used in the MRI • GCM-I. The contour interval is 500 m. The sea surface temperature distributions are shown over the ocean for (a) January, (b) April, (c) July and (d) October, together with land ice distributions indicated with "I", and sea-ice distributions indicated with "=". The contour interval for sea surface temperature is 2°C. The grid points indicated with "L" are lake points.

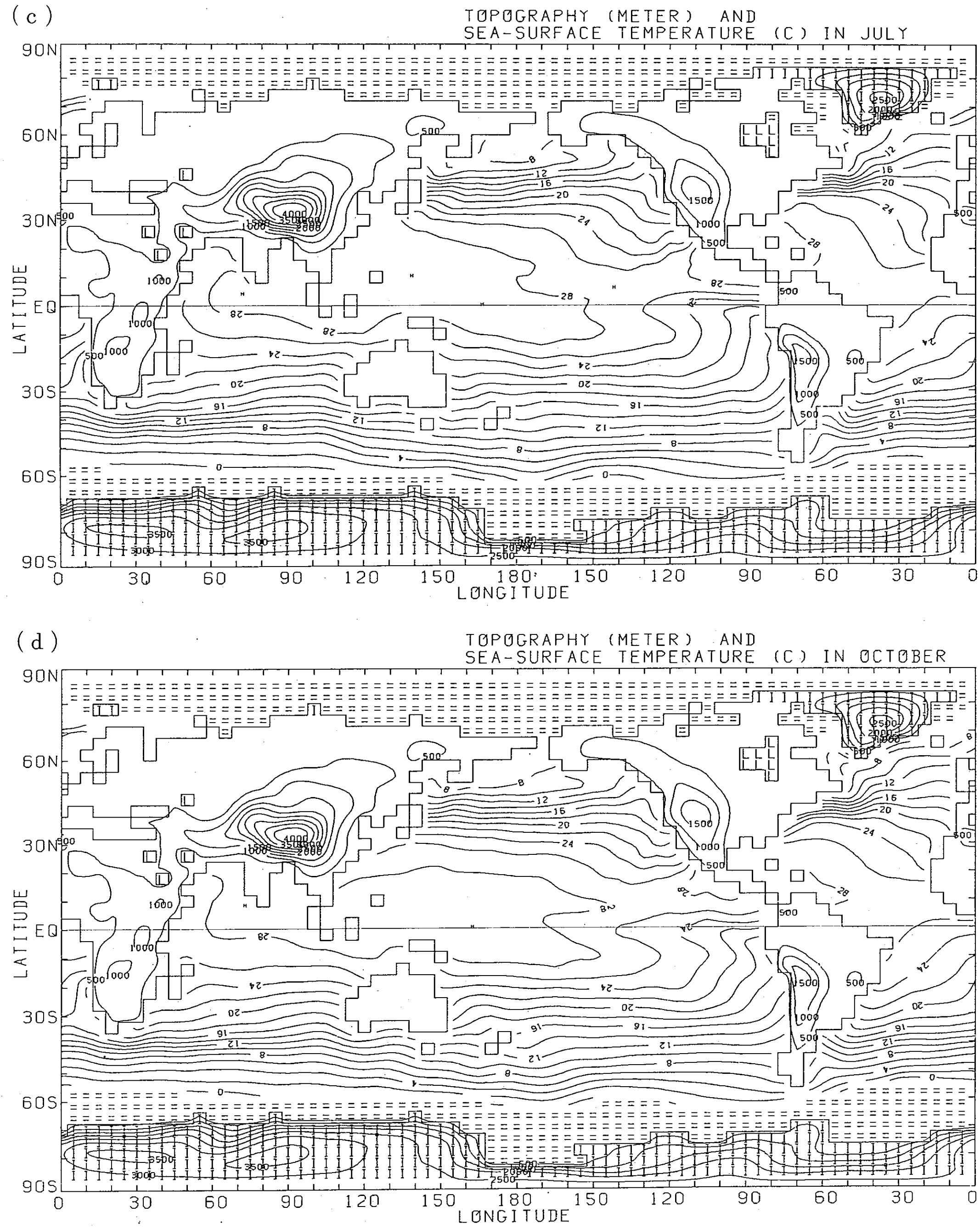

Fig. AII.1(*continued*)

II.2 Numerical constants and functions used in the MRI•GCM-I

Numerical constants and functions used in the MRI•GCM-I are summarized in Tables All.1 and All.2. The names of contants are shown in the left column. Also the conventional symbols or symbols used in the text are shown in the parentheses. In the middle column the values are shown. When the values are derived from other varibles in the program of the MRI•GCM-I, the relations are also shown. The first line of the right column shows the varible name used in the program, and the second line shows the subroutine where the variable is defined (see Fig. AI.1).

Tabel AII.1 Fundamental numerical constants and functinns

solar constant (S_o)	1345 W m^{-2}	S0 COMP3
eccentricity of the earth's orbit (e)	0.01672	 SDET
inclination of the earth's orbit	23° 27′	 SDET
perihelion	January 3.36 (2.36 day)	 SDET
1 year	365 days	DAYPYR BLOCK DATA
mean radius of the earth (a)	6375 km	RAD BLOCK DATA
acceleration of gravity (g)	9.81 m s^{-2}	GRAV BLOCK DATA
gas constant for dry air (R)	287 J kg^{-1} K^{-1}	RGAS BLOCK DATA
latent heat of vaporization (L)	25.12×10^5 J kg^{-1}	HLTM BLOCK DATA
latent heat of sublimation (L_f)	28.48×10^5 J kg^{-1}	HLTF CUP
latent heat of melting (L_i)	3.36×10^5 J kg^{-1}	HLTI, HICE CUP, COMP3
ratio of gas constant to specific heat at constant pressure (κ)	0.286 ($\kappa = R/c_p$)	KAPA BLOCK DATA
specific heat capacity of dry air at constant pressure (c_p)	1003.5 J kg^{-1} K^{-1} $c_p = R/\kappa$	CP CNSTNT

mean surface pressure which determines total mass of the atmosphere on the earth	984 mb	PSF BLOCK DATA
Stefan-Boltzmann constant (σ)	5.67×10^{-8} J $m^{-2}s^{-1}K^{-4}$	STBO RADTN
melting point	273.1 K	TICE COMP3
angular velocity of rotation (Ω)	7.292×10^{-5} s^{-1}	 CNSTNT
Avogadro's number	6.022×10^{26} k mol^{-1}	AVO OZONSS
saturation mixing ratio of water vapor (Tetens' formula) $q^*(T, p)$	$e=6.11\times10^{(7.5\frac{T-273.2}{T-35.9})}$ on water $e=6.11\times10^{(9.5\frac{T-273.2}{T-8.7})}$ on ice $q^*=0.622\frac{e}{p-e}$	(Inline development) related constant QSATEX, QSTIEX in MAIN

Table AII.2 Other numerical constants and functions

surface roughness (Z_o)	0.0002m for ocean 0.0001m for sea-ice 0.005 m for land ice 0.45 m otherwise	Z0 PBL
surface albedo (α_s)	0.07 for ocean 0.14 for bare land 0.3 for frozen land Min (0.85, 0.7+0.15×Z) for snow or ice where Z is height in km 0.4 for bare sea-ice 0.7 for snow on sea-ice 0.5 for melting snow	ALS RADTN
coefficient of horizontal non-linear eddy diffusion (K_o^2)	0.04	K0SQ COMP3
field capacity of soil (ρ W_m h)	1.5 kg m^{-2}	FLDCAP COMP3

critical temperature of ice phase transition in cumulus clouds (T_{cr})	253.1 K	TCR CUP
conversion coefficient from cloud water to rain water (C_o)	0.004 m^{-1} at cloud top 0.002 m^{-1} otherwise	C0, C1 CUP
maximum sustainable cloud water (ℓ_{cr})	0.0	CRITL CUP
base line cloud work function ($A_o(p_d)$)	$2\times(\delta p \times 0.01)^3$ J where δp is cloud depth in mb	A0 (K) CUP
climatological mixing ratio of water vapor (H_2O) in the stratosphere	2.5×10^{-6} (kg/kg)	QST RADTN
carbon dioxide density at NTP ($\rho_{CO2,NTP}$)	1.977 kg m^{-3}	 RADTN
ozone density at NTP ($\rho_{O3,NTP}$)	2.144 kg m^{-3}	RO3NTP RADTN
ozone chemical reaction rates (k_n)	see Eqs. (12.2), (12.4), (12.5), (12.6) and (12.8)	RR (n) OZONSS
photodissociation rates (j_n (p))	see Eq. (12.9)	PHOD (n) OZONSS
reaction rate for ozone surface destruction (K)	8×10^{-4} ms^{-1}	RC OZONSS
eddy diffusivity at the PBL top (D)	10 m^2 s^{-1}	ED OZONSS
entrainment rate across the PBL top (E)	see Eq. (8.24)	ENTRAN PBL
transfer coefficients of heat (C_H) and momentum (C_D)	see Fig. 8.3	CT and CU PBL
bulk heat capacity for ice (C_{ice}), snow (C_{snow}) and soil (C_{soil})	see Eqs. (10.6) and (10.9)	CZH COMP3
efficiency factor of evapo-transpiration (β)	see Eq. (10.18)	EVE PBL
functional form of runoff (R)	see Eq. (10.26)	RUNOFF COMP3

constant related to polytropic atmosphere (a)	0.2	AKAP BLOCK DATA
mixing ratio of carbon dioxide (q_{CO_2})	4.89×10^{-4} (kg/kg) (=320ppm)	 RADTN
pressure scaling factor (α_{H_2O}, α_{CO_2}, α_{O_3})	0.9 for water vapor 0.86 for carbon dioxide 0.3 for ozone	PEXP−1, ACO2, AO3 RADTN
constants for the Dickinson's long wave cooling parameterization (C_0, a_0, β_0, T_0)	see Table 13.2	CSTD, ASTD, BC, TLSTD RADTN
diffusivity factor for the downward radiation	1.66	 RADTN
diffusivity factor for the upward radiation	1.9	 RADTN
reflectivity of clouds (R_c)	see Eq. (13.90)	TACA, TACS RADTN
absorptivity of clouds (A_c)	see Eq. (13.91)	DELABS RADTN

II.3 Time steps and resolutions

Currently, we have three versions of the model, namely, coarse resolution 5-layer model (C5), coarse resolution 12-layer model (C12) and fine resolution 5-layer model (F5). C5 and F5 are the tropospheric models and exclude the process related to ozone and the sponge layer. Values of version dependent parameters are listed in Table AII.3. The time steps for physical process Δt_d is common to all the version and set to be 1 hour.

Table AII.3

version	time step for advective process Δt	resolution in latitude $\Delta\varphi$	resolution in longitude $\Delta\lambda$	model's top p_{top}
C5	450 sec	4 degree	5 degree	100 mb
C12	450 sec	4 degree	5 degree	1 mb
F5	225 sec	2 degree	2.5 degree	100 mb

Appendix III. Selected monthly mean fields produced by the MRI•GCM-I

Selected results taken from a simulation of annual cycle with 5 layer version of the MRI•GCM-I (see Fig. 1.2(a)) are shown in this appendix without any comments on the results. Discussions on them will be found in the forthcoming papers by Tokioka, Kitoh, Yagai and Yamazaki (1985), Kitoh and Tokioka (1985) and Tokioka and Kitoh (1985). The simulated results of the 12-layer MRI•GCM-I are not included here. Those who are interested in them, some preliminary results are found in Tokioka and Yagai (1984).

Horizontal resolution of the model is $\Delta\lambda=5°$ and $\Delta\varphi=4°$. As for the time incrment, $\Delta t=7.5$ min and $\Delta t_d=60$ min are used.

Monthly mean maps are shown for January, April, July and October. For each month, the following fields are included ;

i : Monthly mean sea level pressure. (a) model and (b) observation

ii : Monthly mean geopotential field at 500 mb. (a) model and (b) observation

iii : Monthly mean wind and stream lines at 900 mb. (a) model and (b) observation

iv : Same as iii but for 200 mb

v : Monthly mean velocity potential and divergent wind of the model at 200 mb.

vi : Seasonal mean precipitation. (a) model and (b) observation

vii : Monthly mean evaporation of the model.

viii : Monthly mean sensible heat flux at the surface of the model.

ix : Monthly mean net downward flux of solar radiation at the top of the atmosphere. (a) model and (b) observed value

x : Monthly mean net upward flux of terrestrial radiation at the top of the atmosphere. (a) model and (b) observed value

xi : Monthly mean net downward flux of radiation at the top of the atmosphere. (a) model and (b) observed value

xii : Monthly mean net downward flux of solar radiation of the model at the surface.

xiii : Monthly mean net upward flux of terrestrial radiation of the model at the surface.

xiv : Monthly mean net downward flux of radiation of the model at the surface.

xv : Monthly mean total heating of air column of the model.

xvi : Monthly mean snow depth of the model.

xvii : Monthly mean total cloudiness of the model.

xviii : Monthly mean zonally averaged temperature. (a) model and (b) observation xix : Monthly mean zonally averaged zonal wind. (a) model and (b) observation

xx : Monthly mean meridional stream function. (a) model and (b) based on observation

xxi : Monthly mean zonally averaged total heating rate of the model.

(a—1)

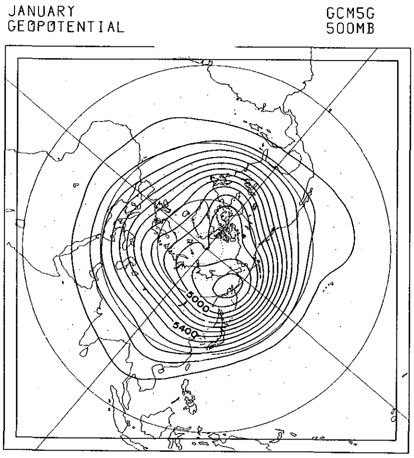

(a—2)

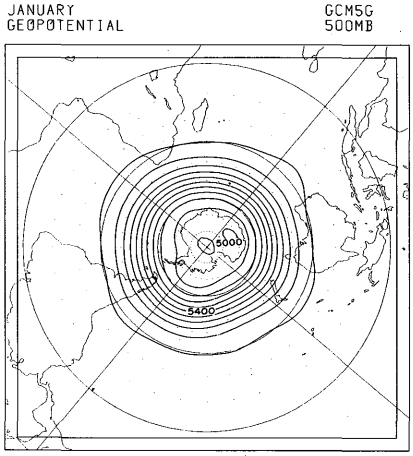

(b—1)

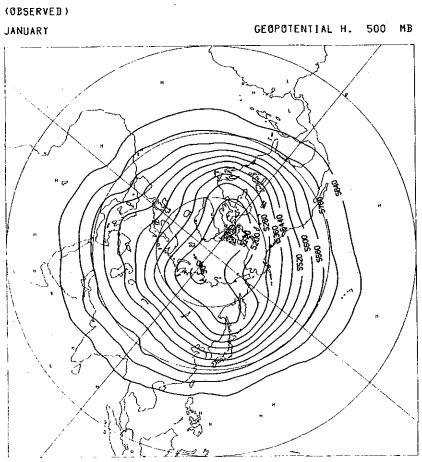

(b—2)

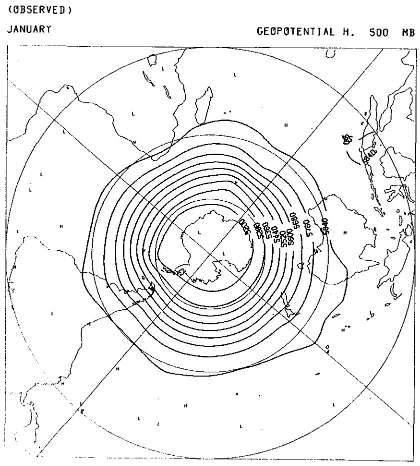

Fig. AIII.1.ii Monthly mean geopotential field at 500 mb for January. (a-1) model and (b-1) observation (Oort, 1983) for the northen hemisphere. (a-2) model and (b-2) observation (Oort, 1983) for the southern hemisphere. Contour interval is 80 gpm.

(a)

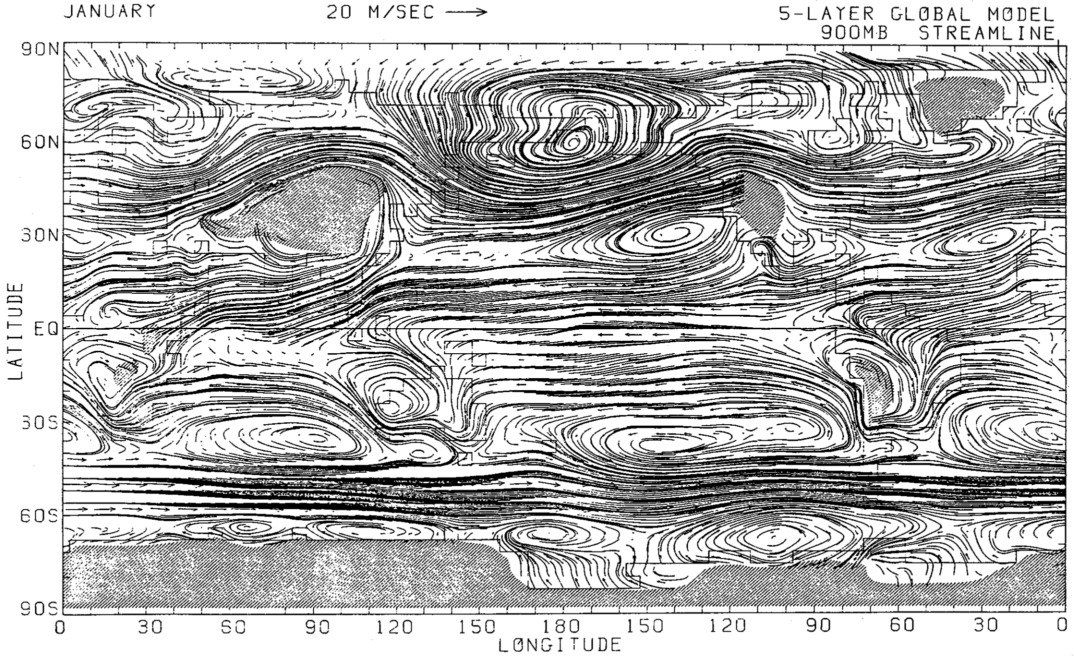

(b)

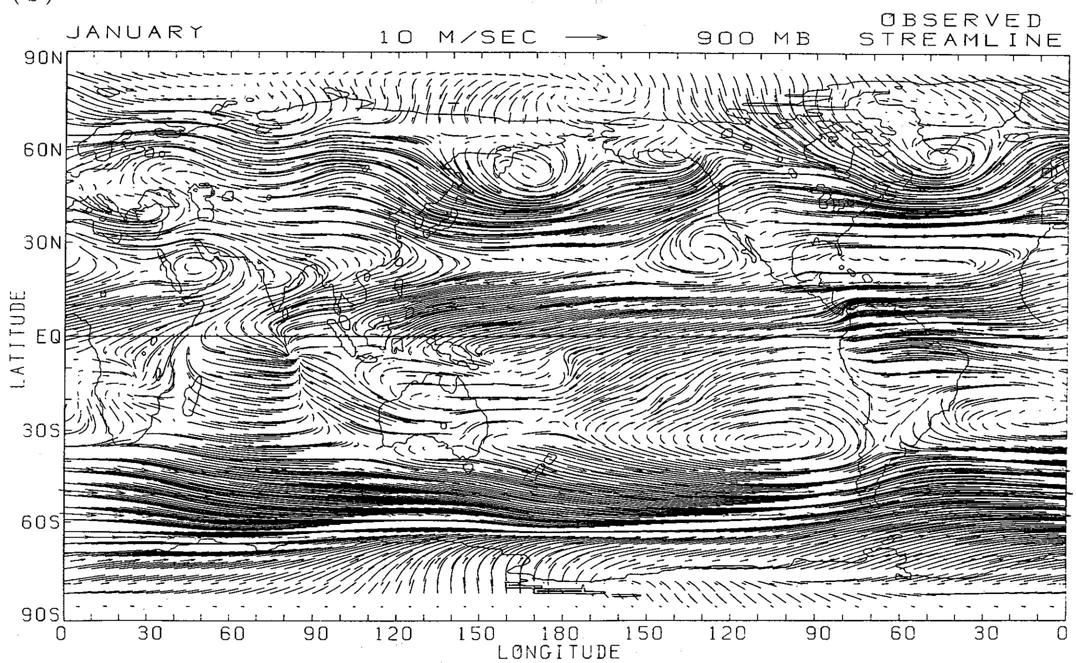

Fig. AIII.1.iii Global distribution of monthly mean wind and stream lines at 900 mb for January. (a) model and (b) observation (based on Oort (1983)).

(a)

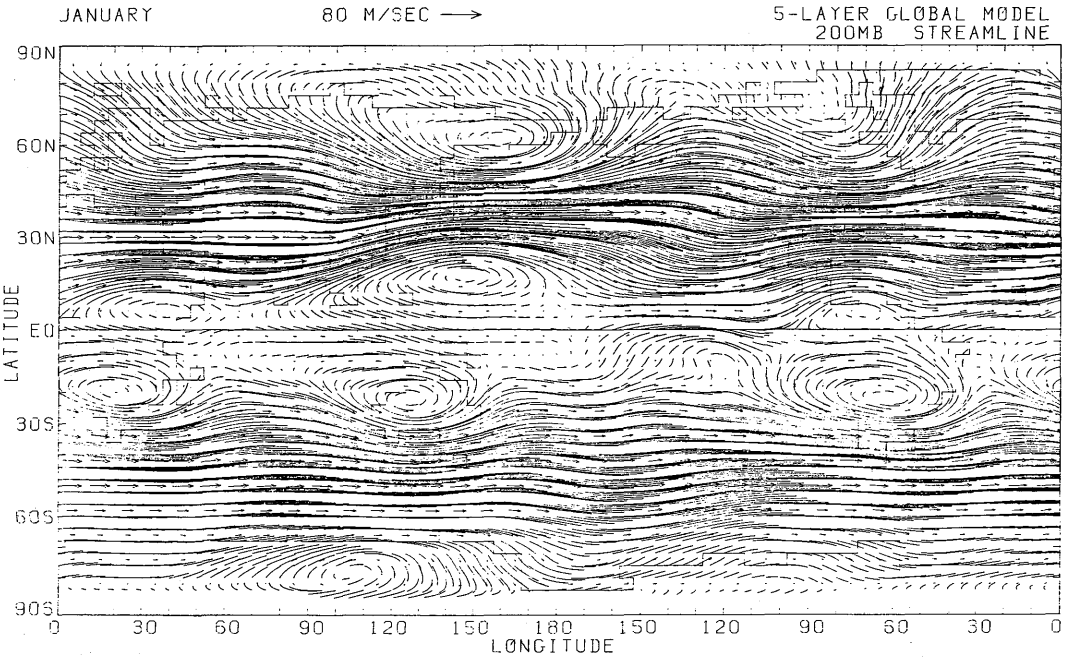

(b)

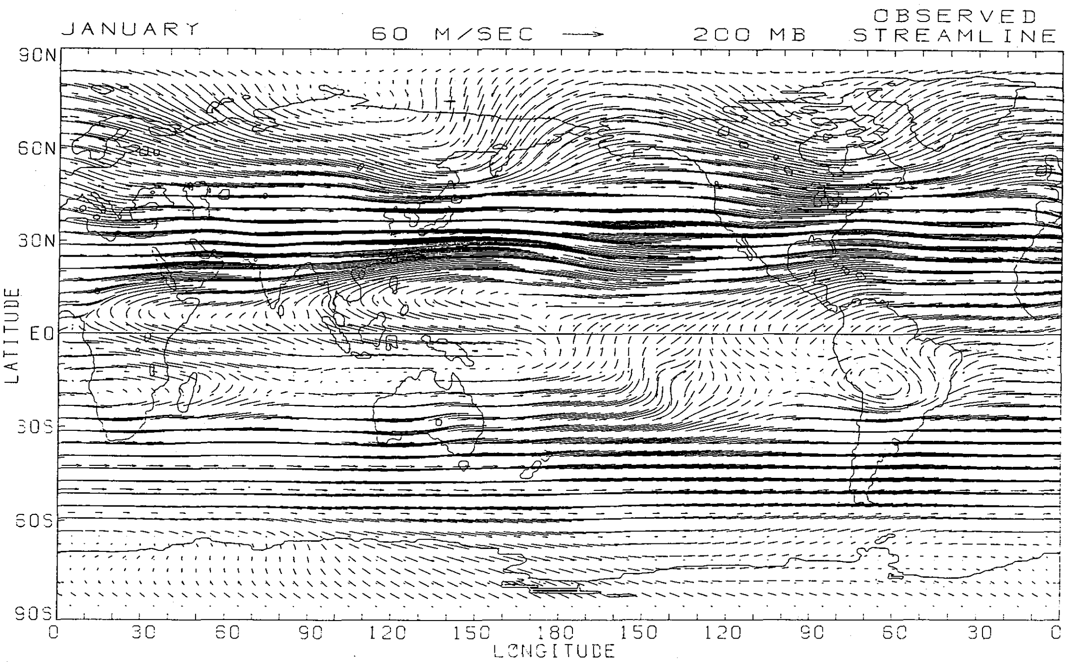

Fig. AIII.1.iv Same as in Fig. AIII.1.iii but for 200 mb.

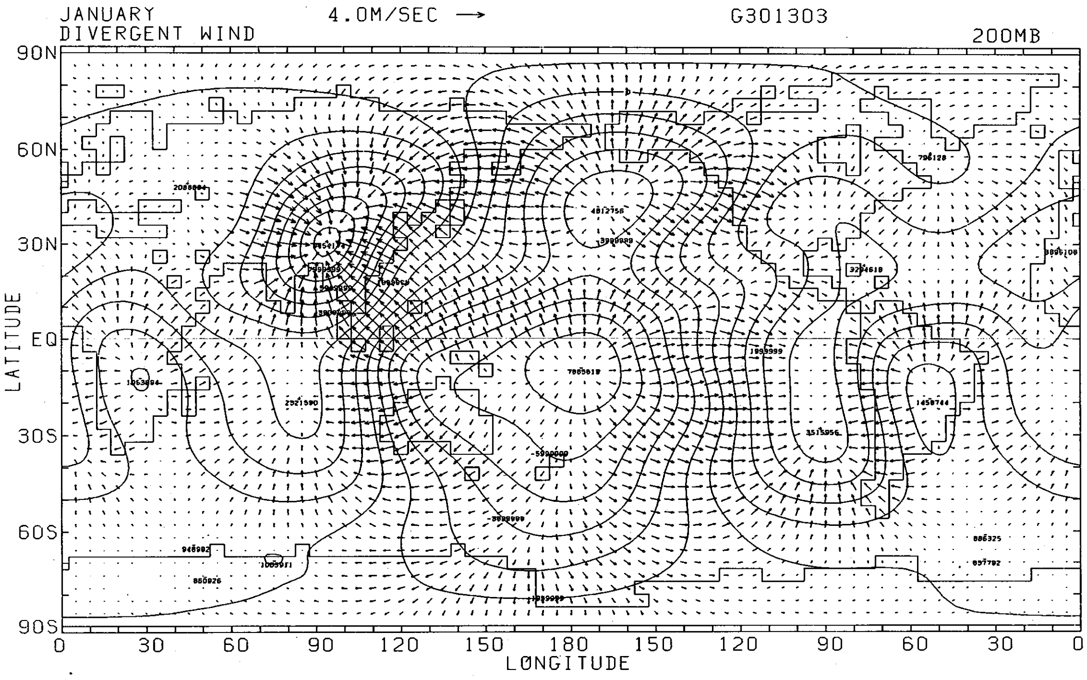

Fig. AIII.1.v Global distribution of monthly mean velocity potential and divergent wind of the model at 200 mb for January. Contour interval is $10^6 m^2 s^{-1}$.

(a)

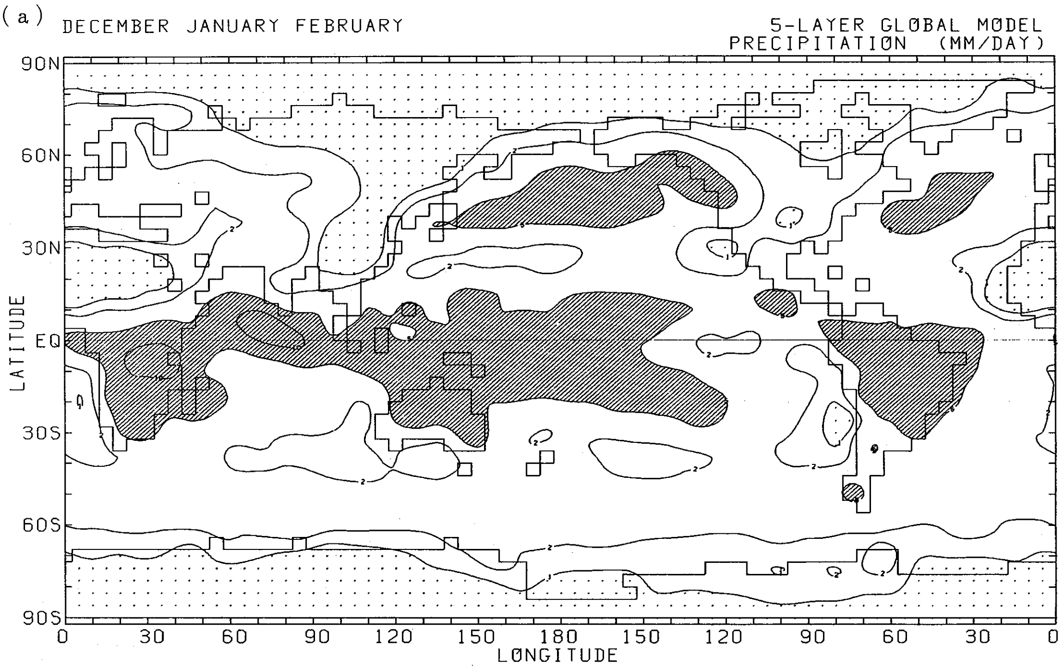

(b)

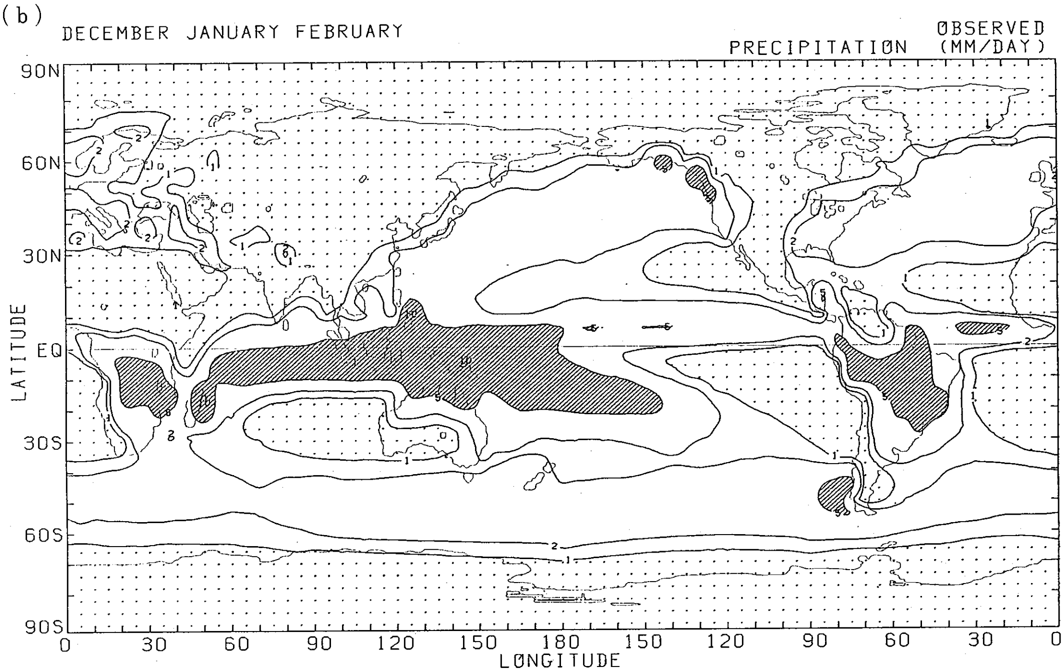

Fig. AIII.1.vi Global distribution of total precipitation for December, January and February. (a) model and (b) observation (Schutz and Gates, 1972). (unit : mm/d) Areas over 5mm/d and less than 1mm/d are covered with shades and dots, respectively.

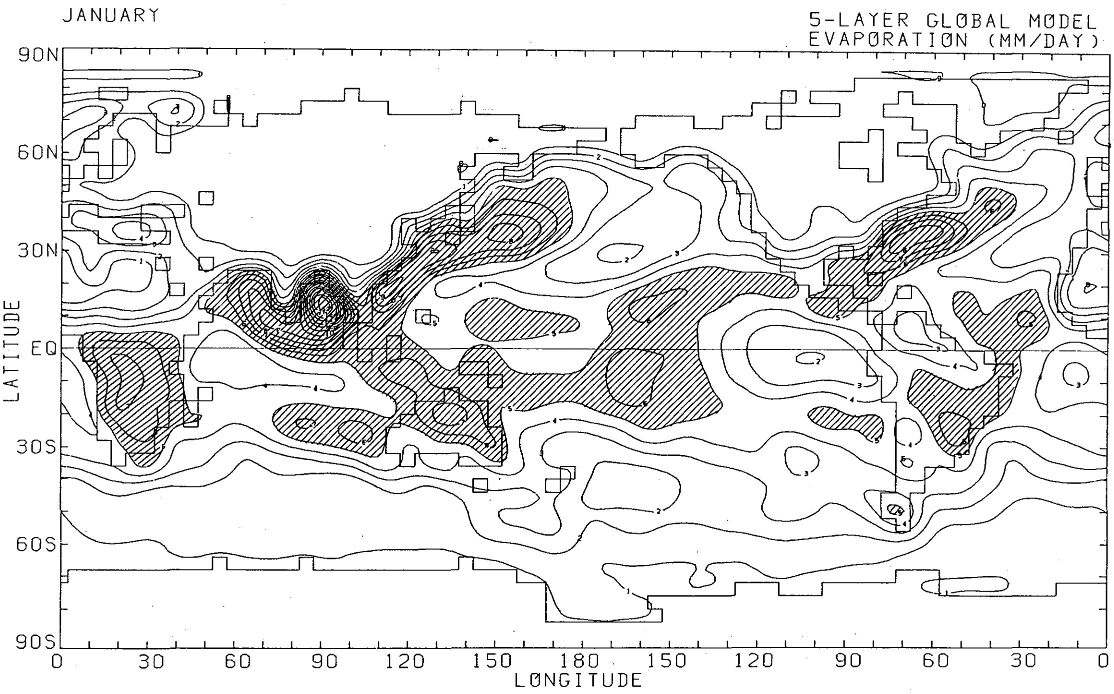

Fig. AIII.1.vii Global distribution of evaporation of the model at the surface for January. (unit : mm/d). Areas over 5mm/d are covered with shades.

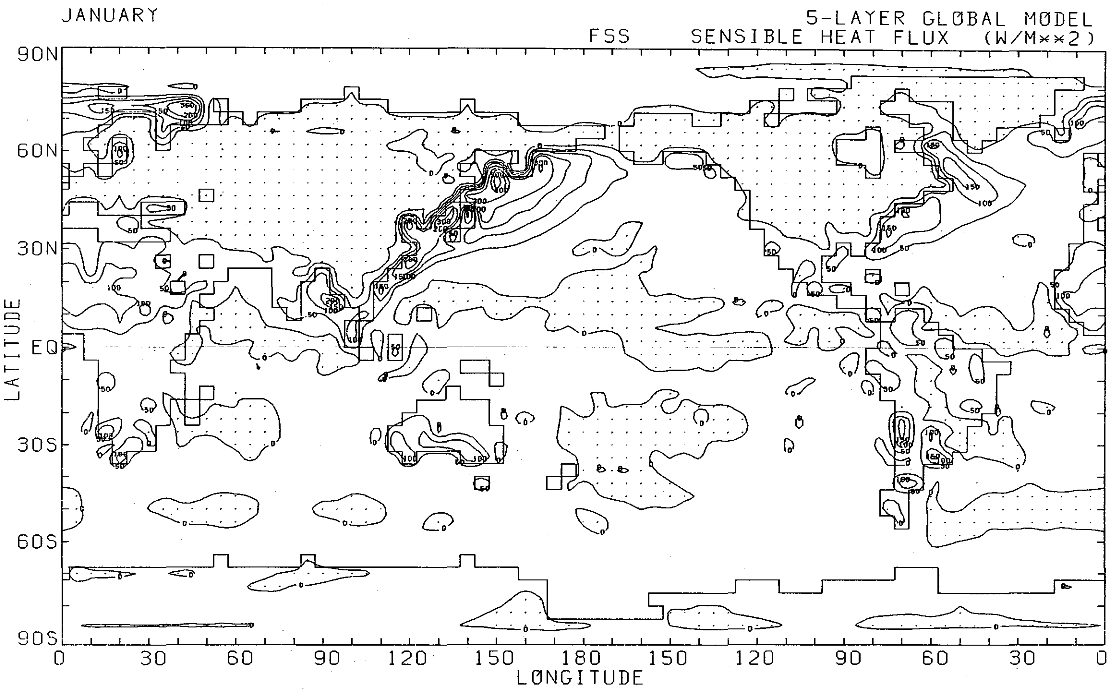

Fig. AIII.1.viii Global distribution of upward sensible heat flux of the model at the surface for January. Contour interval is 50 W m^{-2}. Negative areas are covered with dots.

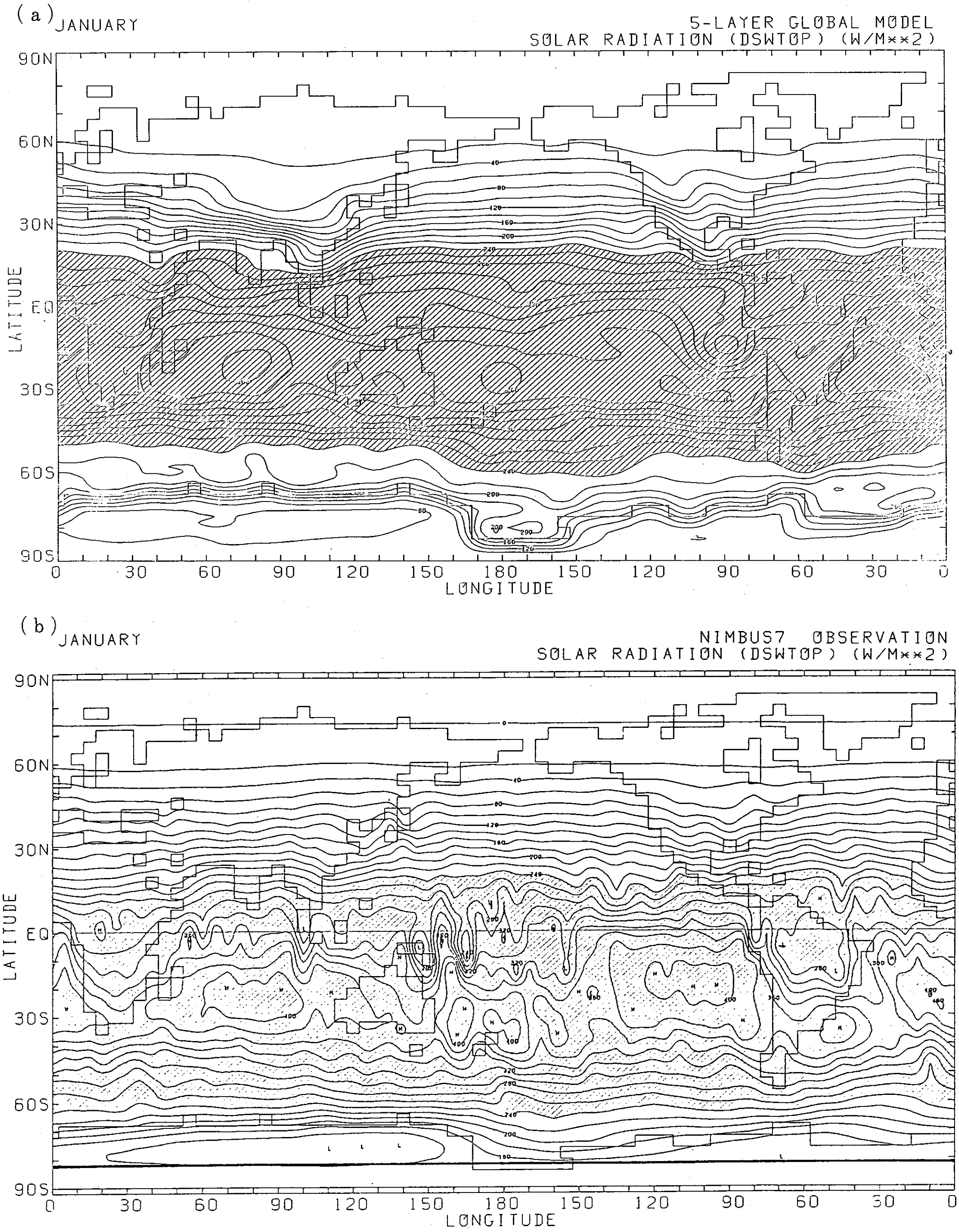

Fig. AIII.1.ix Global distribution of monthly mean net downward flux of solar radiation at the top of the atmosphere for January. (a) model and (b) observed value (Jacobowitz *et al.*, 1984). Contour interval is 20 W m^{-2}. Areas over 240 W m^{-2} are shaded.

(a)

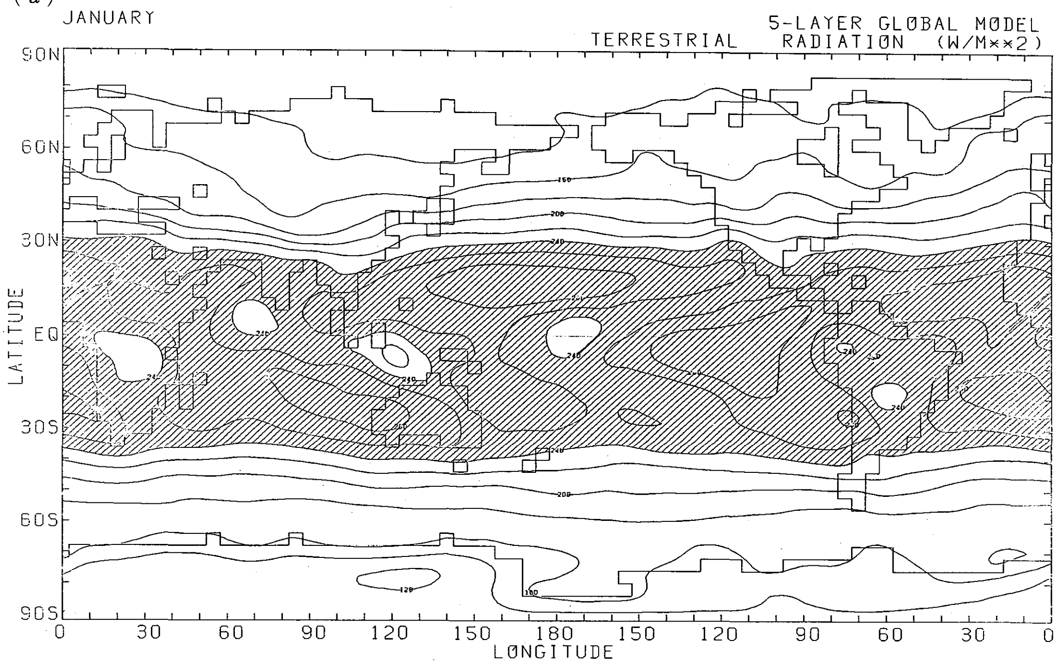

(b)

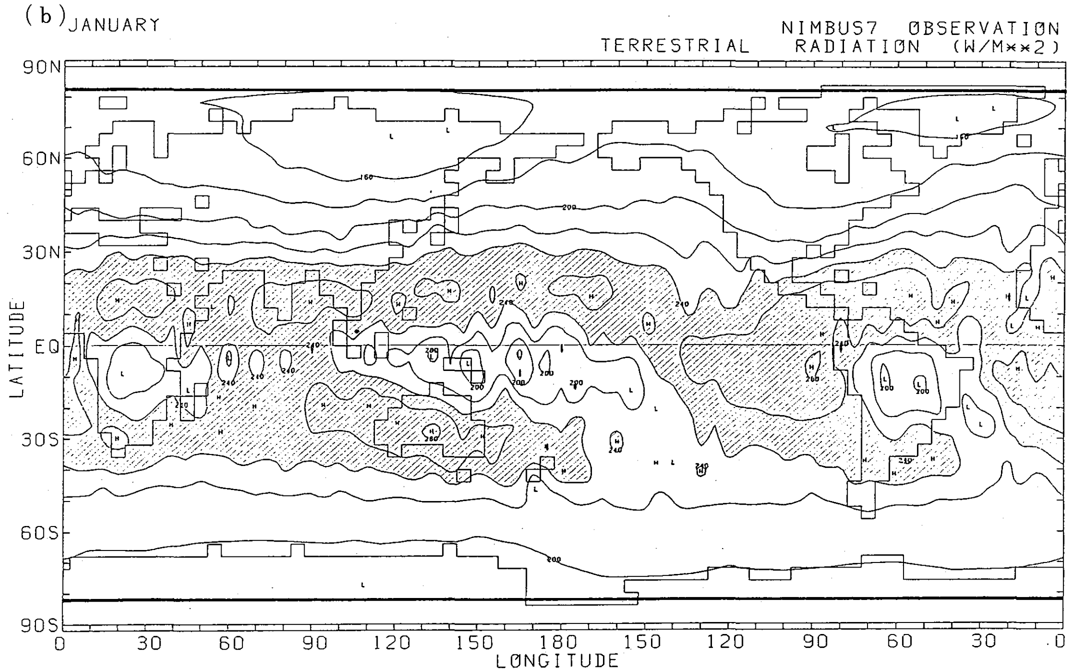

Fig. AIII.1.x Global distribution of monthly mean net upward flux of terrestrial radiation at the top of the atmosphere for January. (a) model and (b) observed value (Jacobowitz *et al.*, 1984). Contour interval is 20 W m^{-2}. Areas over 240 W m^{-2} are shaded.

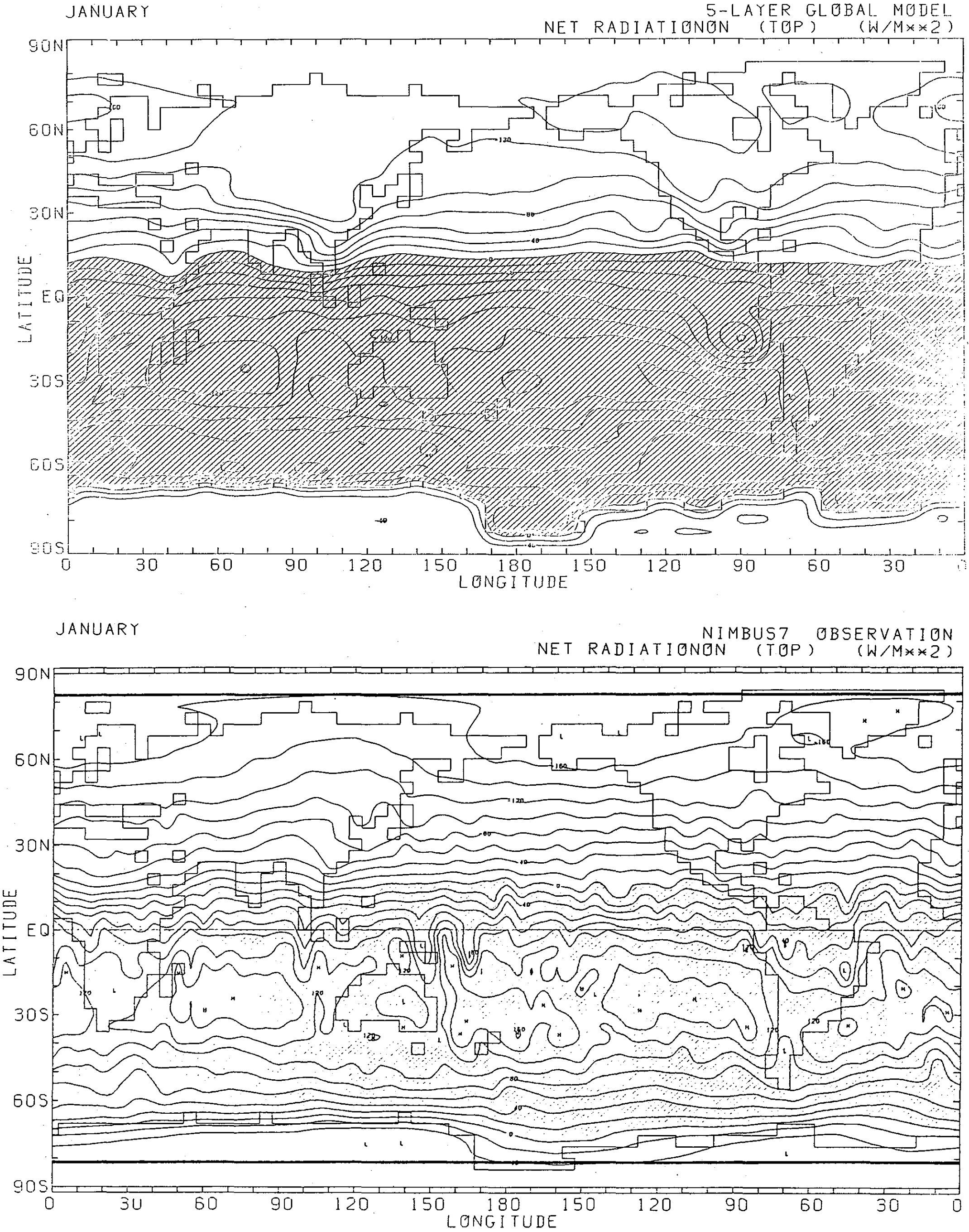

Fig. AIII.1.xi Global distribution of monthly mean net downward flux of radiation at the top of the atmosphere for January. (a) model and (b) observed value (Jacobowitz *et al.*, 1984). Contour interval is 20 W m^{-2}. Positive areas are shaded.

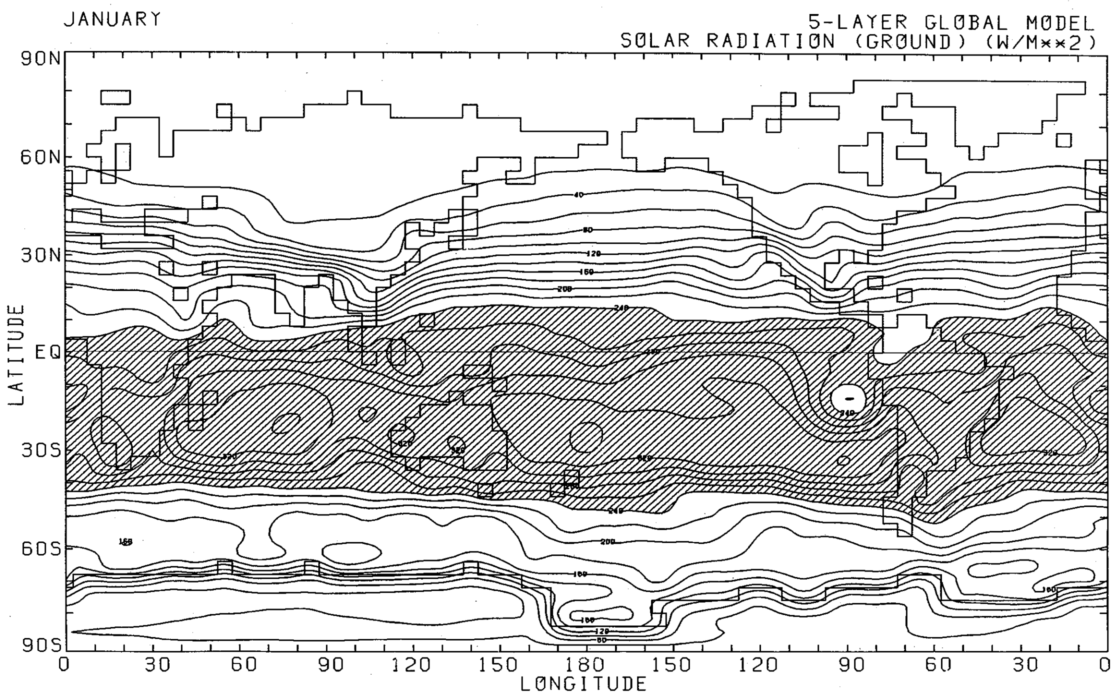

Fig. AIII.1.xii Global distribution of monthly mean net downward flux of solar radiation at the surface of the model for January. Contour interval is 20 W m^{-2}. Areas over 240 W m^{-2} are shaded.

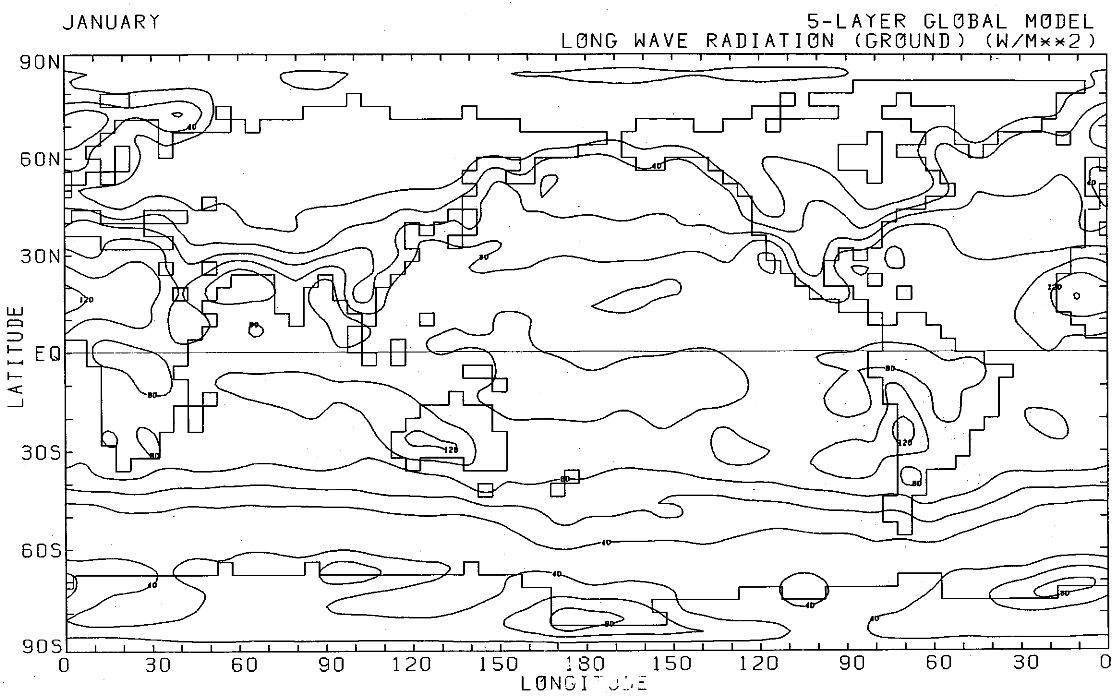

Fig. AIII.1.xiii Global distribution of monthly mean net upward flux of terrestrial radiation at the surface of the model for January. Contour interval is 20 W m^{-2}.

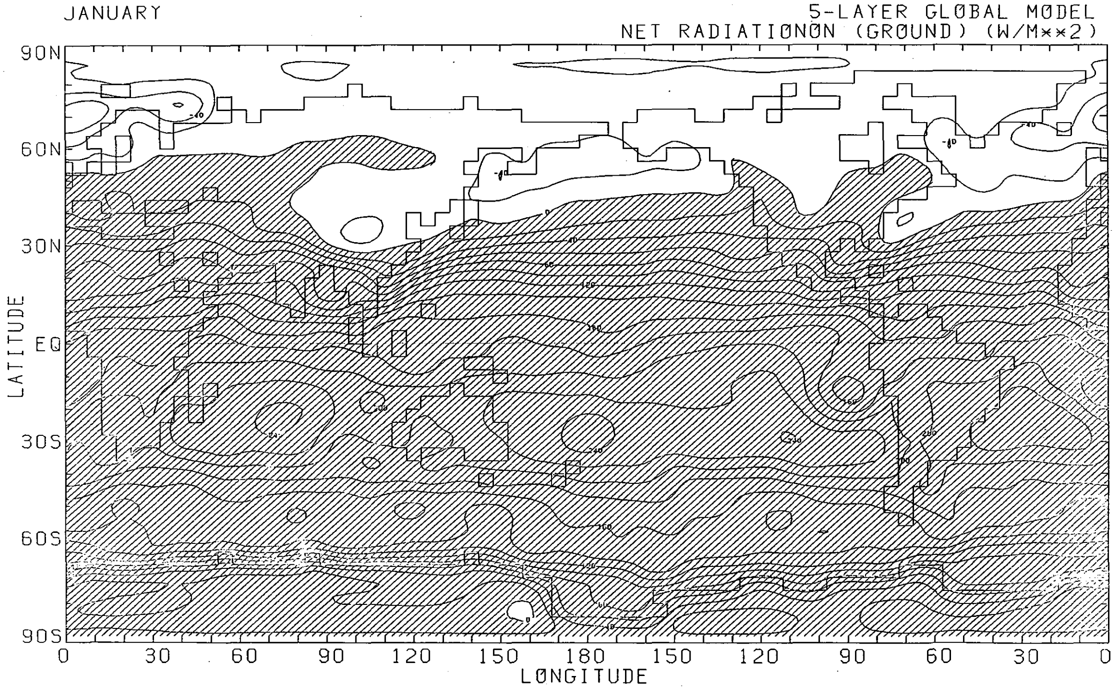

Fig. AIII.1.xiv Global distribution of monthly mean net downward flux of radiation at the surface of the model for January. Contour interval is 20 W m^{-2}. Positive areas are shaded.

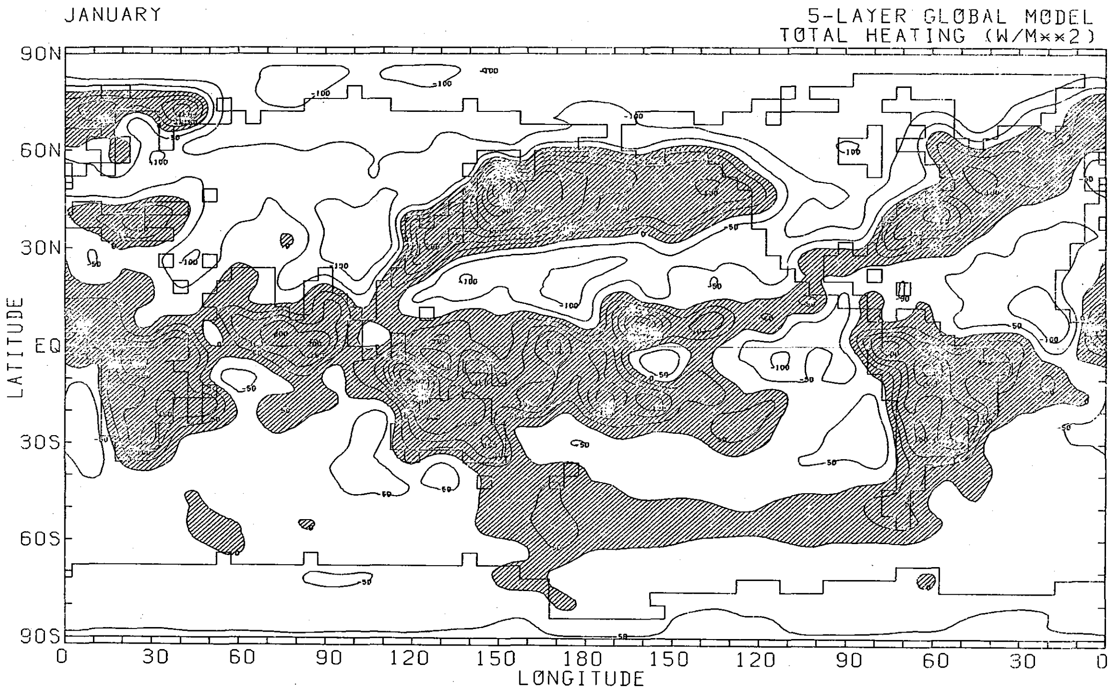

Fig. AIII.1.xv Global distribution of monthly mean total heating of air column of the model for January. Contour interval is 50 W m^{-2}. Positive areas are covered with shades.

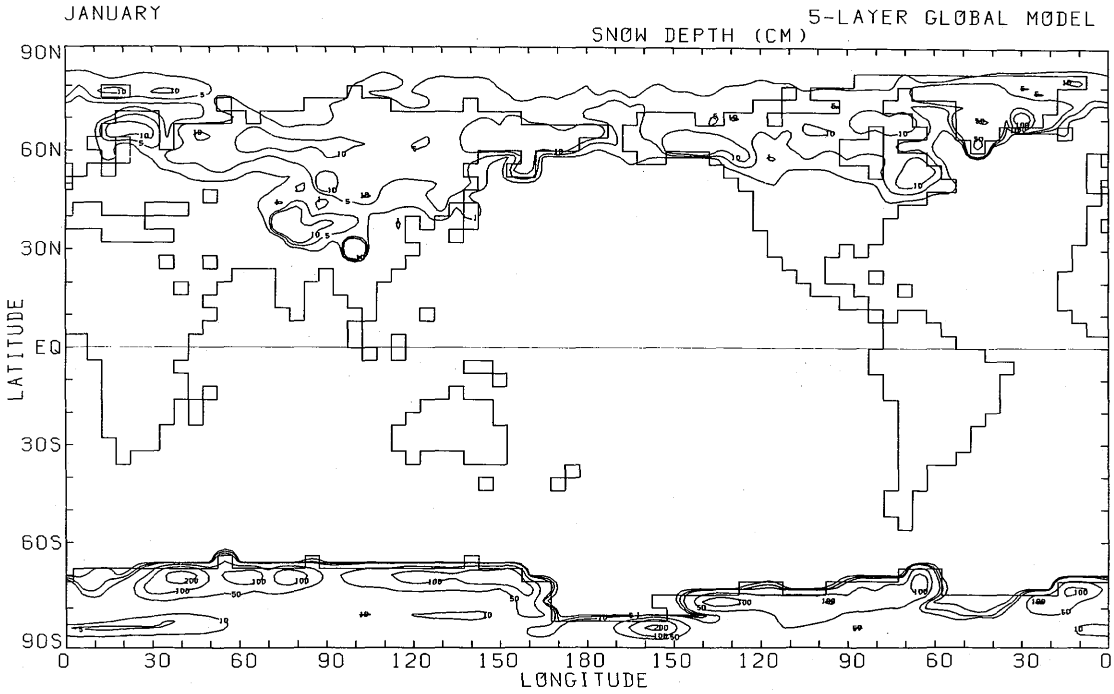

Fig. AIII.1.xvi Global distribution of monthly mean snow depth of the model for January. (unit : cm)

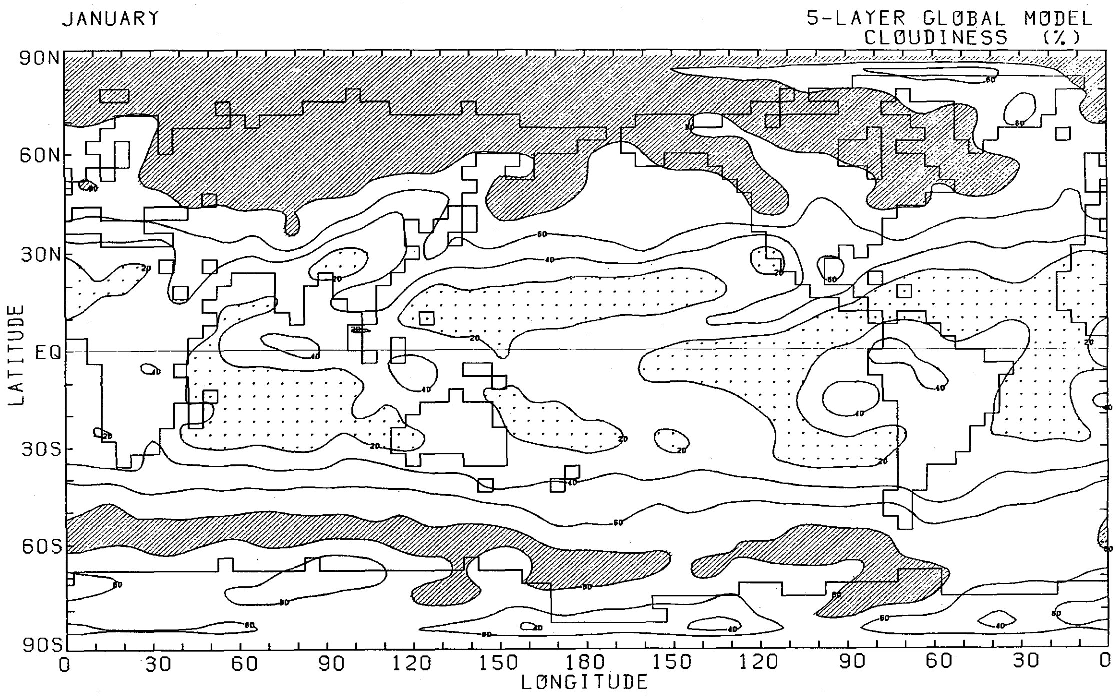

Fig. AIII.1.xvii Global distribution of monthly mean total cloudiness of the model for January. Areas over 80% and less than 20% cloudiness are covered with shades and dots, respectively.

(a)

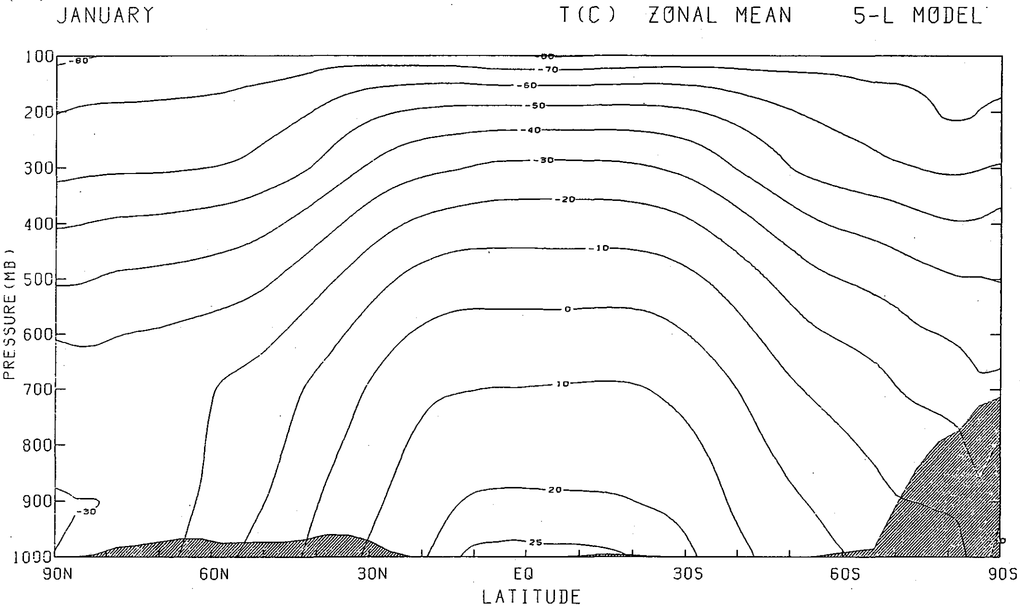

(b)

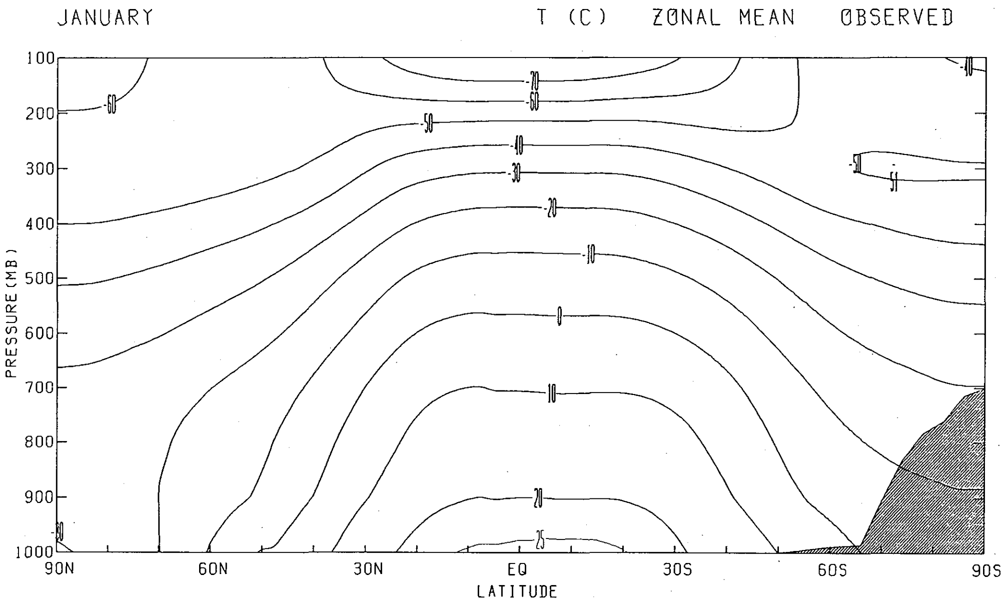

Fig. AIII.1.xviii Meridional distribution of monthly mean zonally averaged temperature for January. (a) model and (b) observation (Oort, 1983). Contour interval is 10C.

(a)

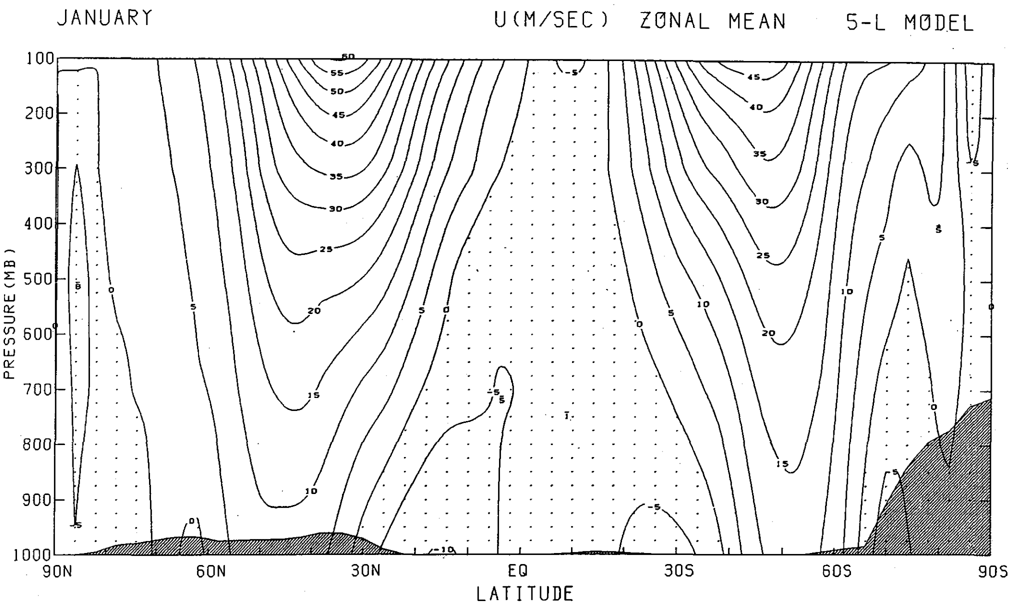

(b)

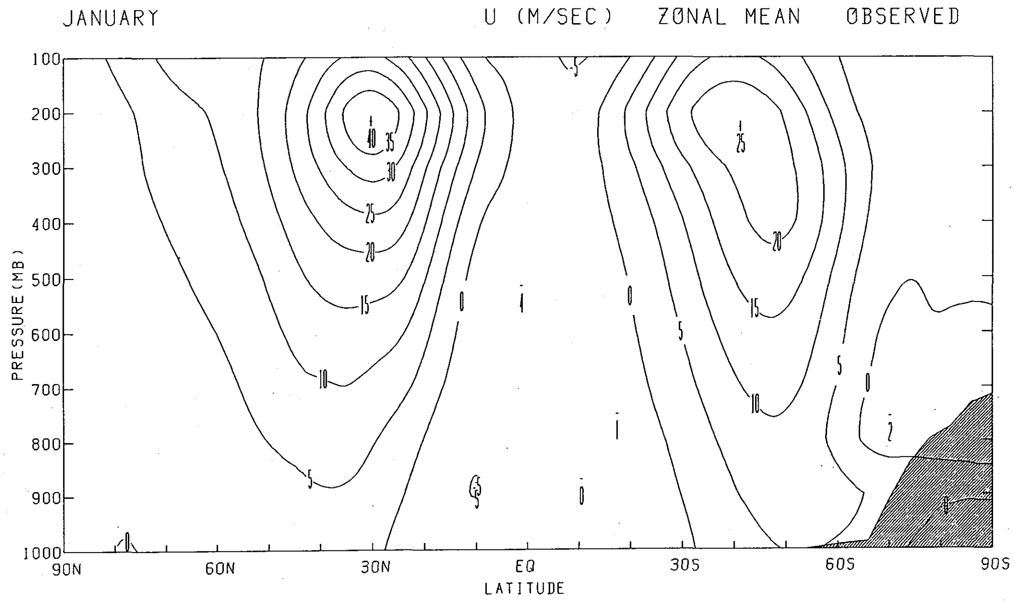

Fig. AIII.1.xix Meridional distribution of monthly mean zonally averaged zonal wind for January. (a) model and (b) observation (Oort, 1983). Contour interval is 5 m s^{-1}.

(a)

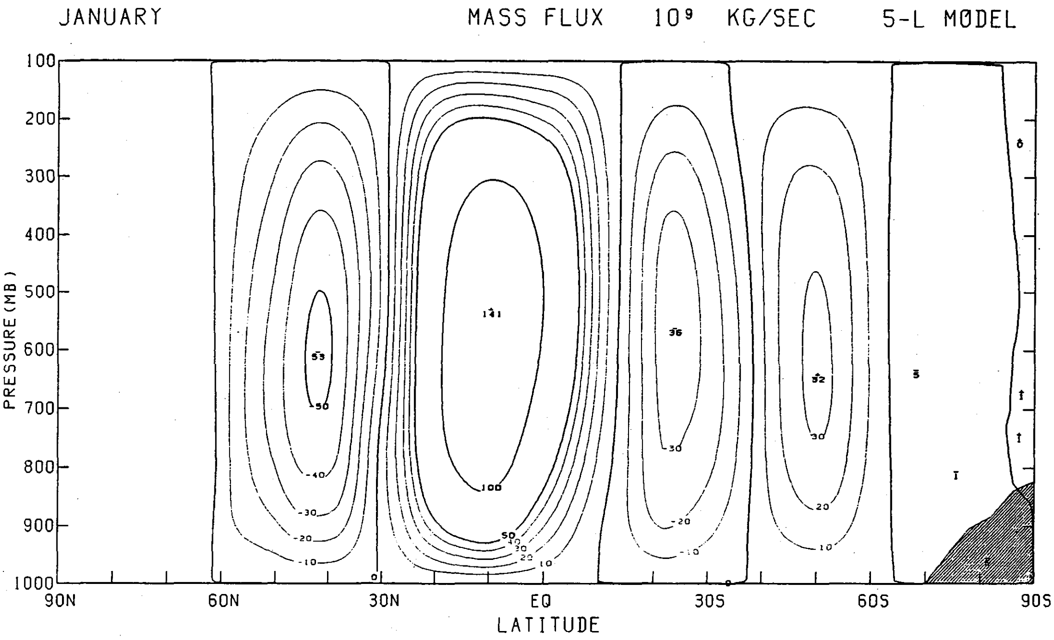

(b)

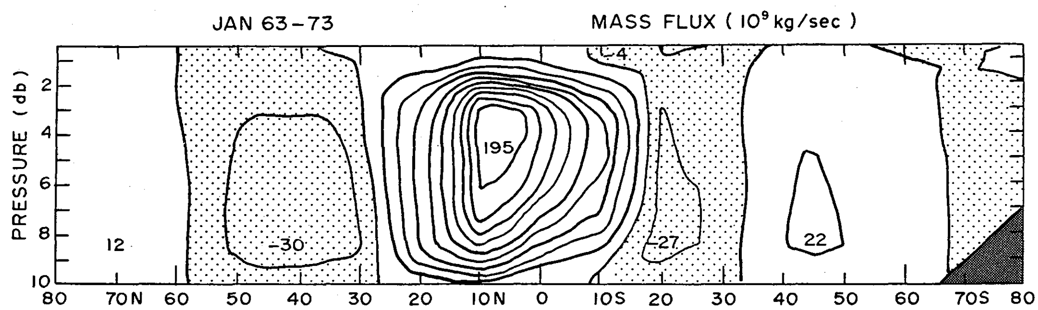

Fig. AIII.1.xx Meridional distribution of monthly mean meridional stream function for January. (a) model and (b) observed analysis by Oort (1983).

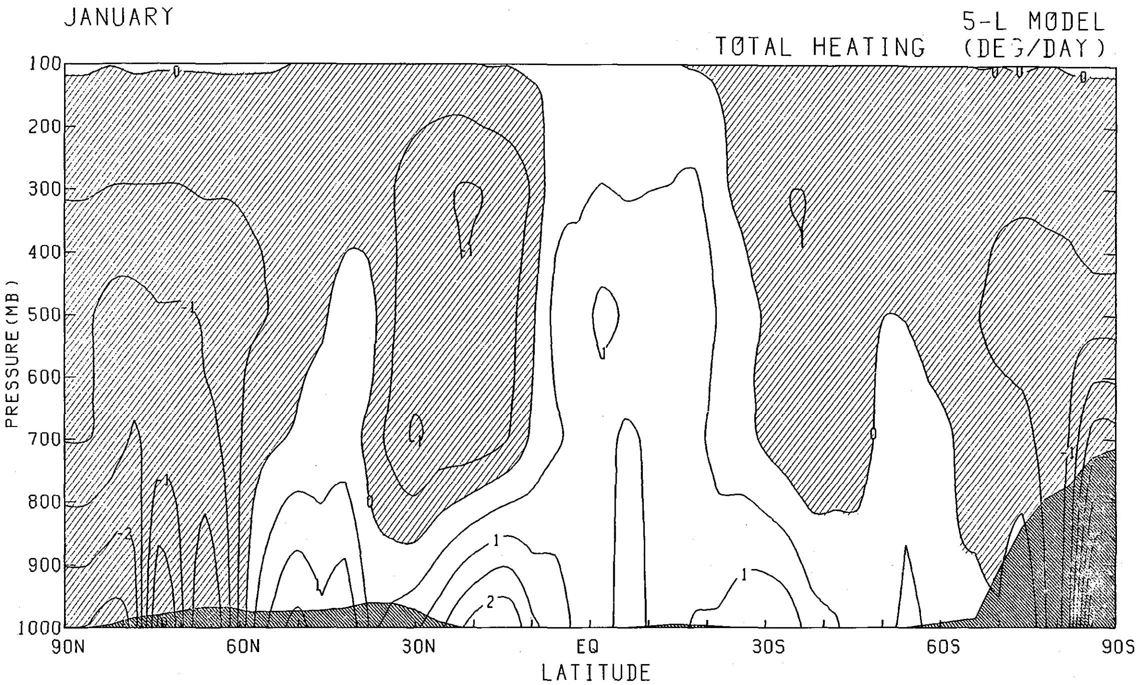

Fig. AIII.1.xxi Meridional distribution of monthly mean zonally averaged total heating rate of the model for January. Contour interval is 0.5 K d^{-1}. Cooling areas are covered with shades.

(a)

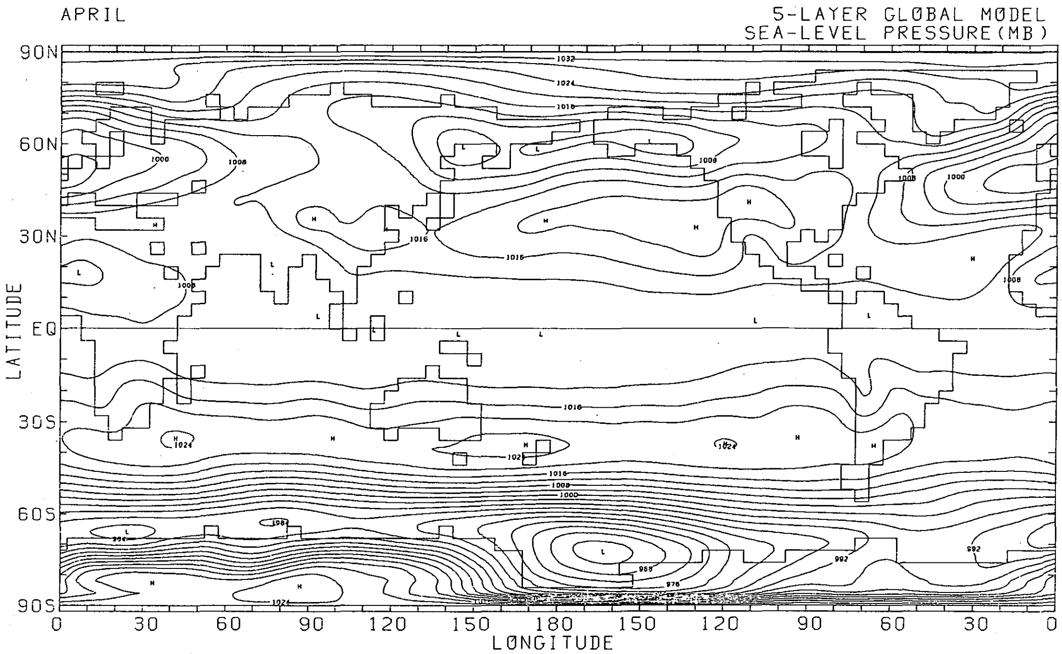

(b)

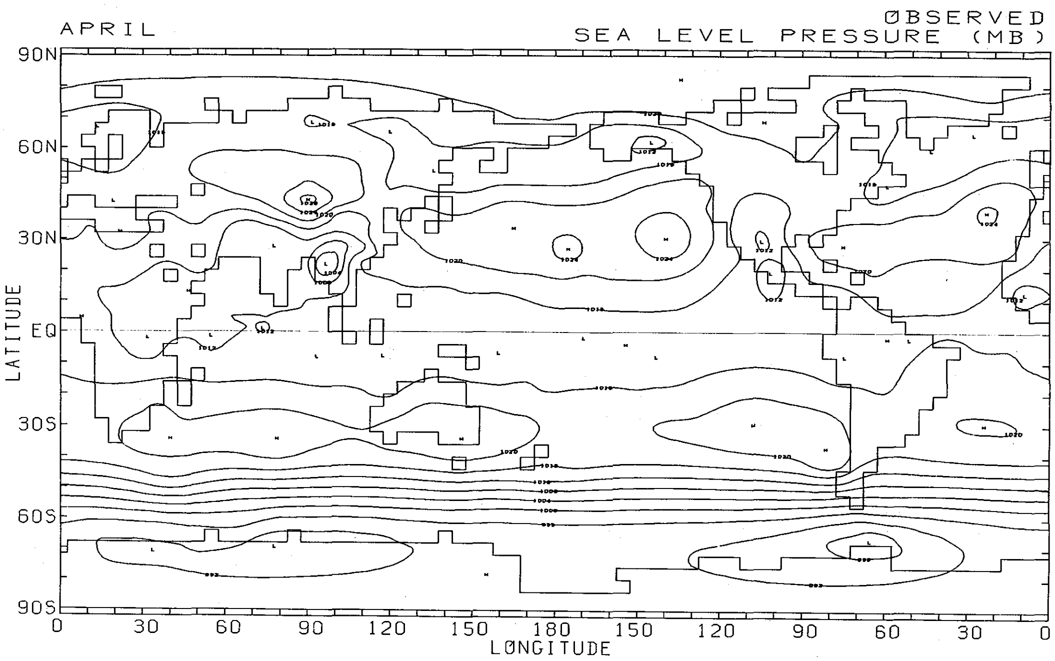

Fig. AIII.2.i Same as in Fig. AIII.1.i but for April.

(a — 1)

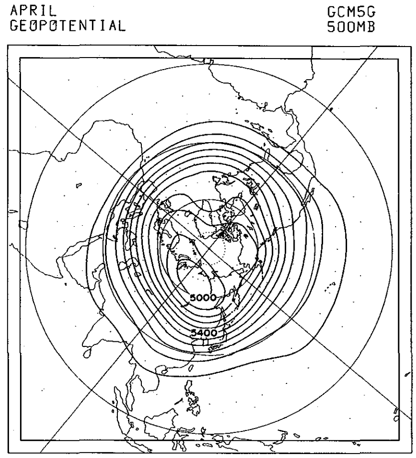

(a — 2)

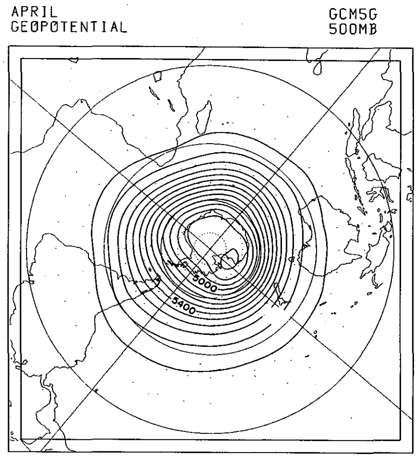

(b — 1)

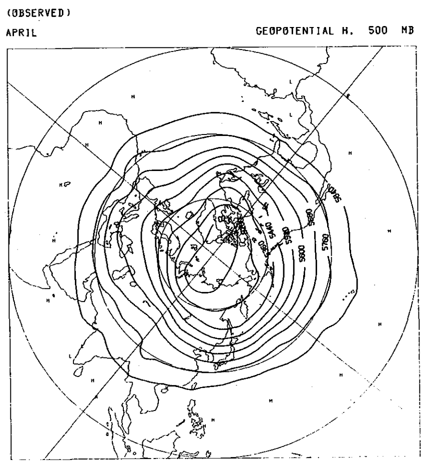

(b — 2)

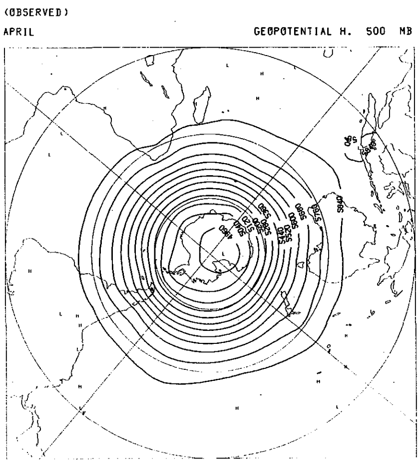

Fig. AIII.2.ii Same as in Fig. AIII.1.ii but for April.

(a)

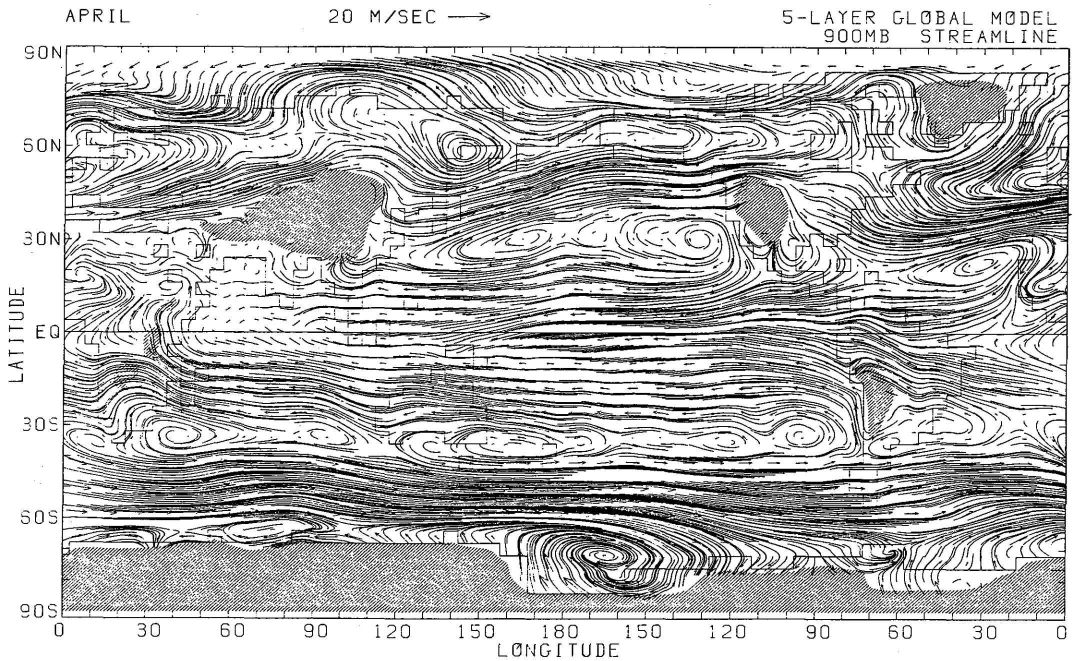

(b)

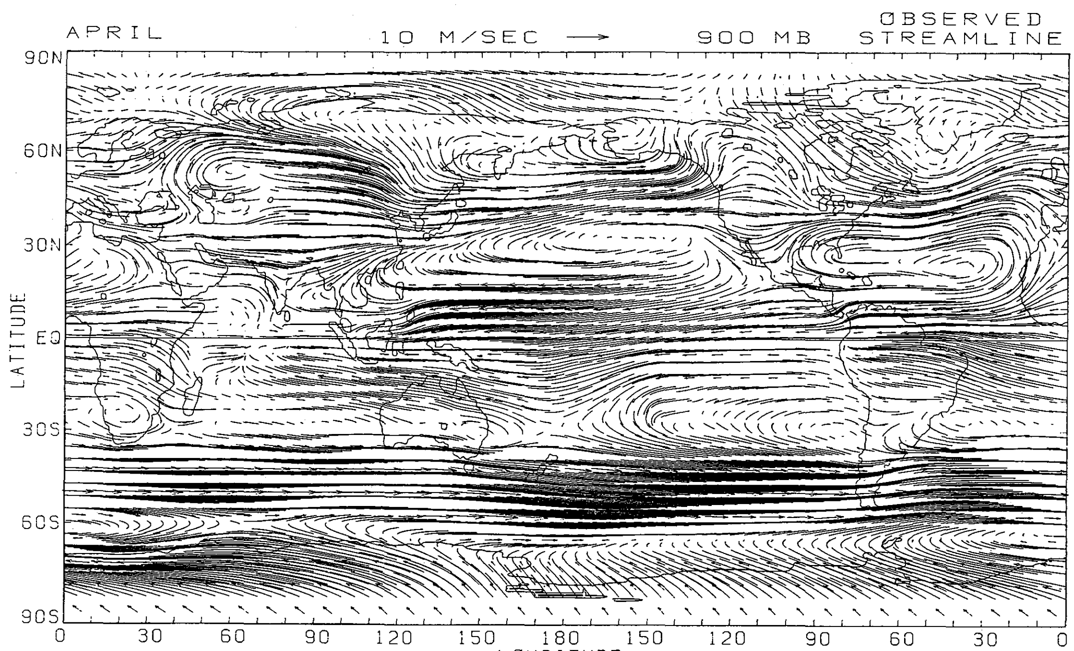

Fig. AIII.2.iii Same as in Fig. AIII.1.iii but for April.

(a)

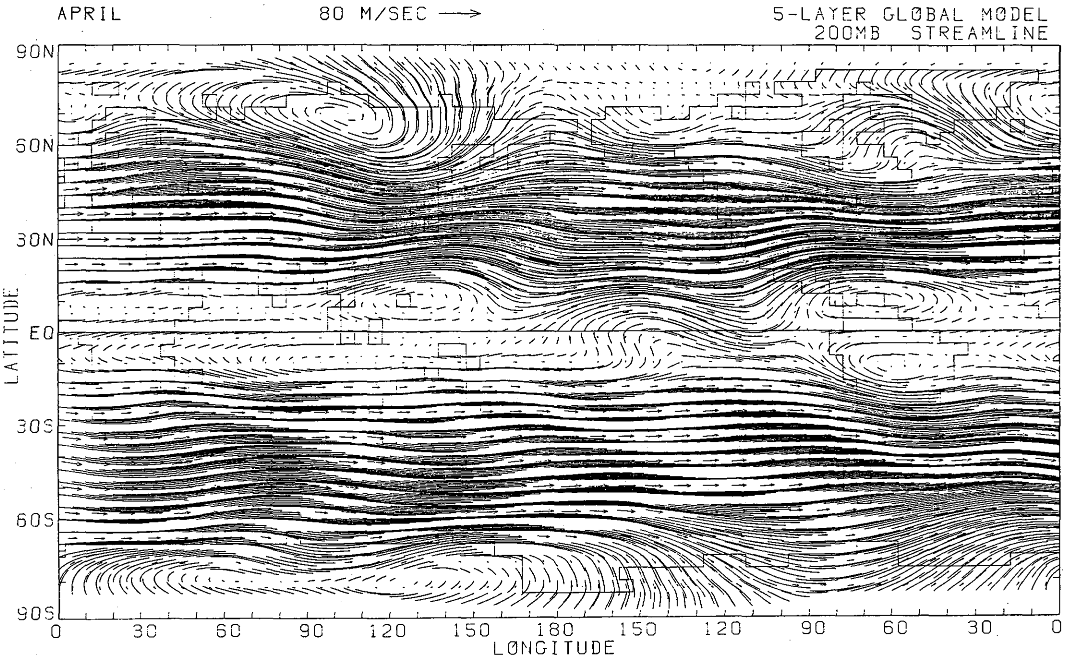

(b)

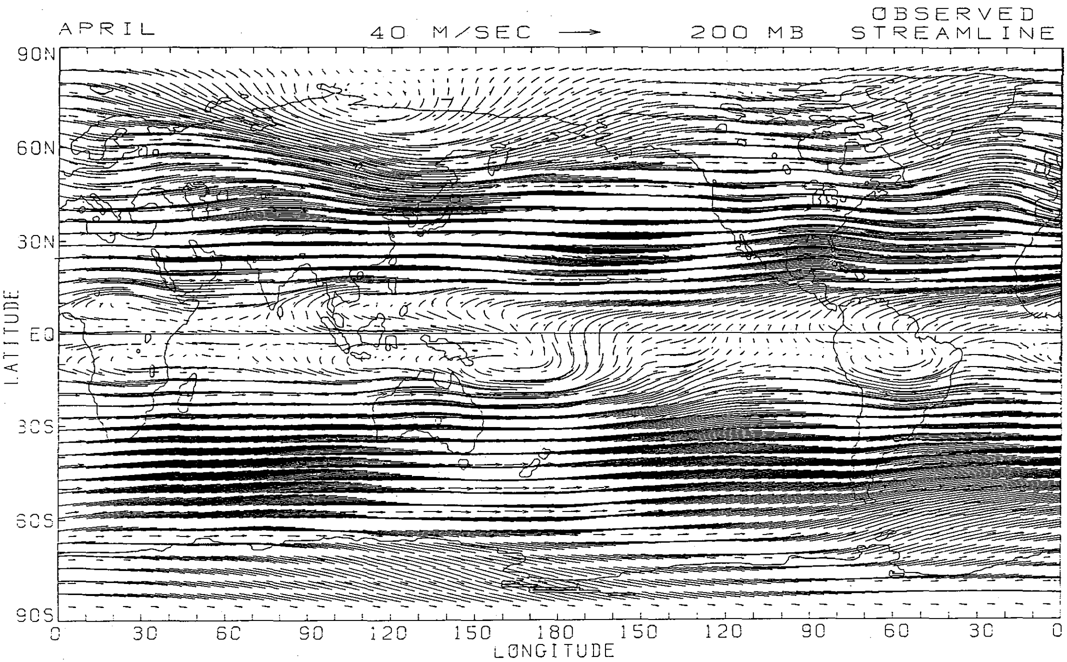

Fig. AIII.2.iv Same as in Fig. AIII.1.iv but for April.

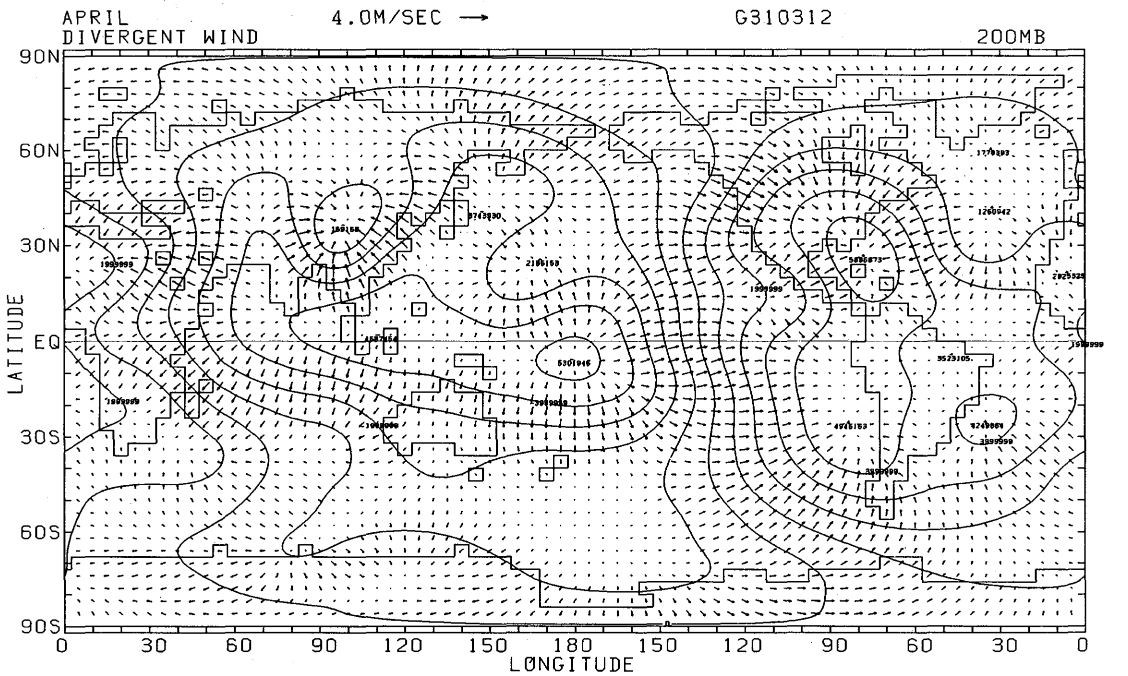

Fig. AIII.2.v Same as in Fig. AIII.1. v but for April.

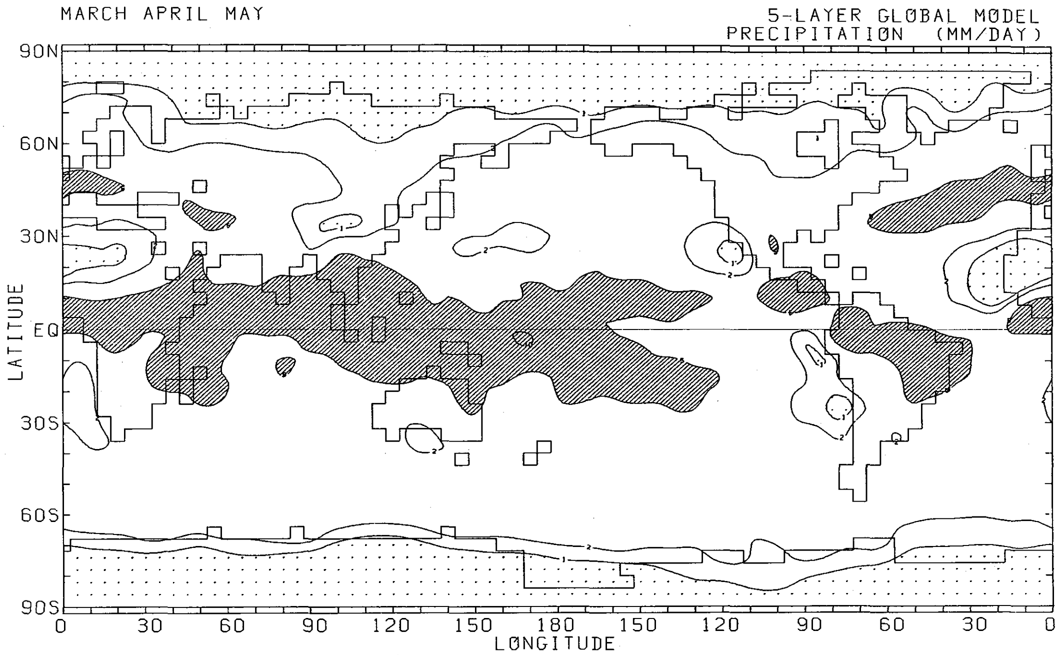

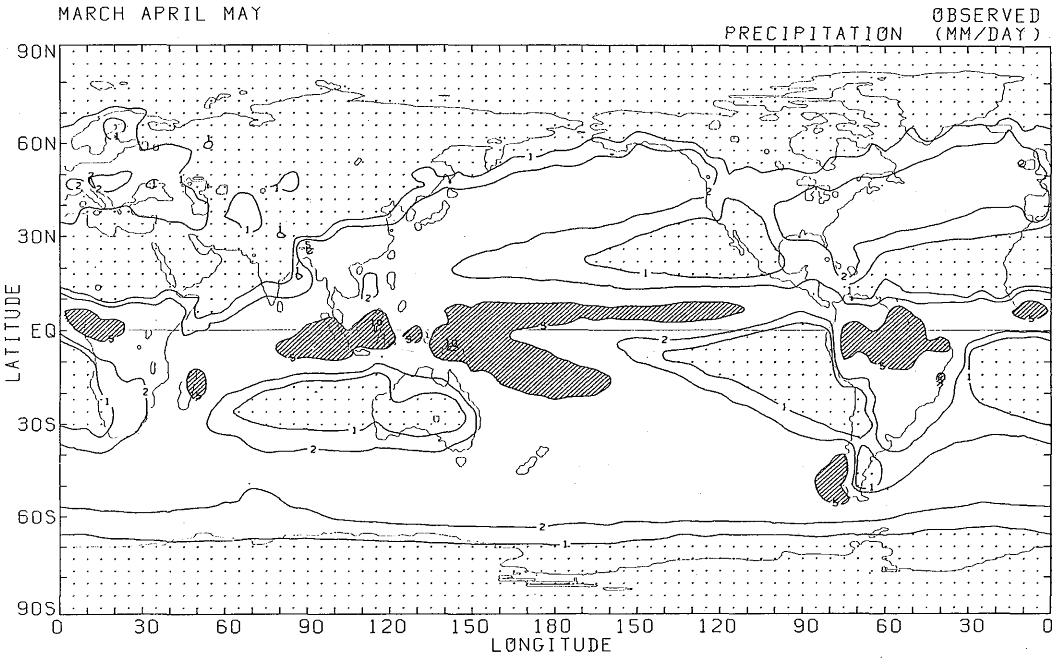

Fig. AIII.2.vi Same as in Fig. AIII.1.vi but for March, April and May.

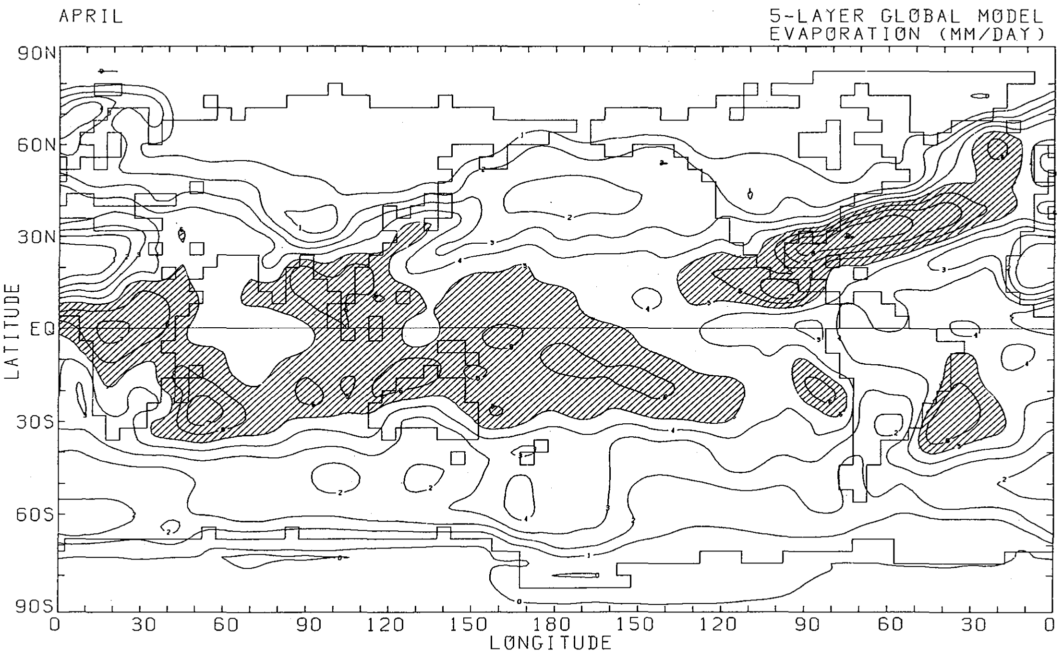

Fig. AIII.2.vii Same as in Fig. AIII.1.vii but for April.

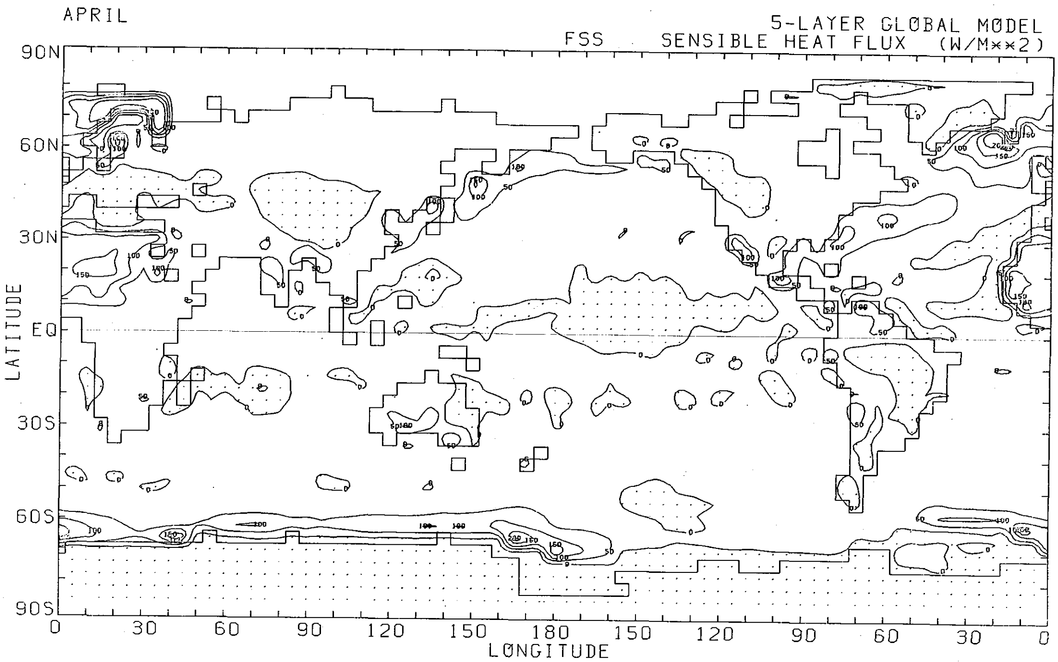

Fig. AIII.2.viii Same as in Fig. AIII.1.viii but for April.

(a)

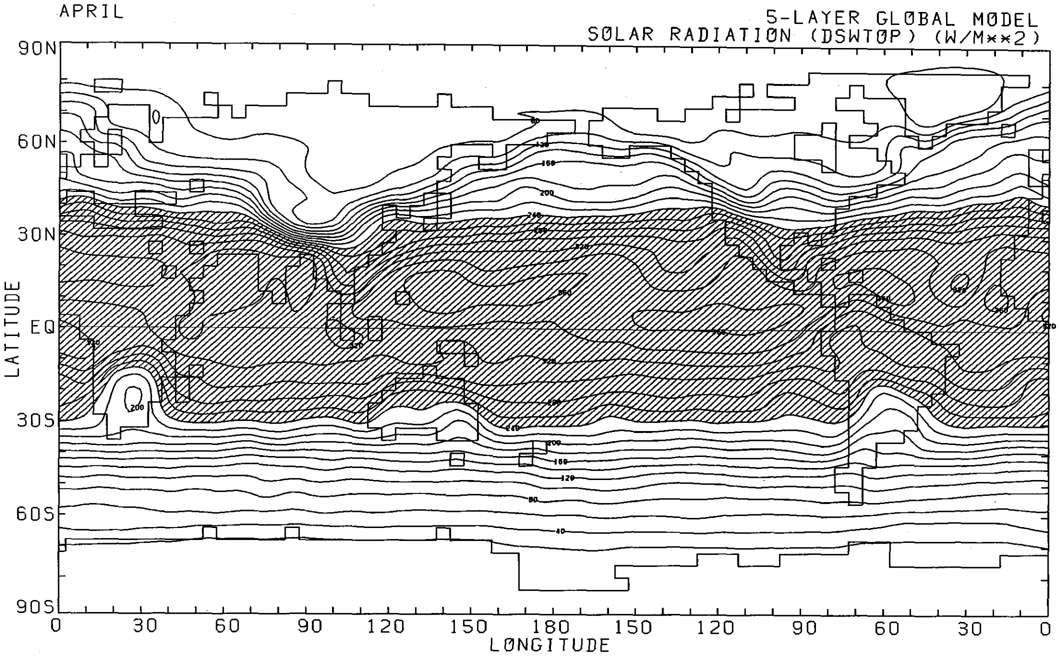

(b)

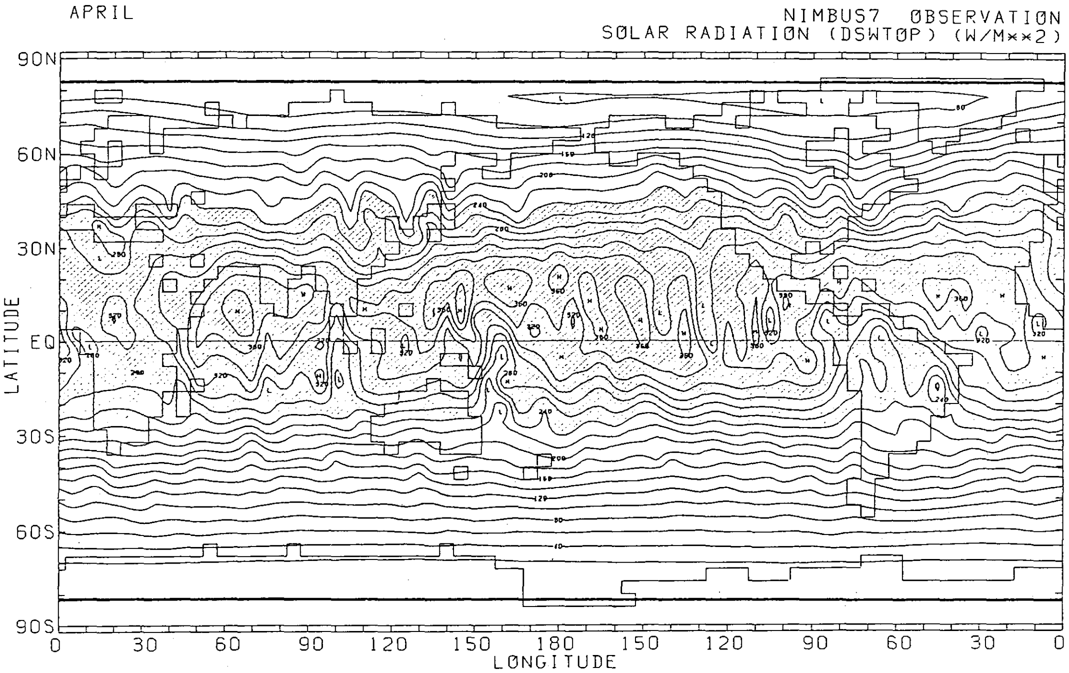

Fig. AIII.2.ix Same as in Fig. AIII.1.ix but for April.

(a)

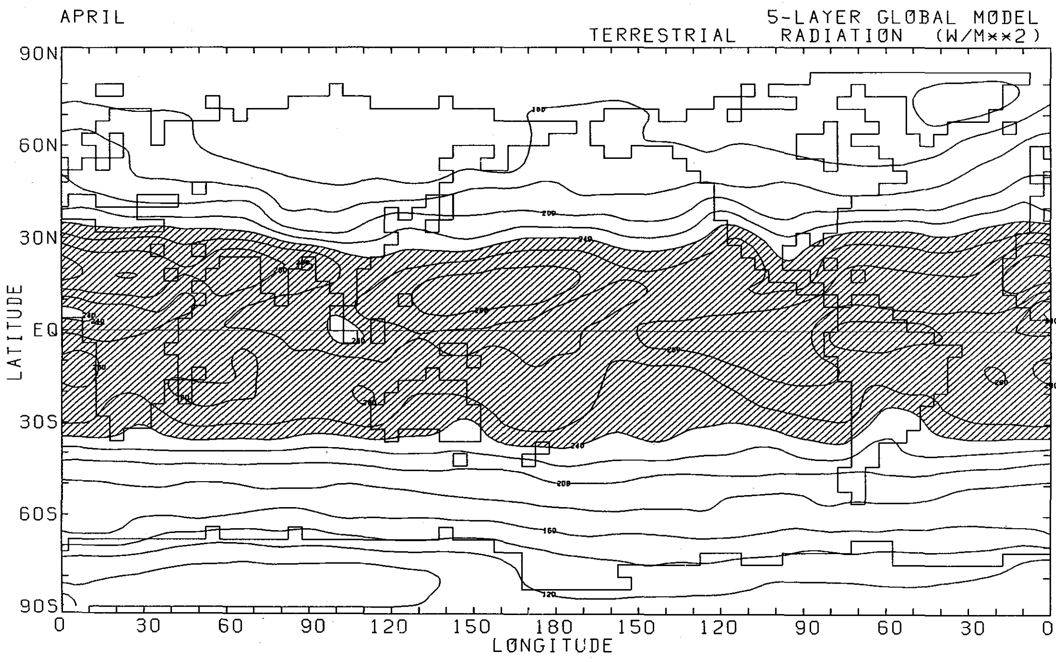

(b)

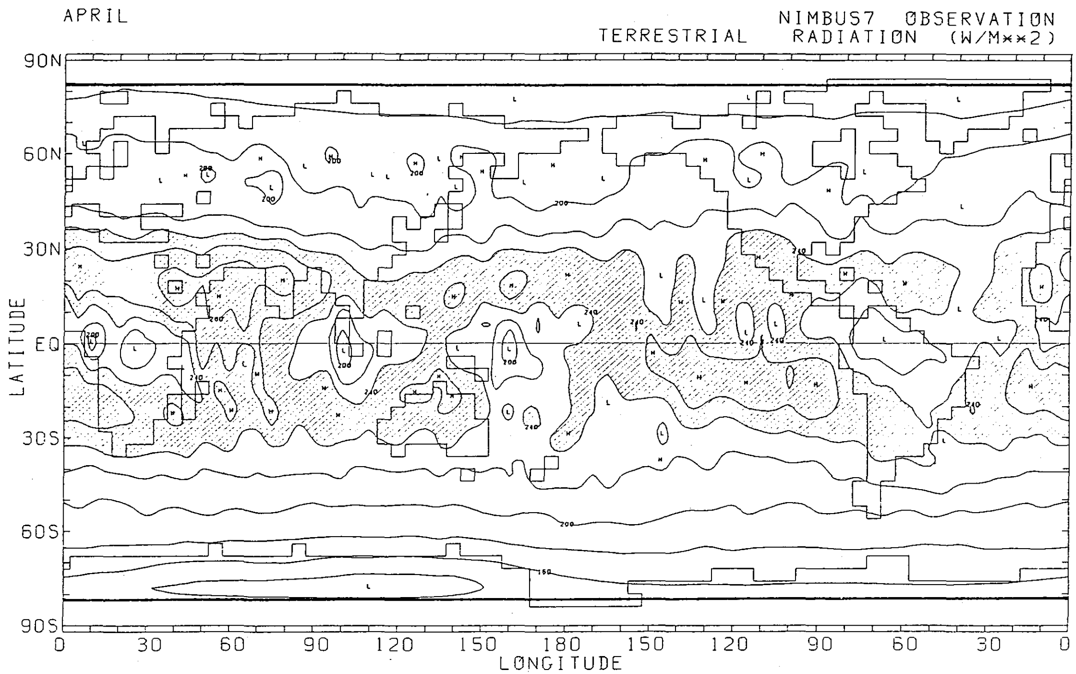

Fig. AIII.2.x Same as in Fig. AIII.1.x but for April.

(a)

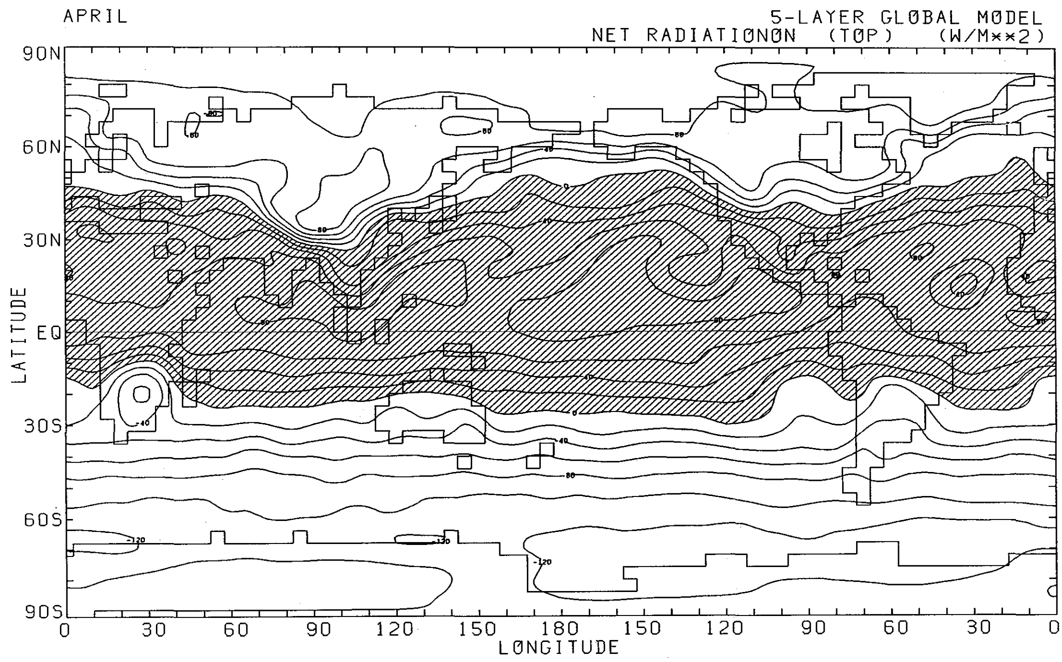

(b)

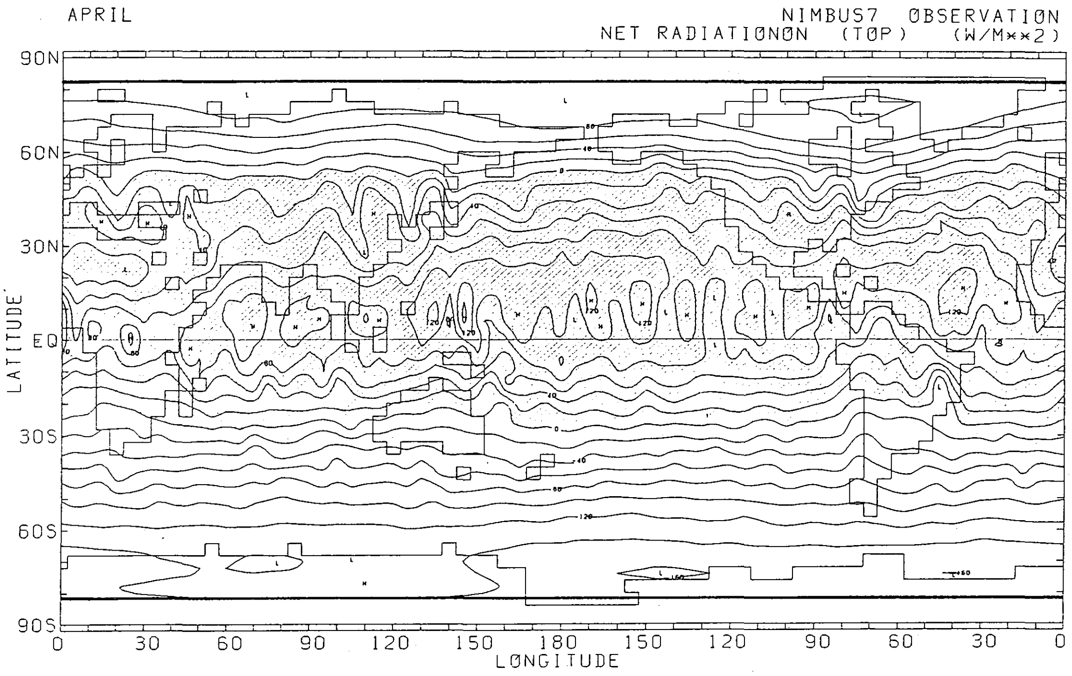

Fig. AIII.2.xi Same as in Fig. AIII.1.xi but for April.

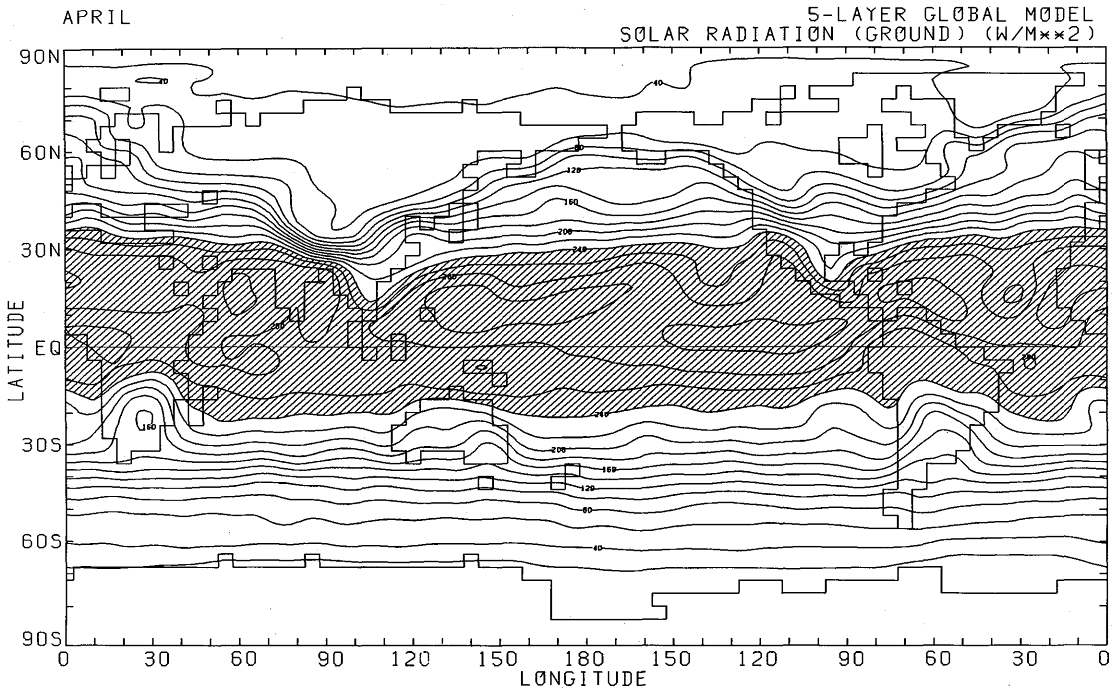

Fig. AIII.2.xii Same as in Fig. AIII.1.xii but for April.

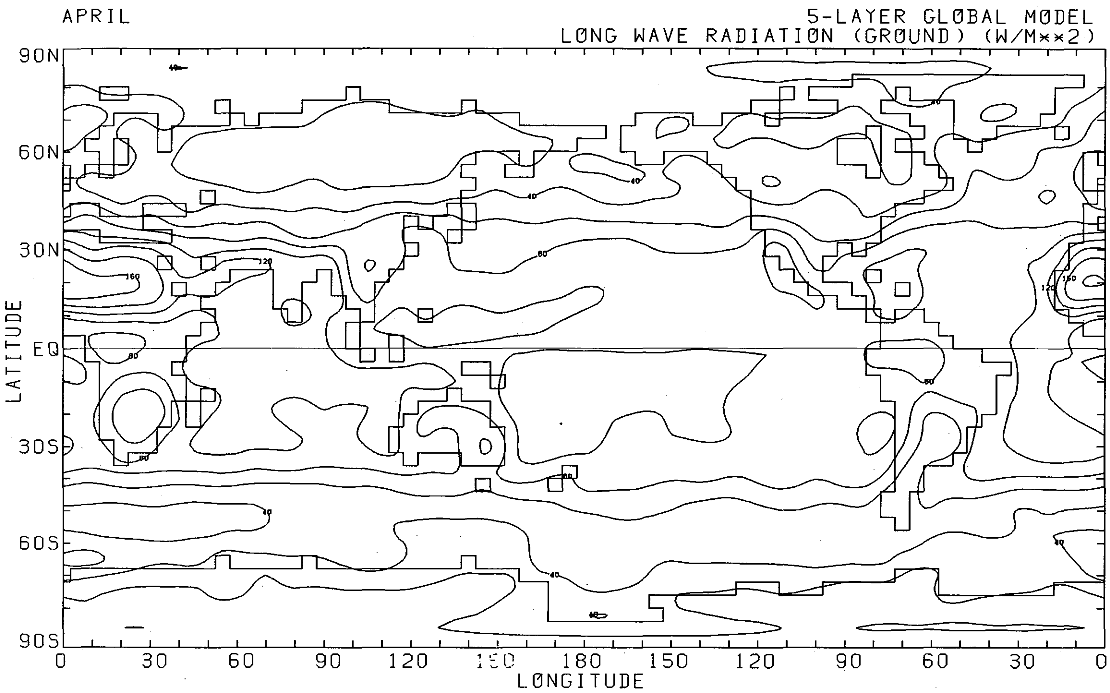

Fig. AIII.2.xiii Same as in Fig. AIII.1.xiii but for April.

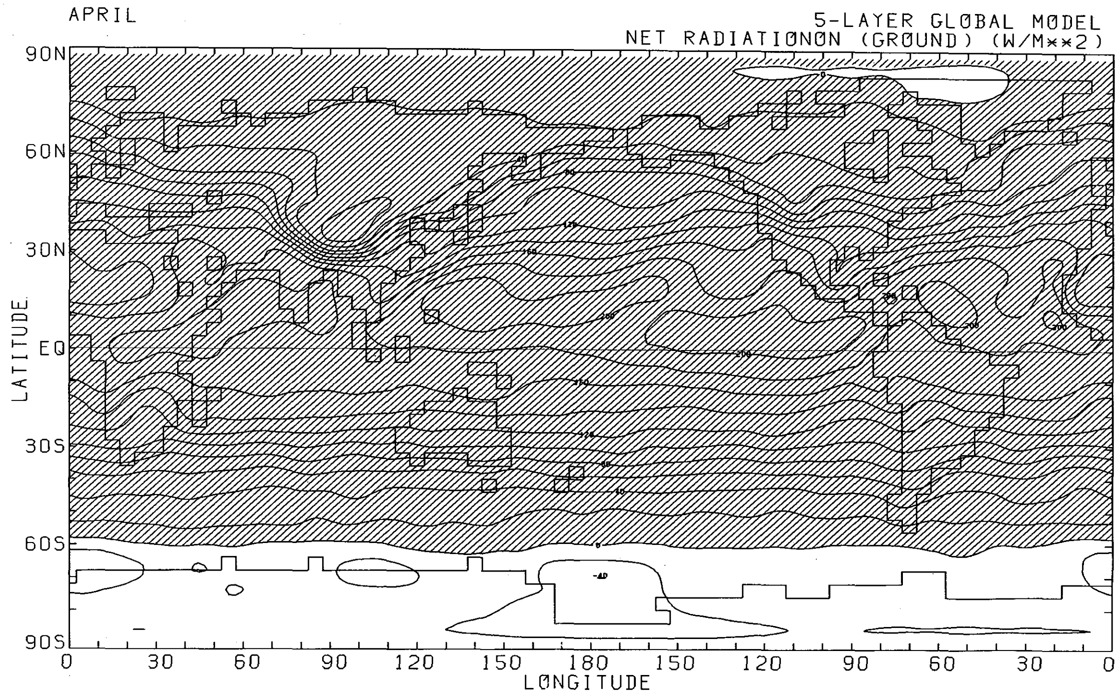

Fig. AIII.2.xiv Same as in Fig. AIII.1.xiv but for April.

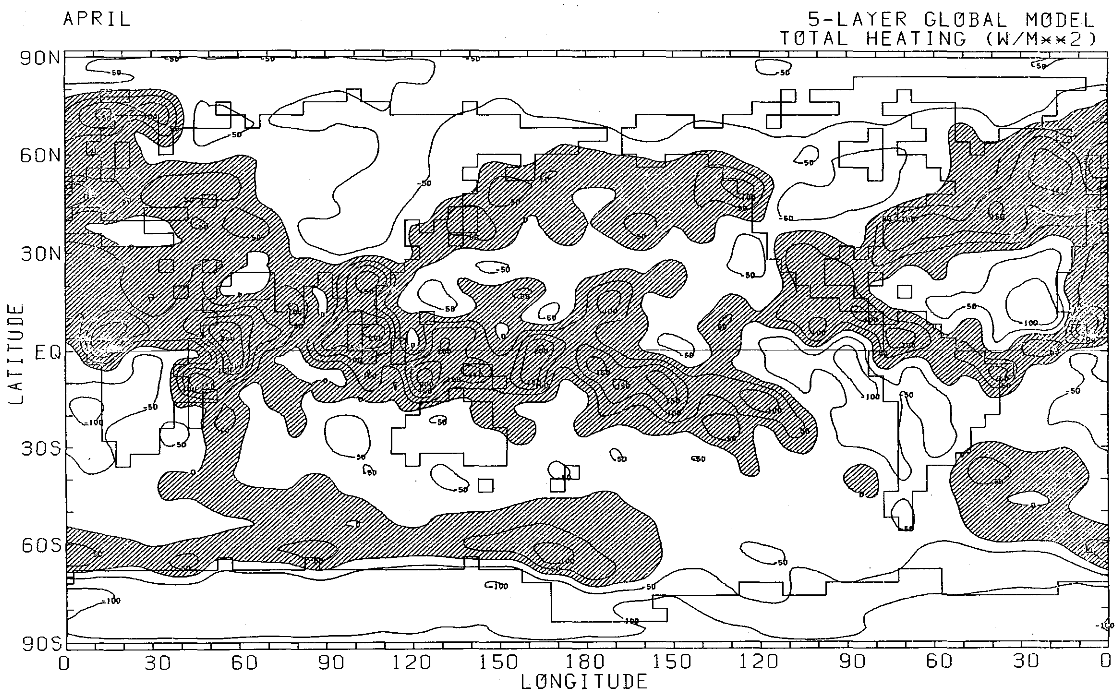

Fig. AIII.2.xv Same as in Fig. AIII.1.xv but for April.

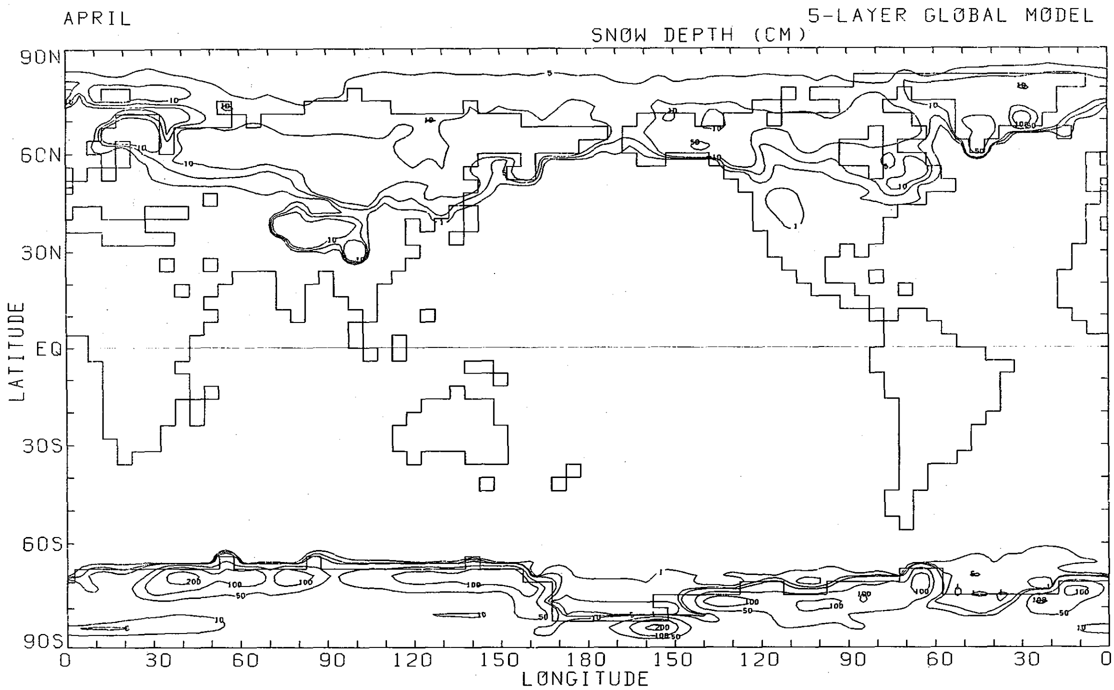

Fig. AIII.2.xvi Same as in Fig. AIII.1.xvi but for April.

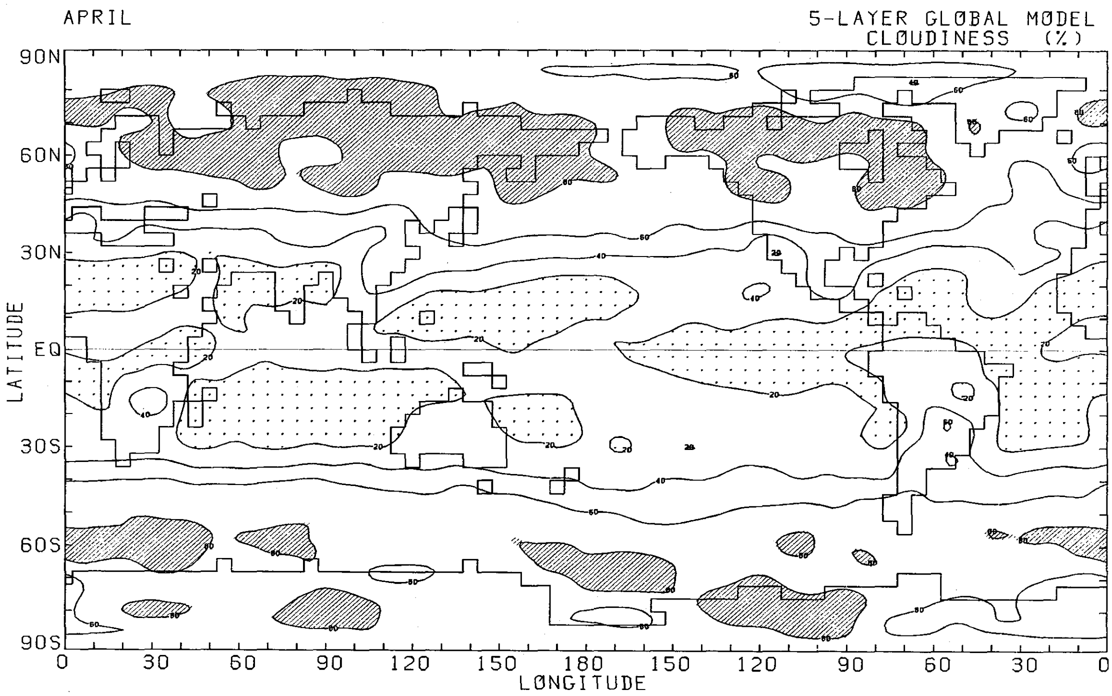

Fig. AIII.2.xvii Same as in Fig. AIII.1.xvii but for April.

(a)

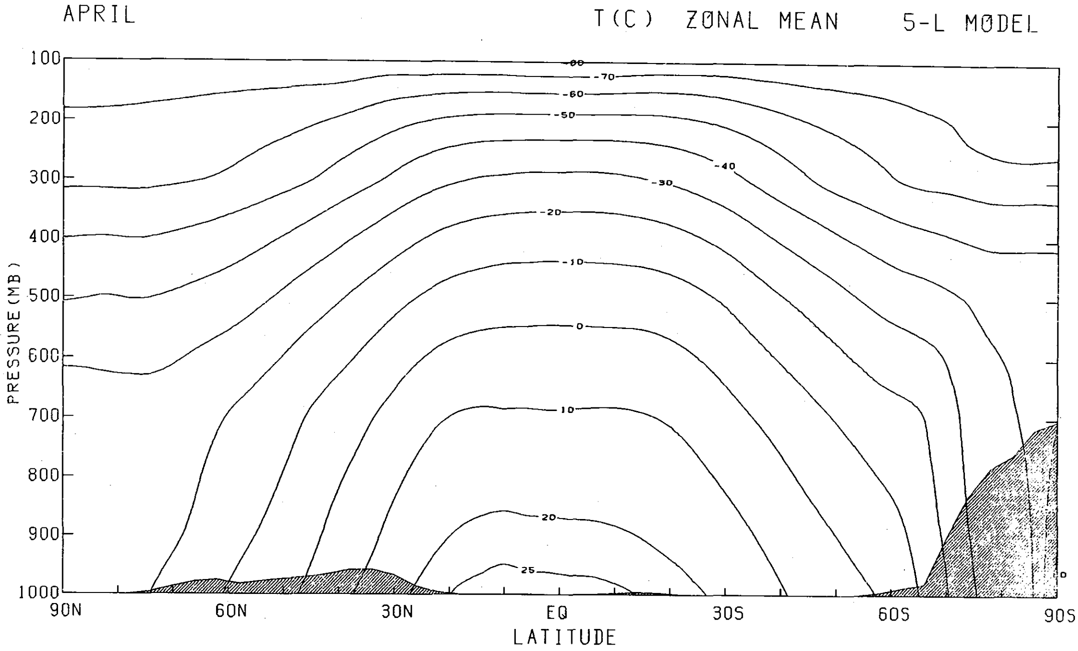

(b)

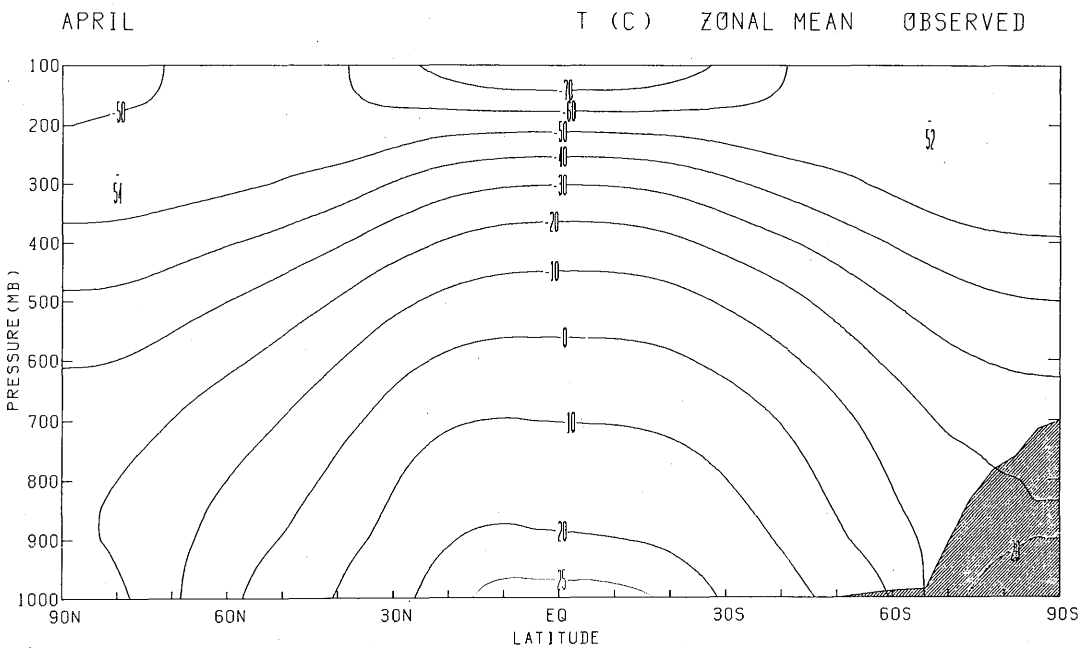

Fig. AIII.2.xviii Same as in Fig. AIII.1.xviii but for April.

(a)

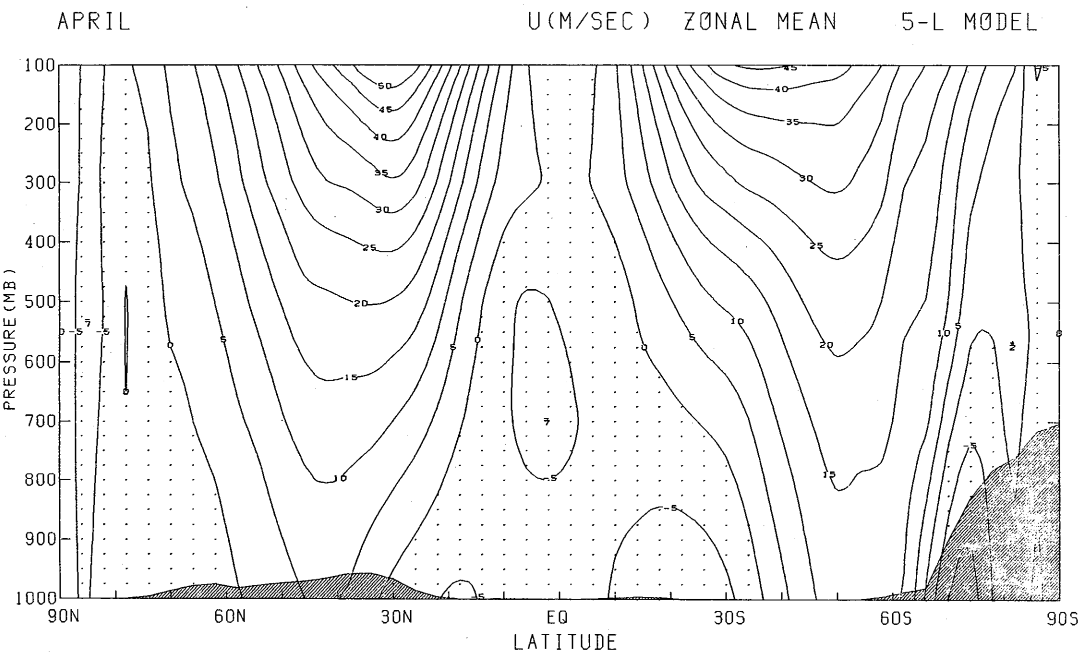

(b)

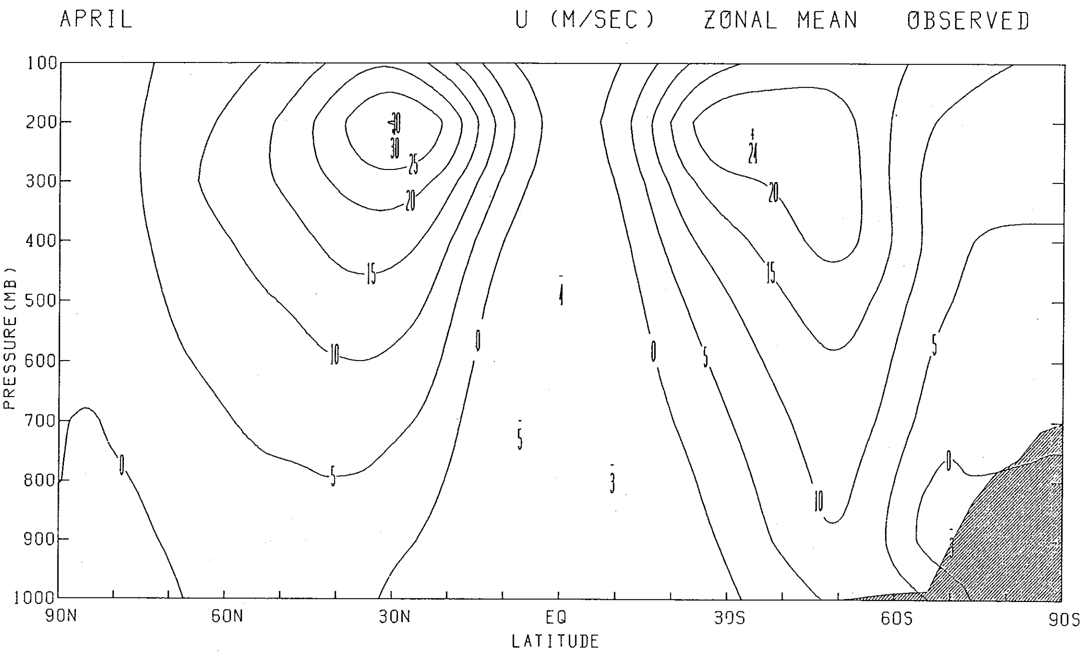

Fig. AIII.2.xix Same as in Fig. AIII.1.xix but for April.

(a)

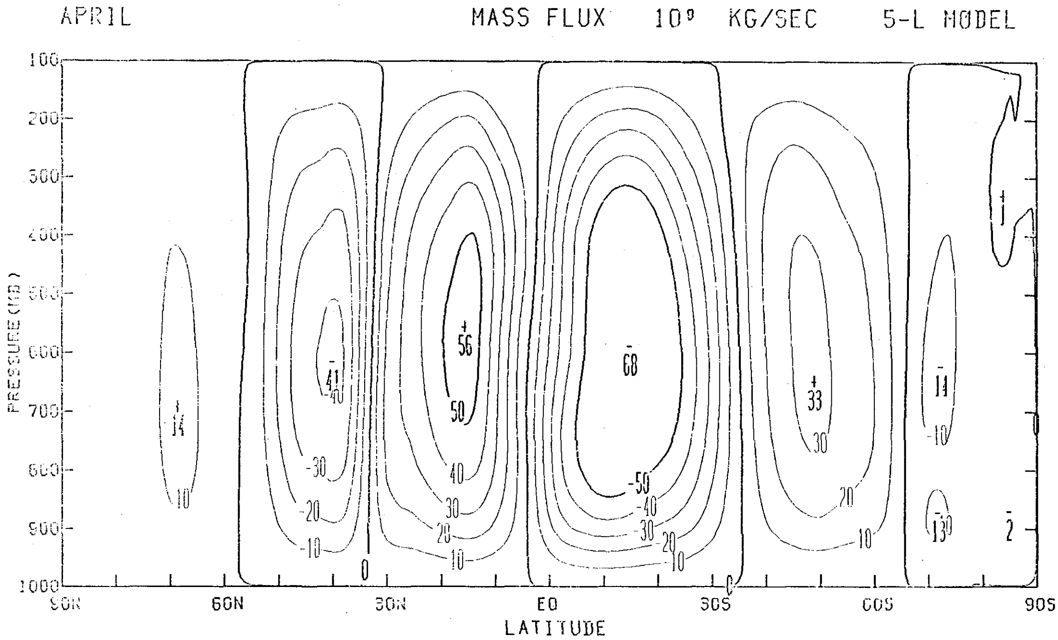

(b)

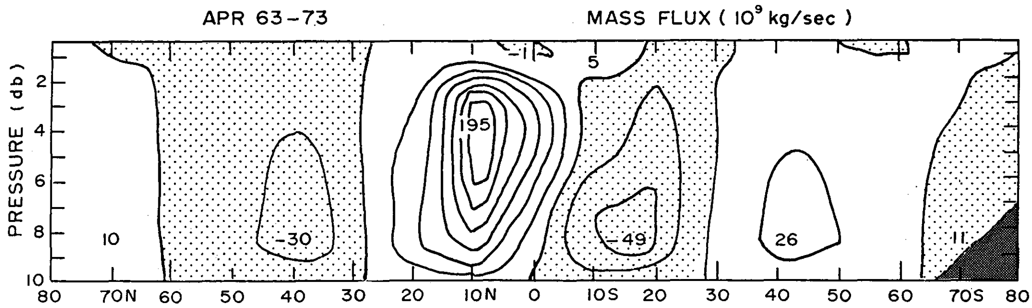

Fig. AIII.2.xx Same as in Fig. AIII.1.xx but for April.

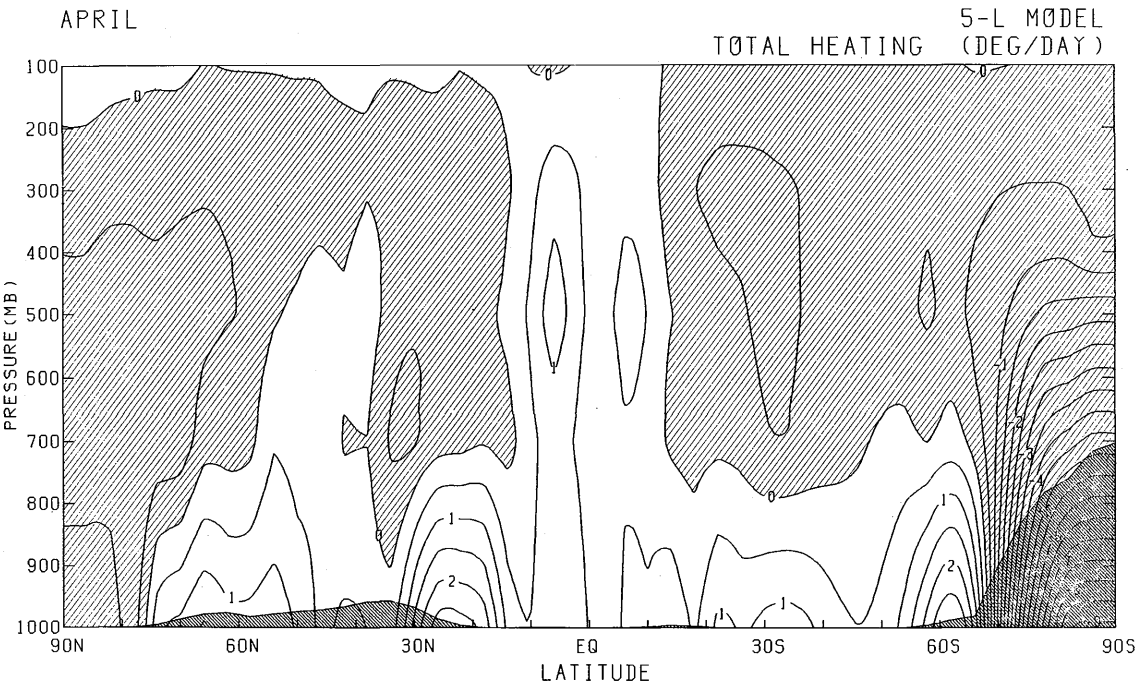

Fig. AIII.2.xxi Same as in Fig. AIII.1.xxi but for April.

(a)

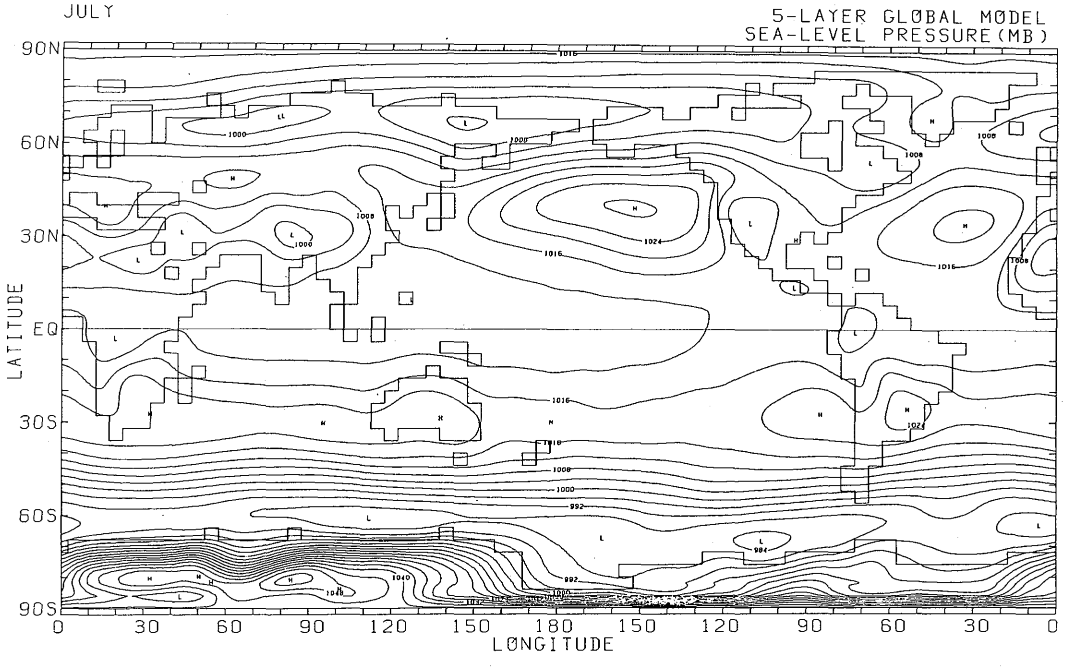

(b)

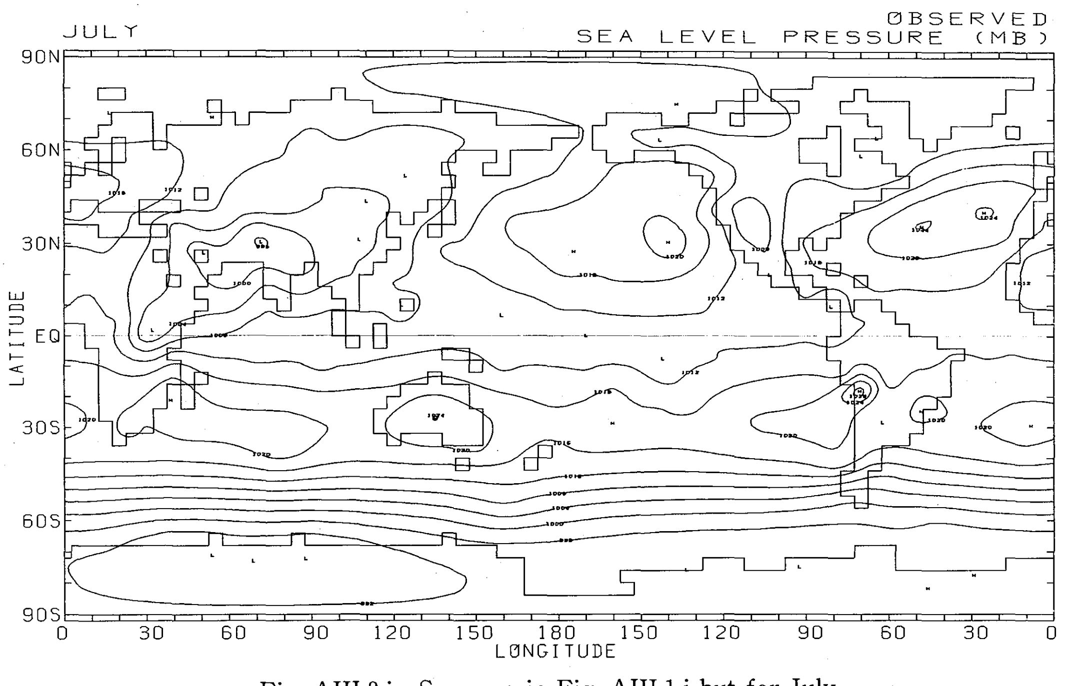

Fig. AIII.3.i Same as in Fig. AIII.1.i but for July.

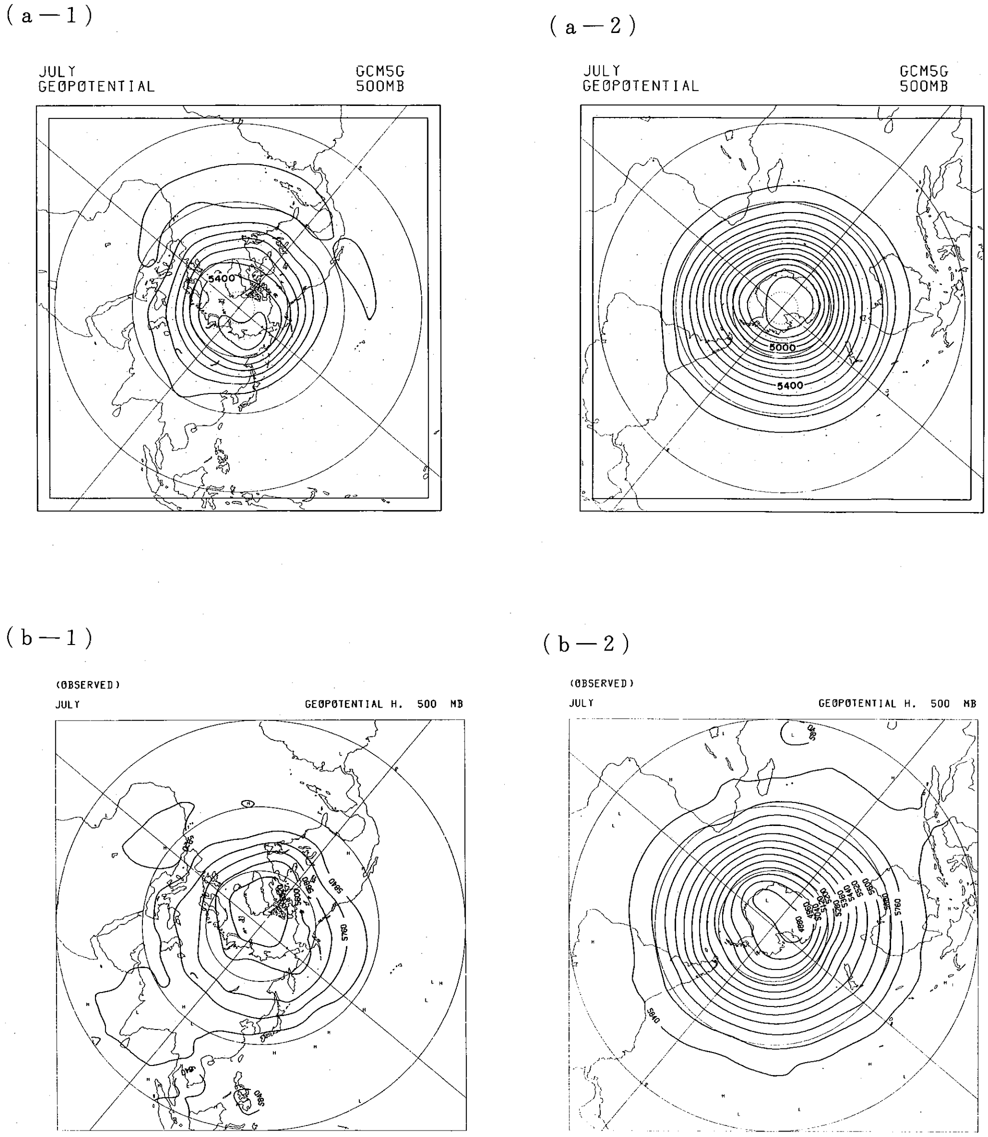

Fig. AIII.3.ii Same as in Fig. AIII.1.ii but for July.

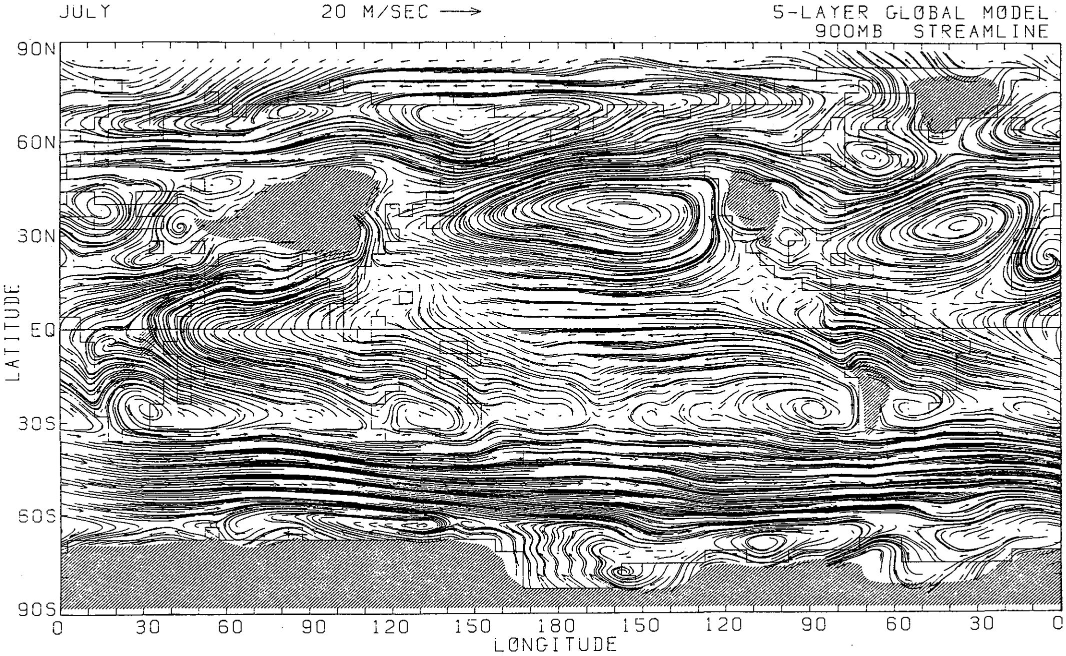

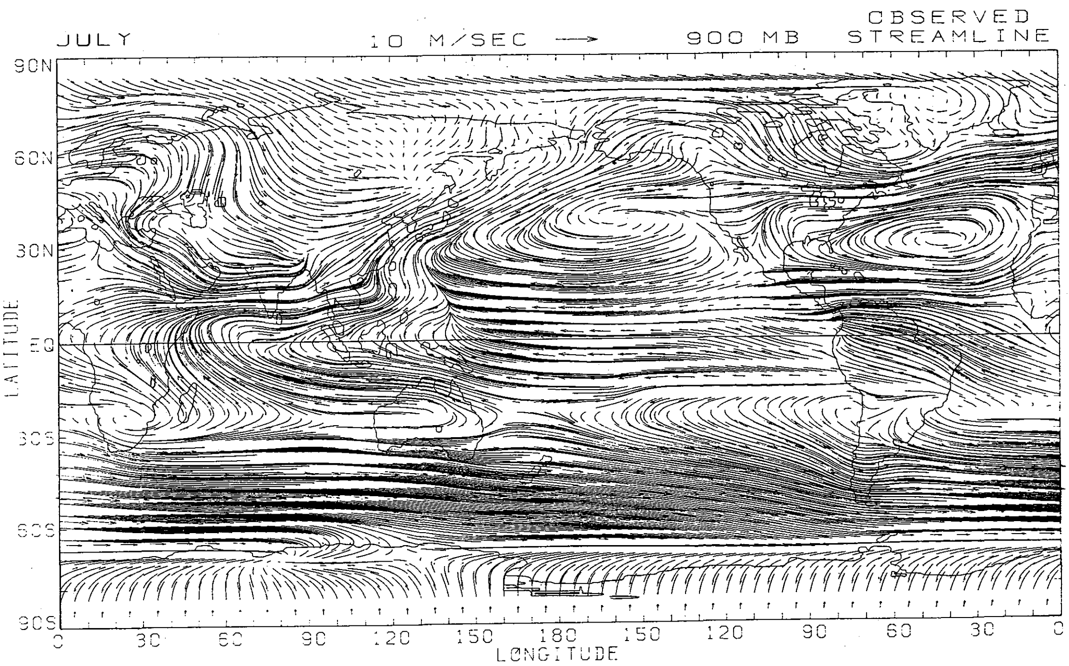

Fig. AIII.3.iii Same as in Fig. AIII.1.iii but for July.

(a)

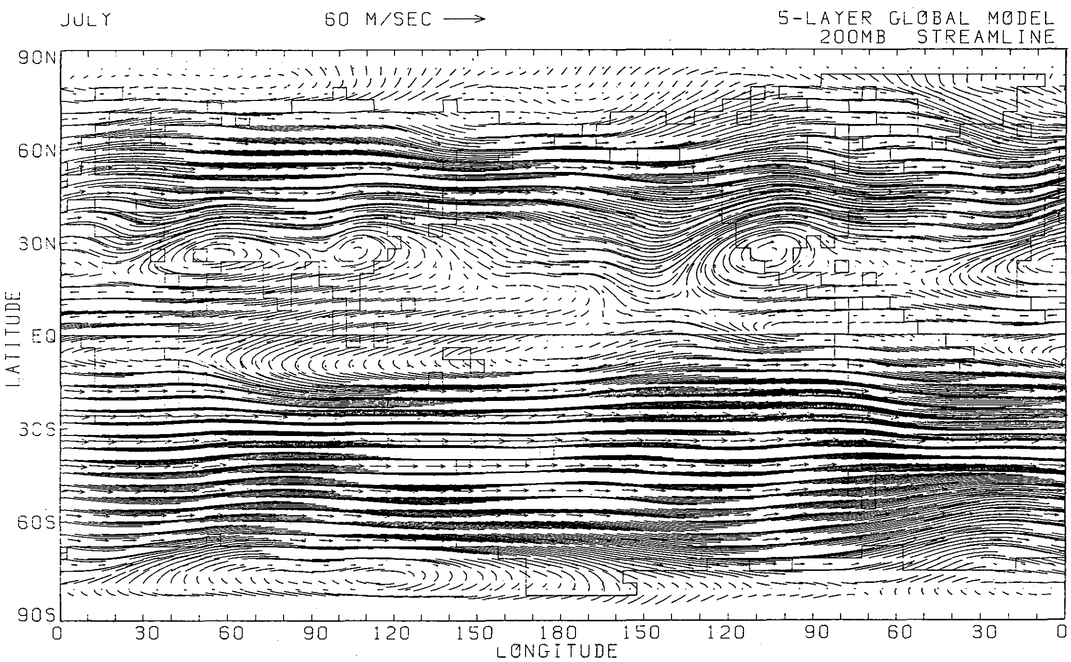

(b)

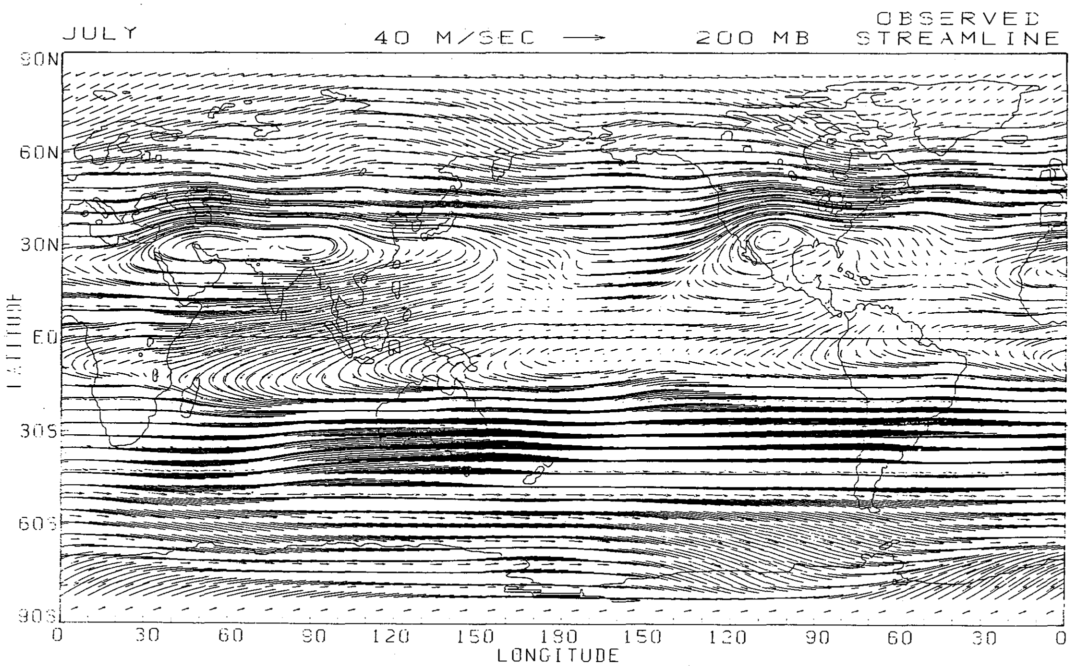

Fig. AIII.3.iv Same as in Fig. AIII.1.iv but for July.

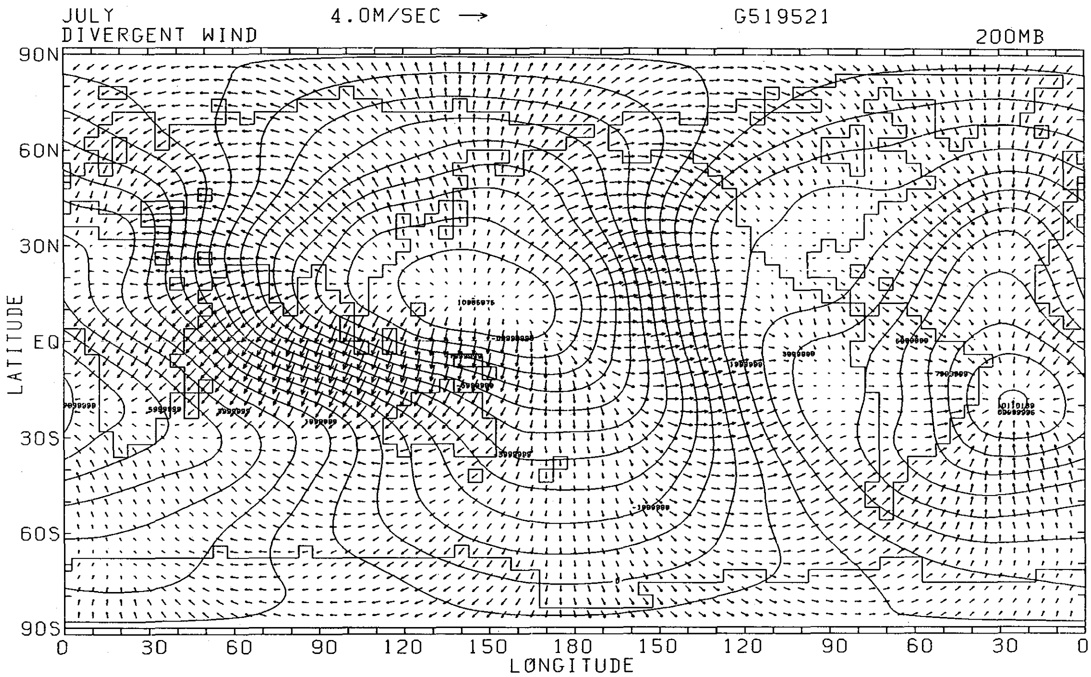

Fig. AIII.3.v Same as in Fig. AIII.1.v but for July.

(a)

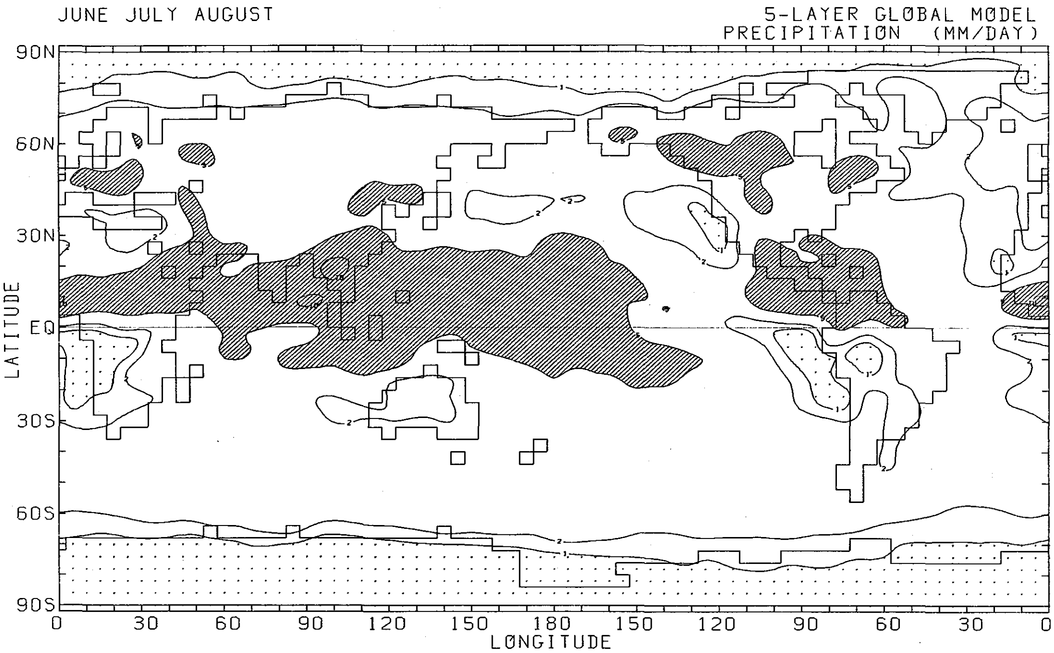

(b)

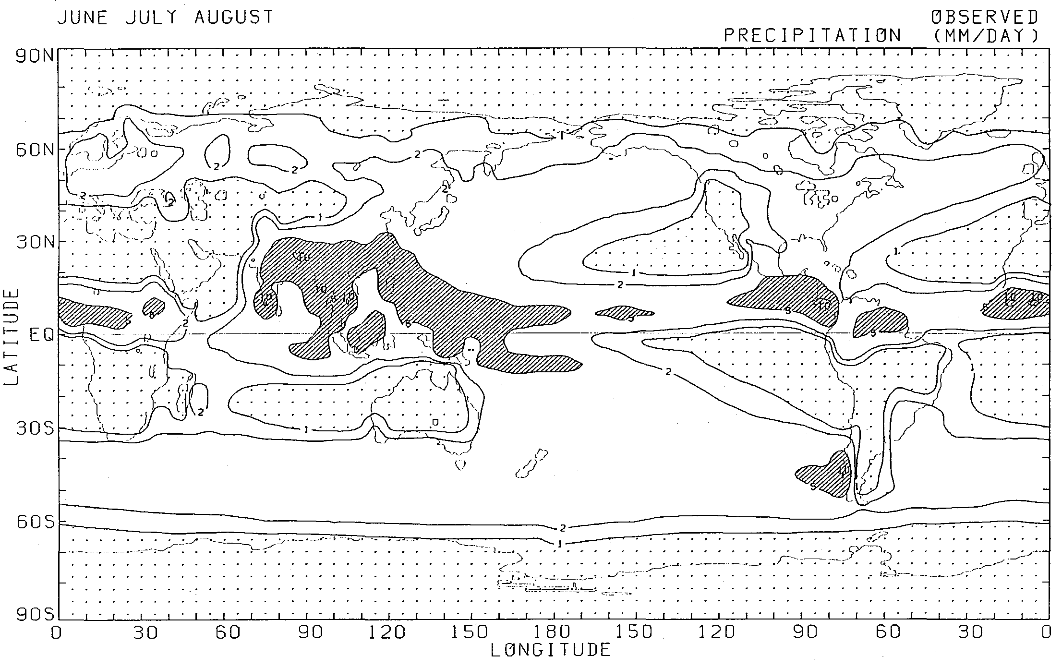

Fig. AIII.2.vi Same as in Fig. AIII.1.vi but for June, July and August.

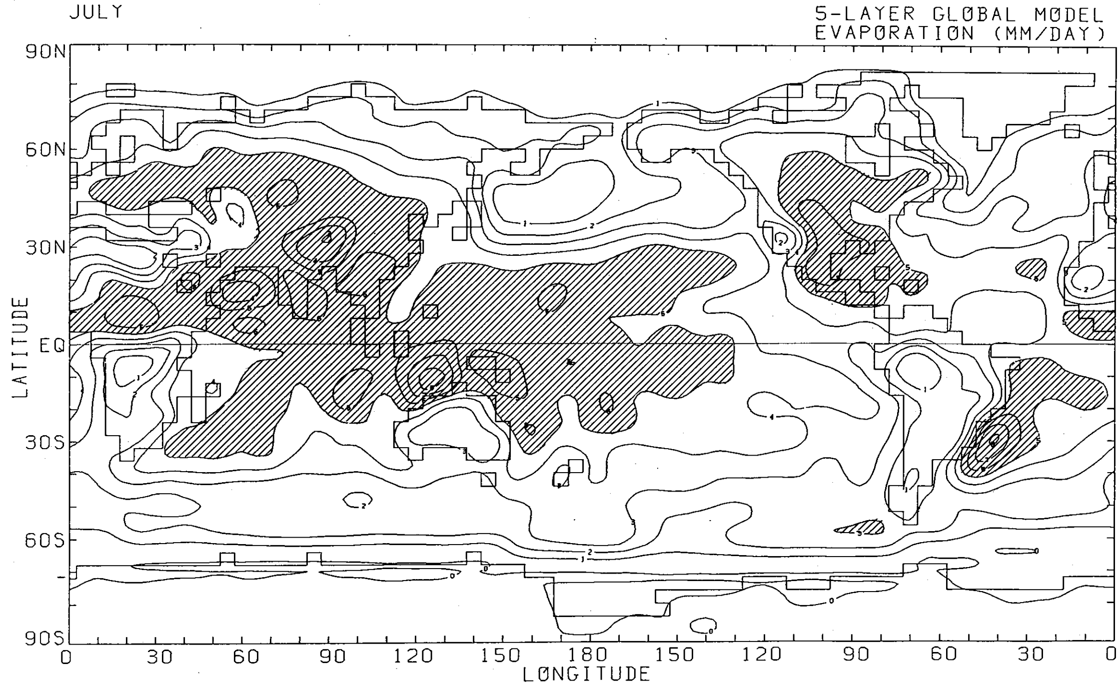

Fig. AIII.3.vii Same as in Fig. AIII.1.vii but for July.

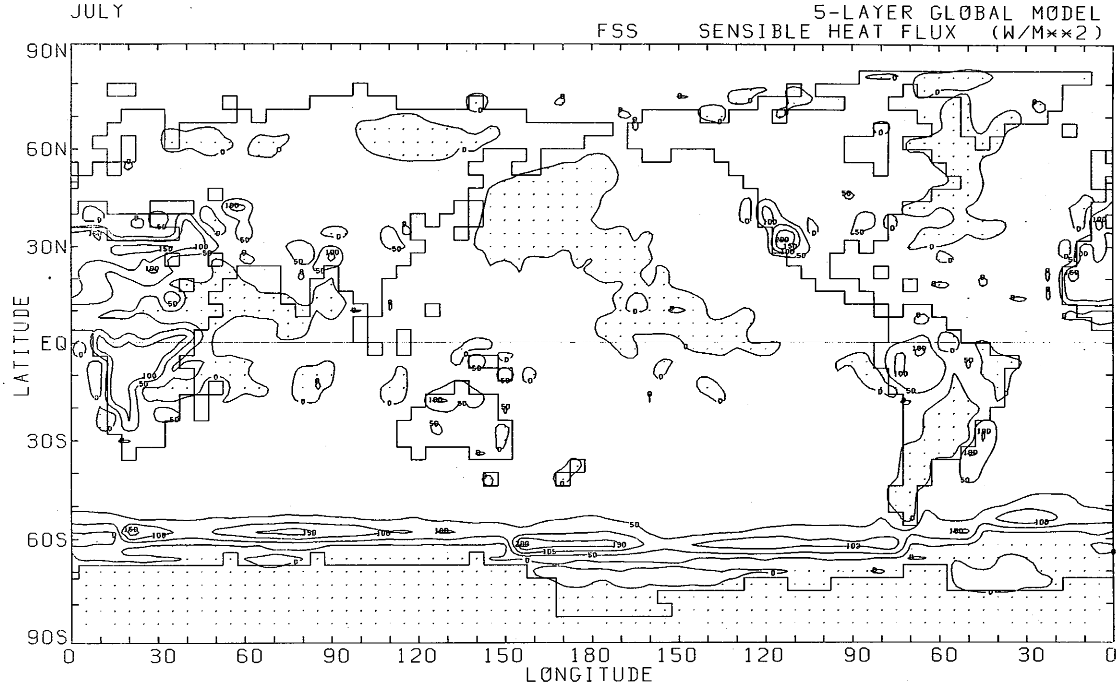

Fig. AIII.3.viii Same as in Fig. AIII.1.viii but for July.

(a)

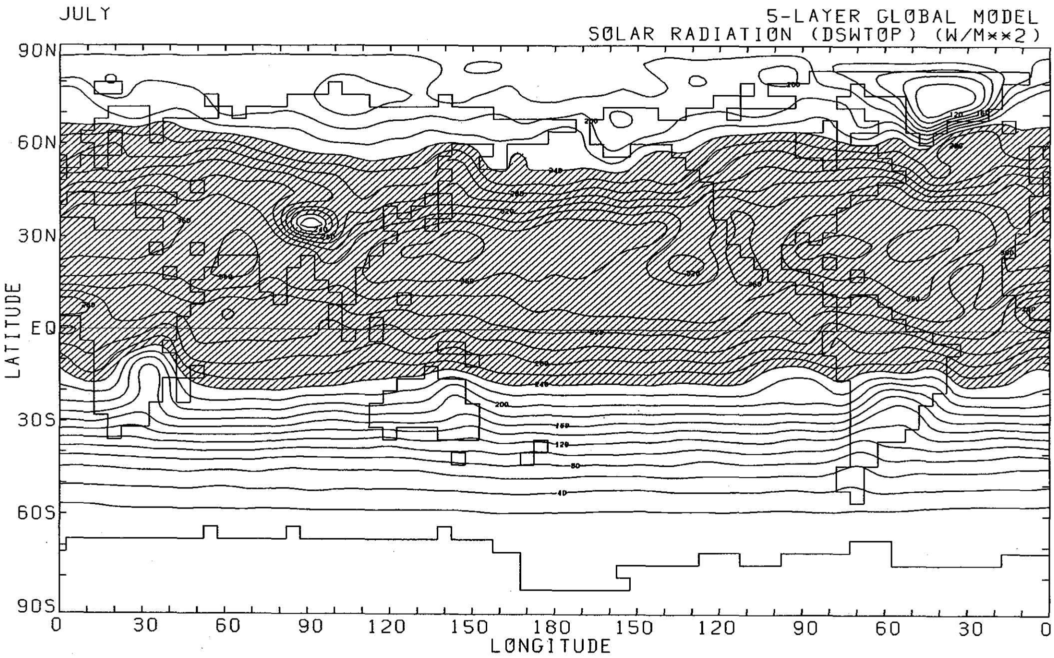

(b)

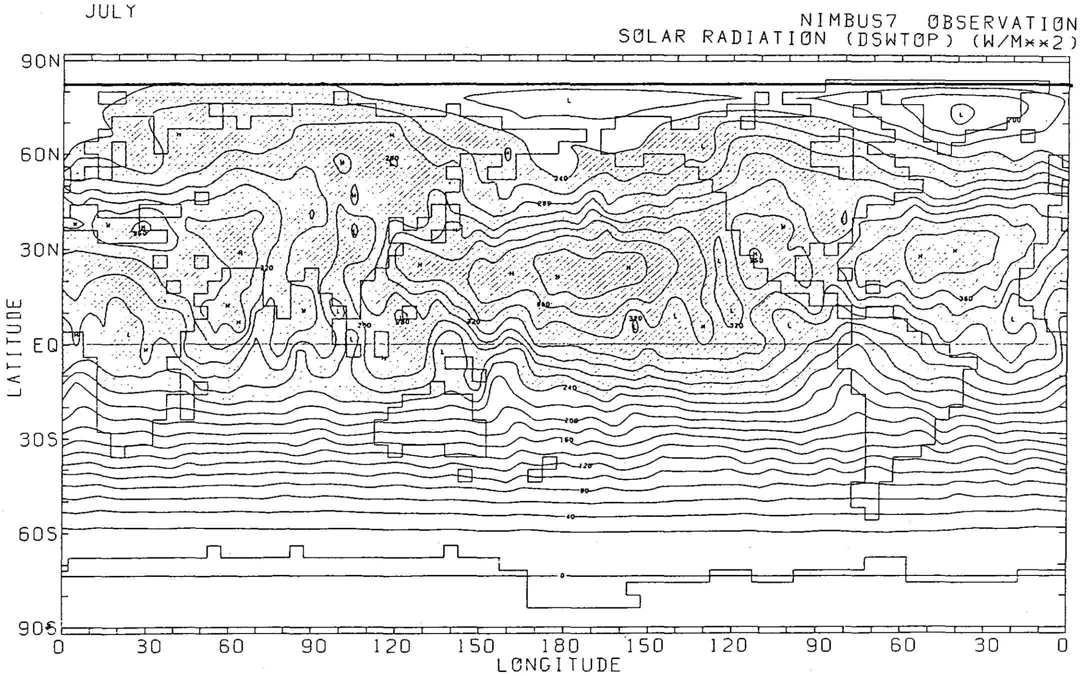

Fig. AIII.3.ix Same as in Fig. AIII.1.ix but for July.

(a)

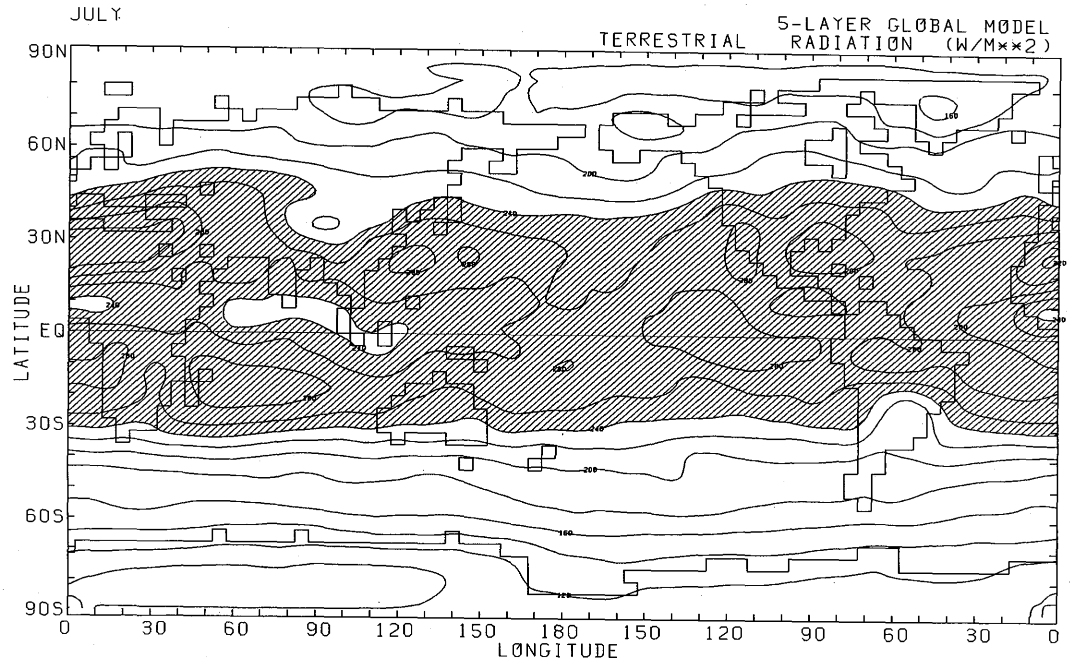

(b)

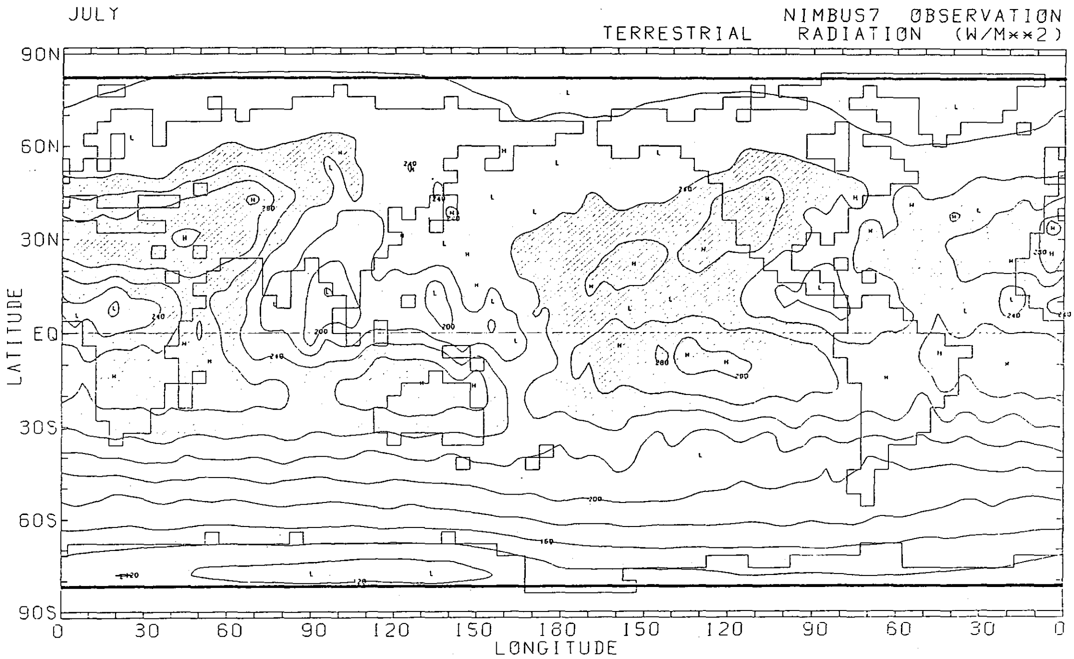

Fig. AIII.3.x Same as in Fig. AIII.1.x but for July.

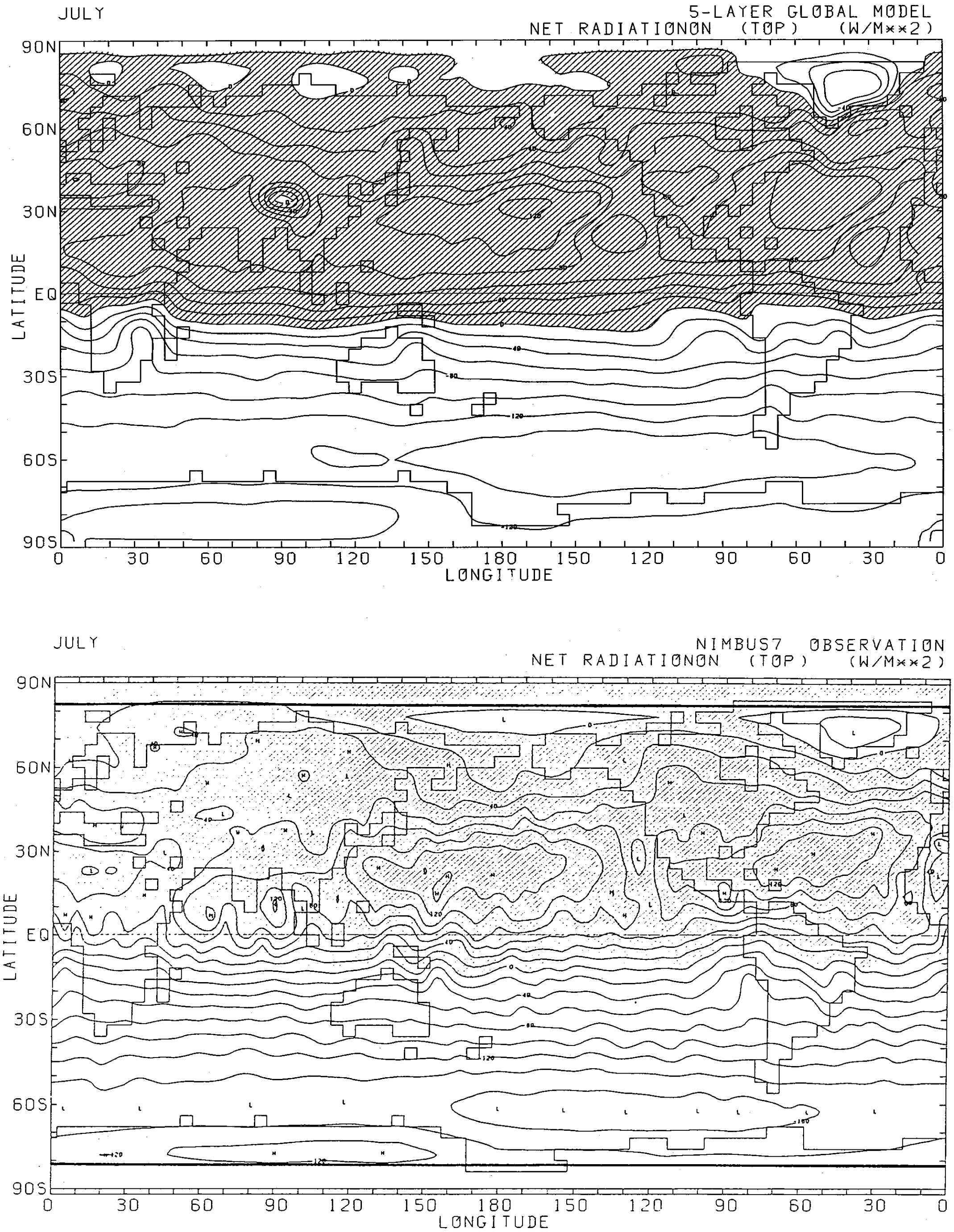

Fig. AIII.3.xi Same as in Fig. AIII.1.xi but for July.

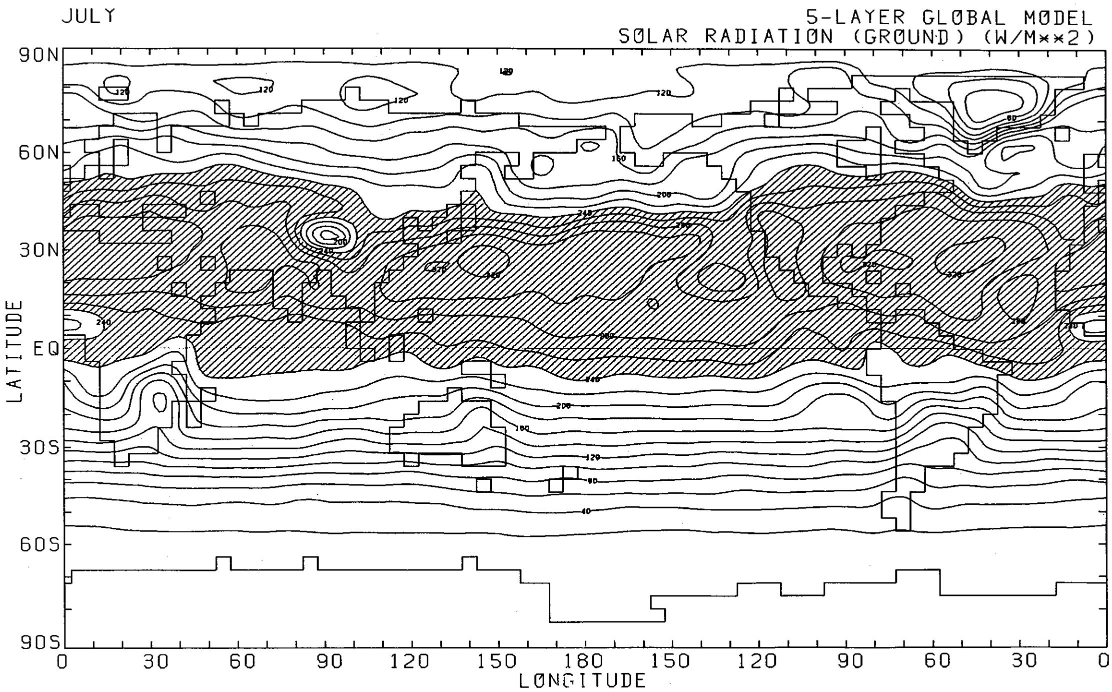

Fig. AIII.3.xii Same as in Fig. AIII.1.xii but for July.

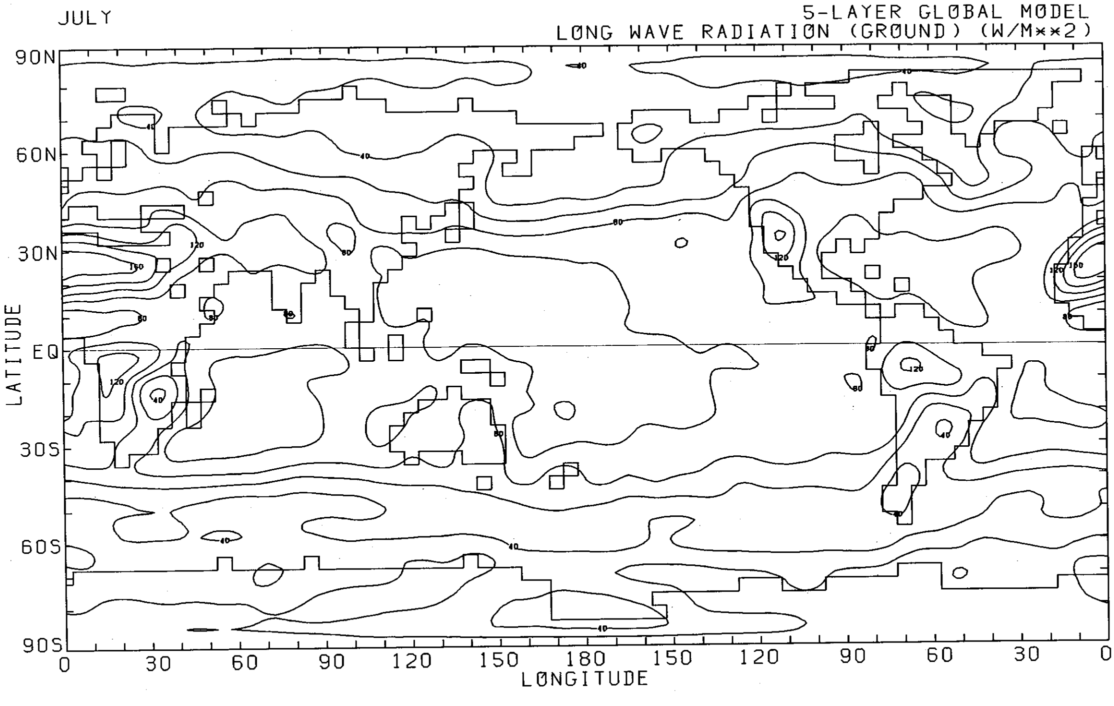

Fig. AIII.3.xiii Same as in Fig. AIII.1.xiii but for July.

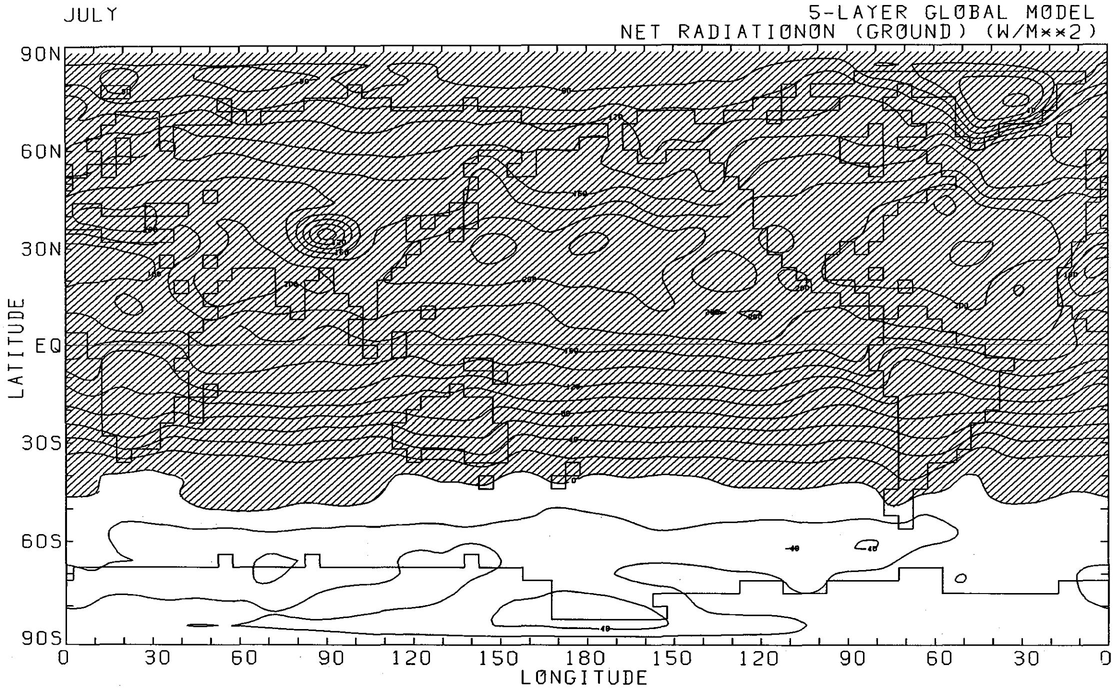

Fig. AIII.3.xiv Same as in Fig. AIII.1.xiv but for July.

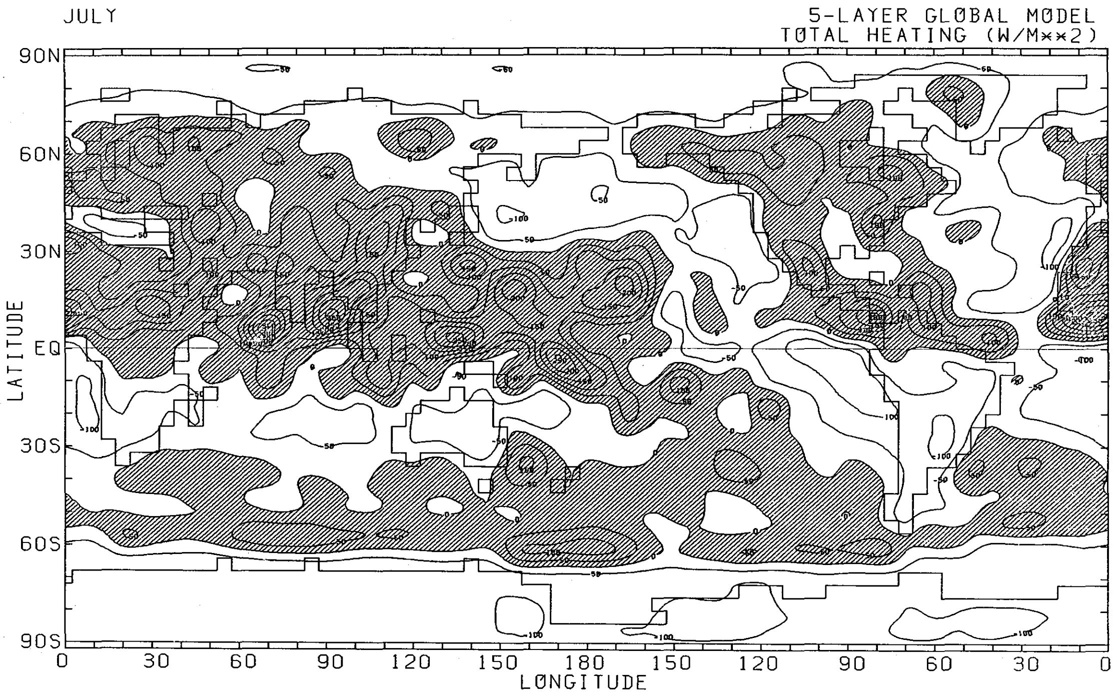

Fig. AIII.3.xv Same as in Fig. AIII.1.xv but for July.

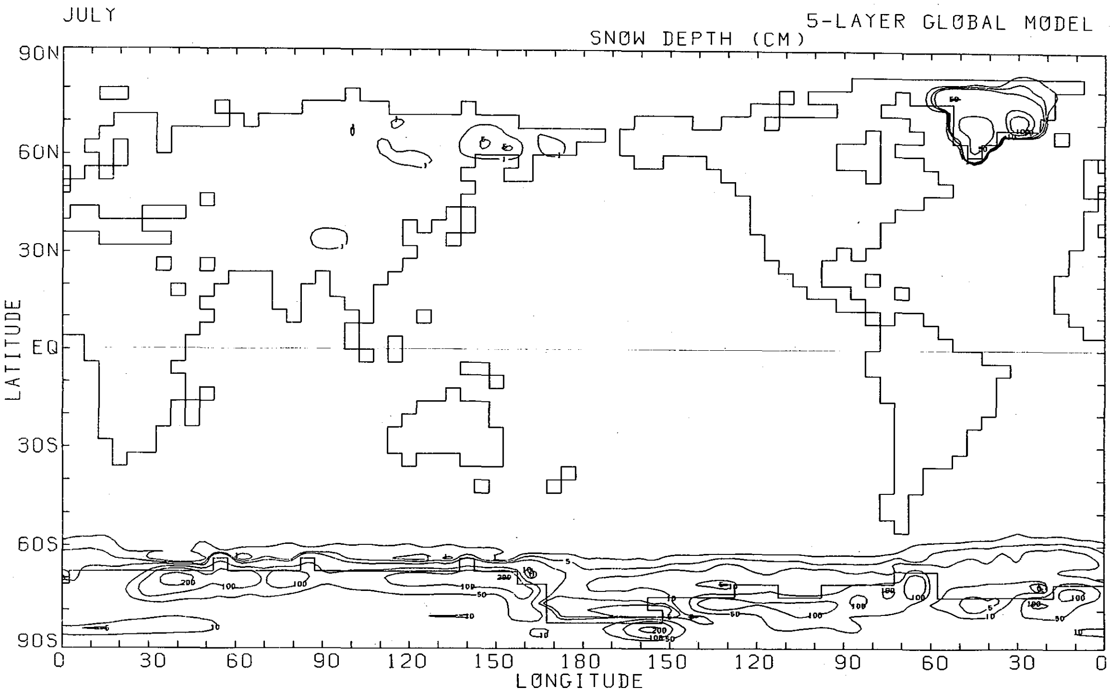

Fig. AIII.3.xvi Same as in Fig. AIII.1.xvi but for July.

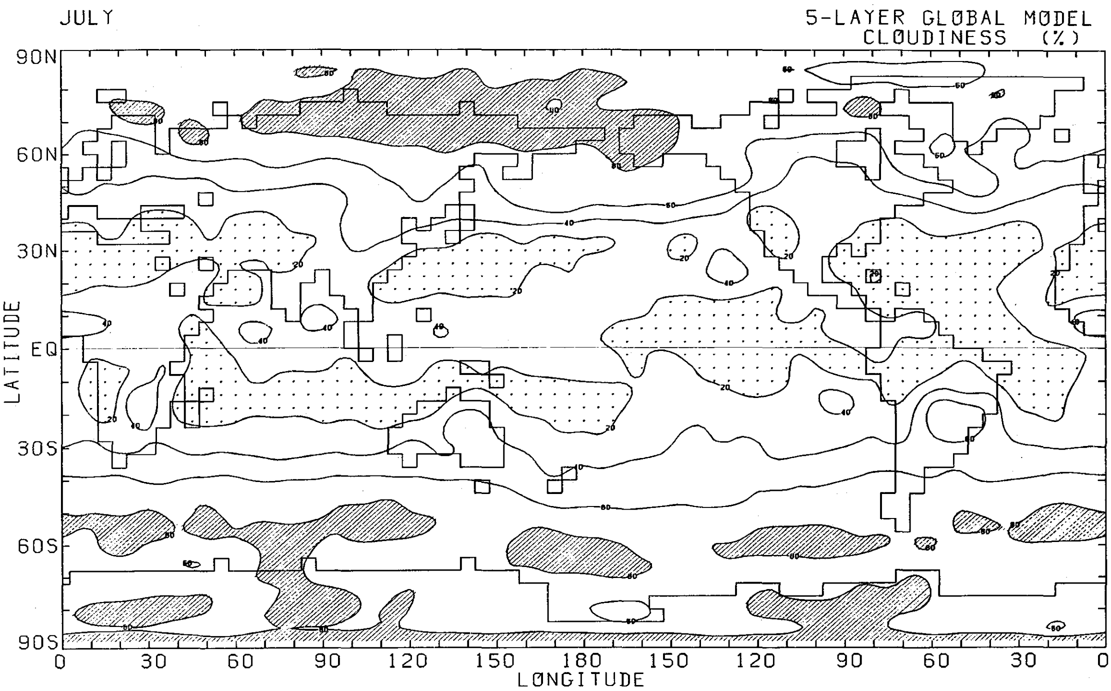

Fig. AIII.3.xvii Same as in Fig. AIII.1.xvii but for July.

(a)

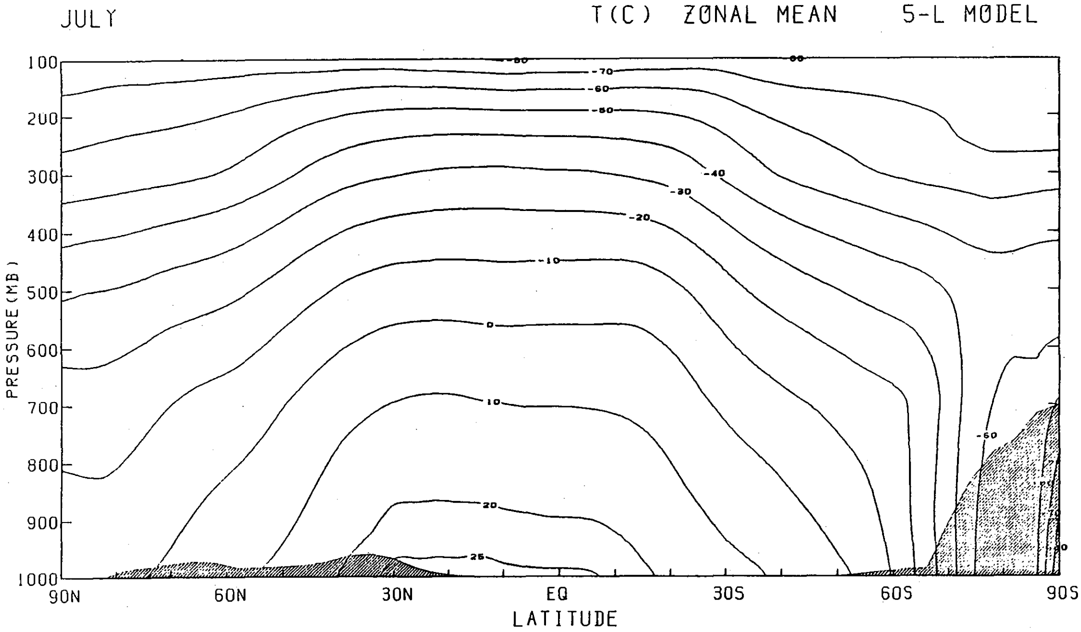

(b)

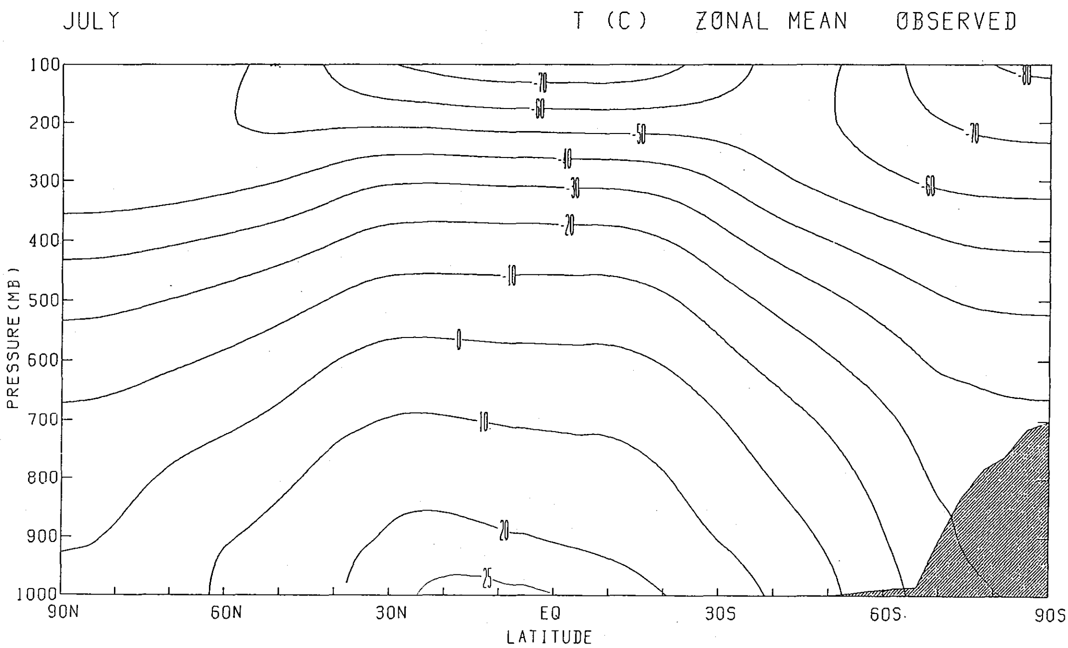

Fig. AIII.3.xviii Same as in Fig. AIII.1.xviii but for July.

(a)

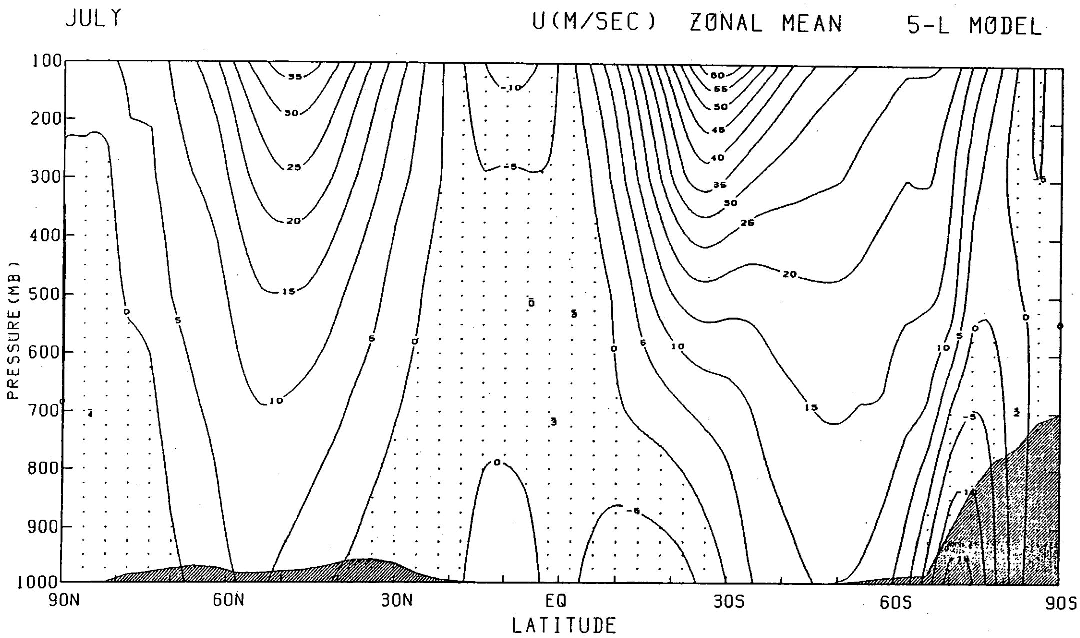

(b)

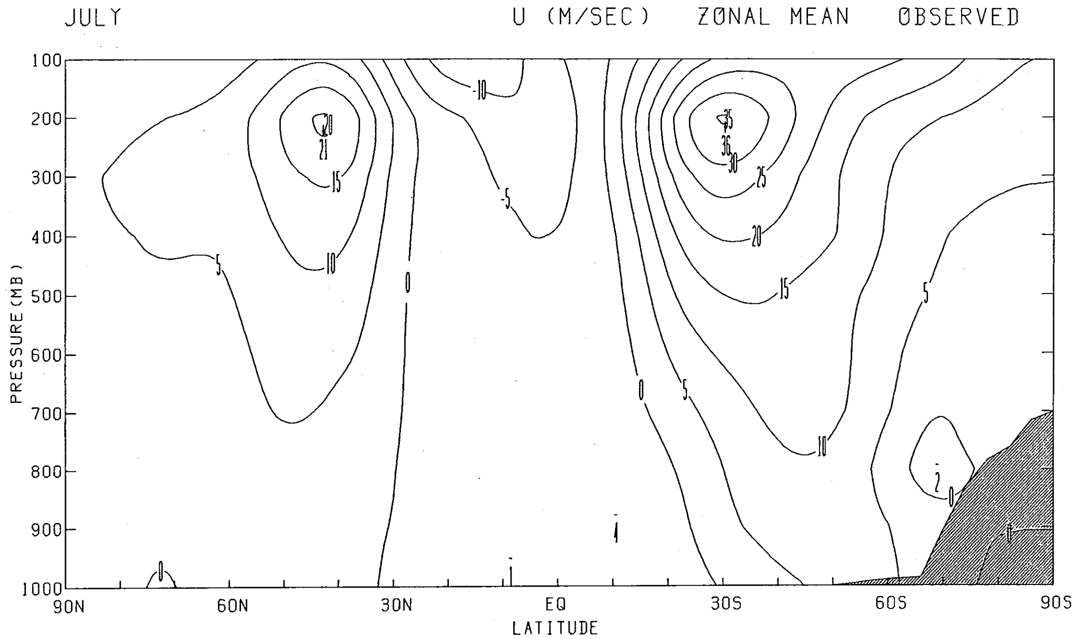

Fig. AIII.3.xix Same as in Fig. AIII.1.xix but for July.

(a)

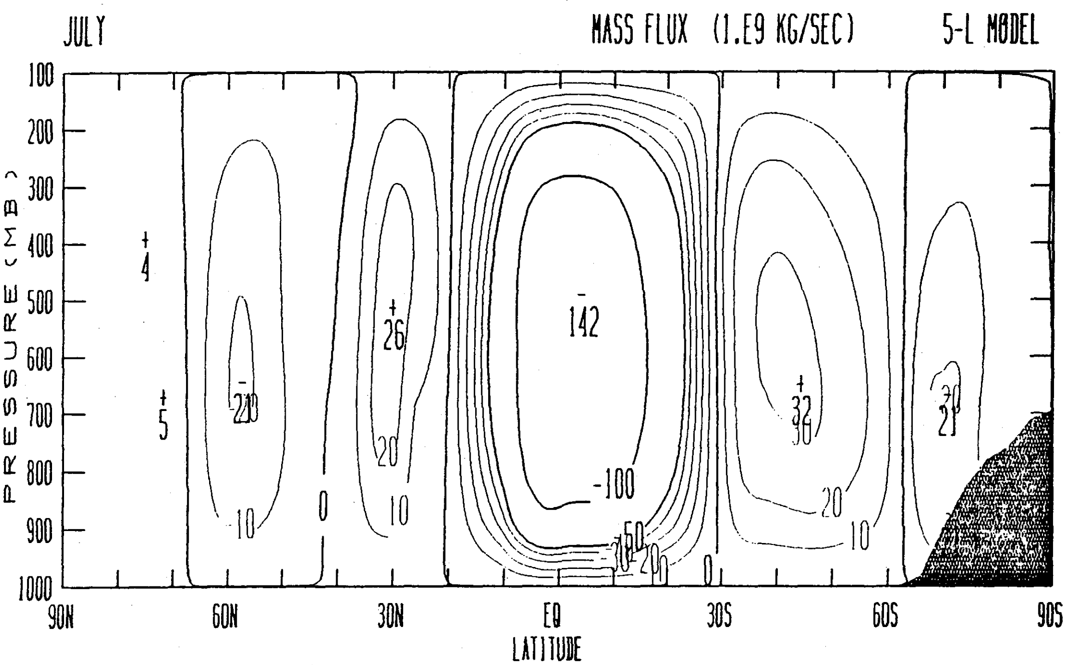

(b)

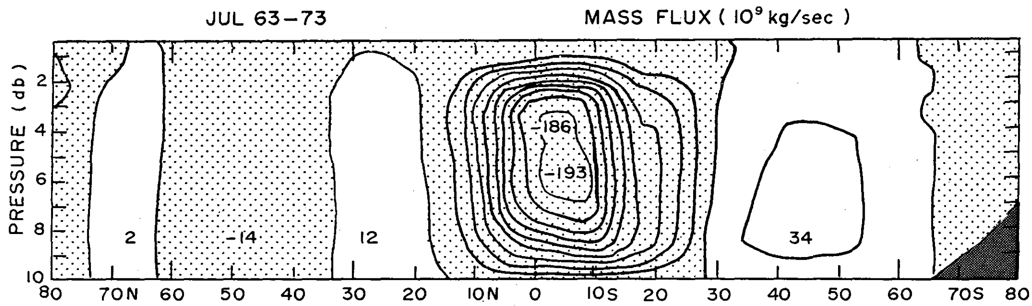

Fig. AIII.3.xx Same as in Fig. AIII.1.xx but for July.

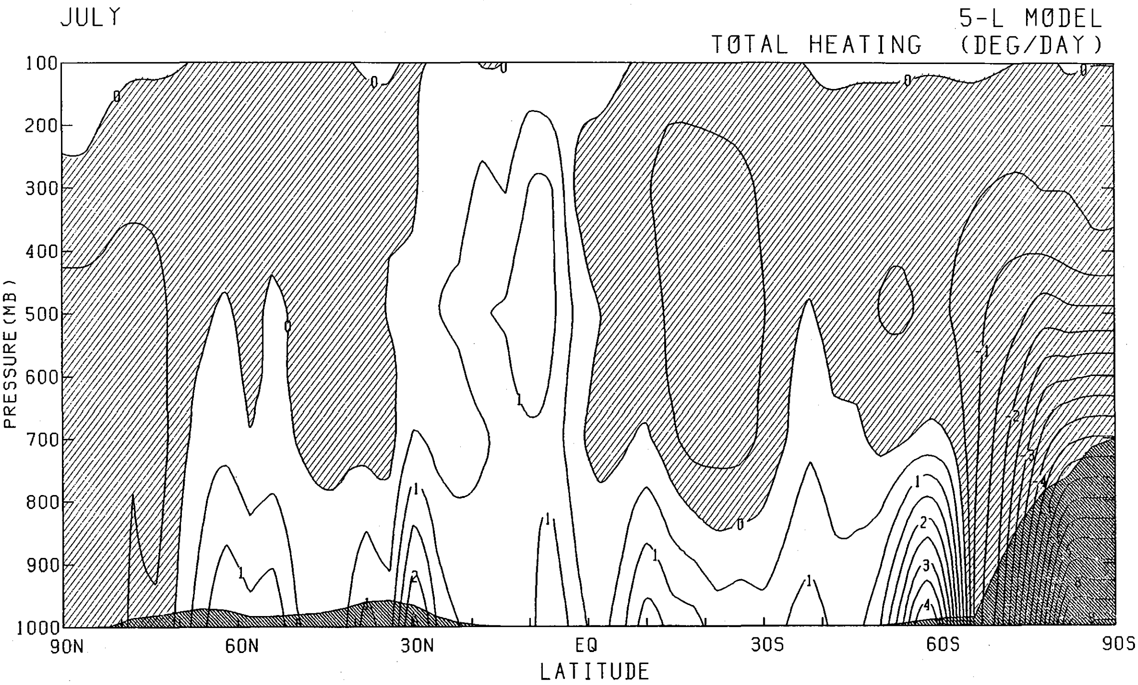

Fig. AIII.3.xxi Same as in Fig. AIII.1.xxi but for July.

(a)

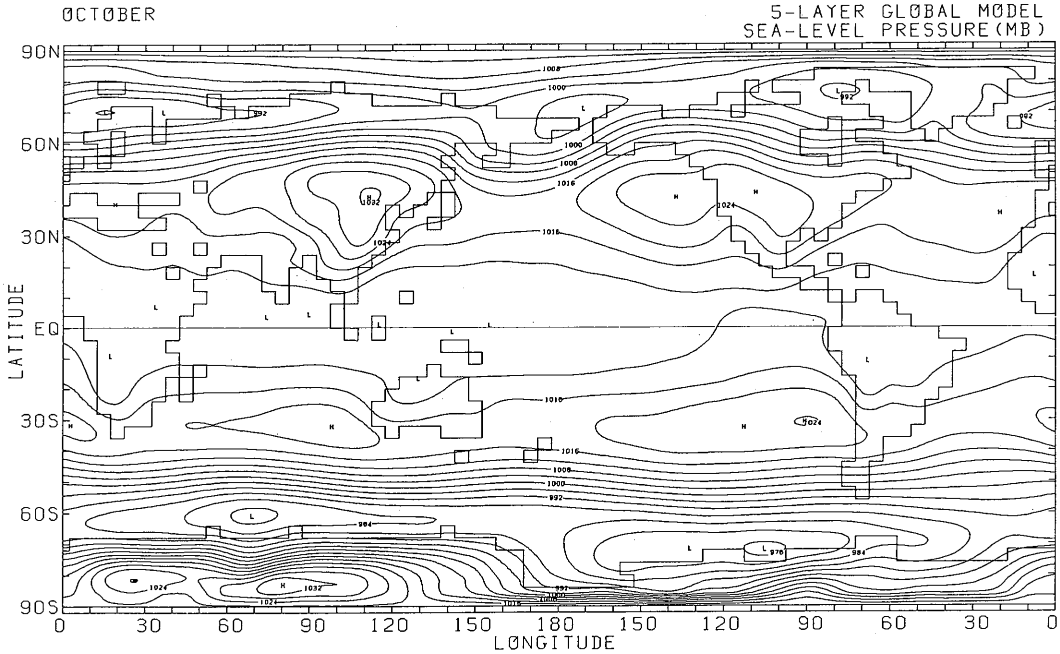

(b)

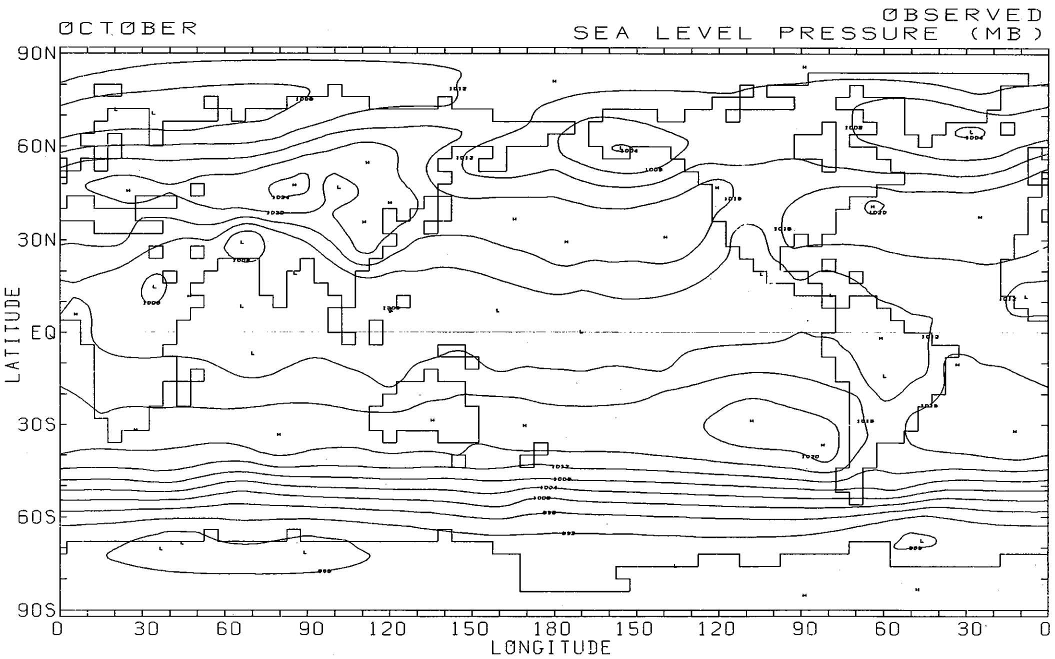

Fig. AIII.4.i Same as in Fig. AIII.1.i but for October.

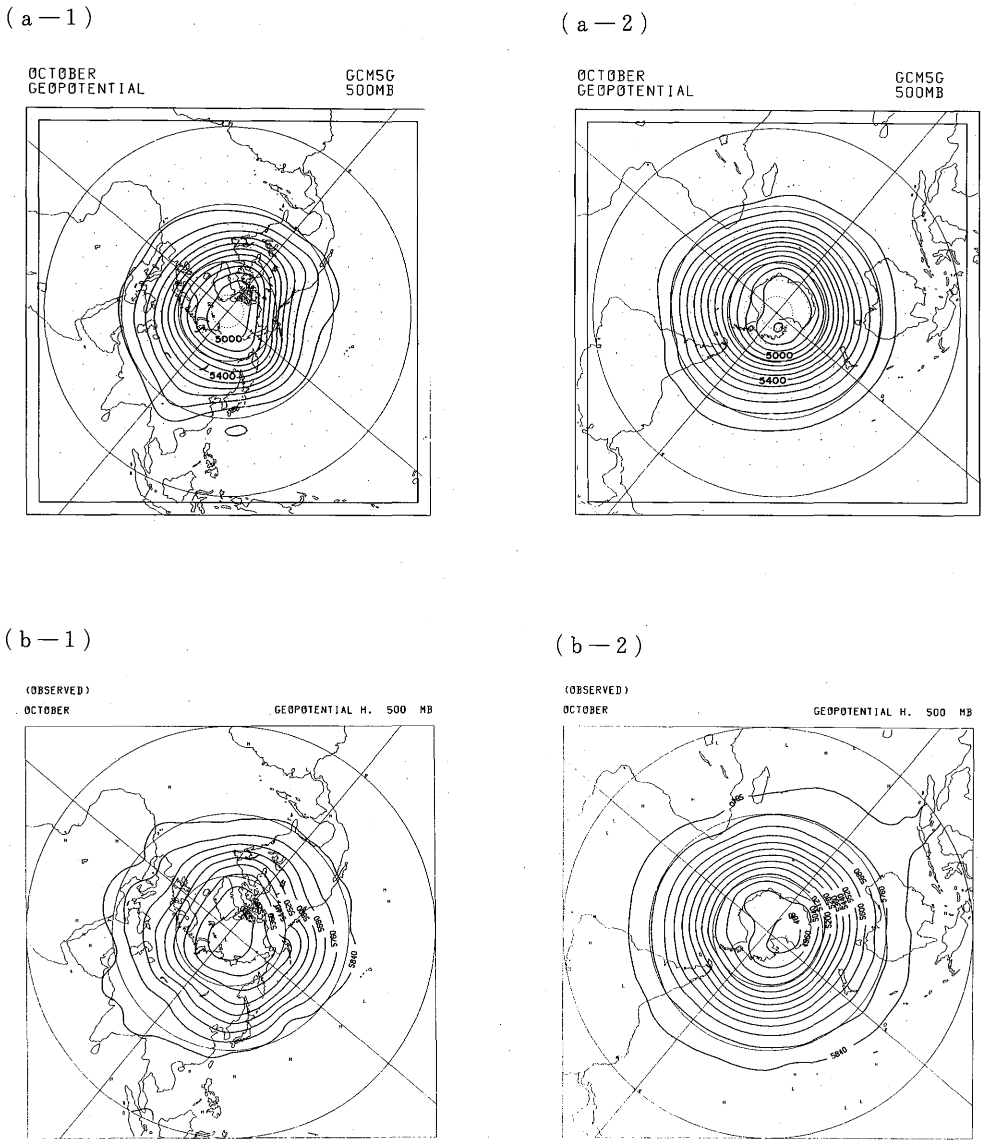

Fig. AIII.4.ii Same as in Fig. AIII.1.ii but for October.

(a)

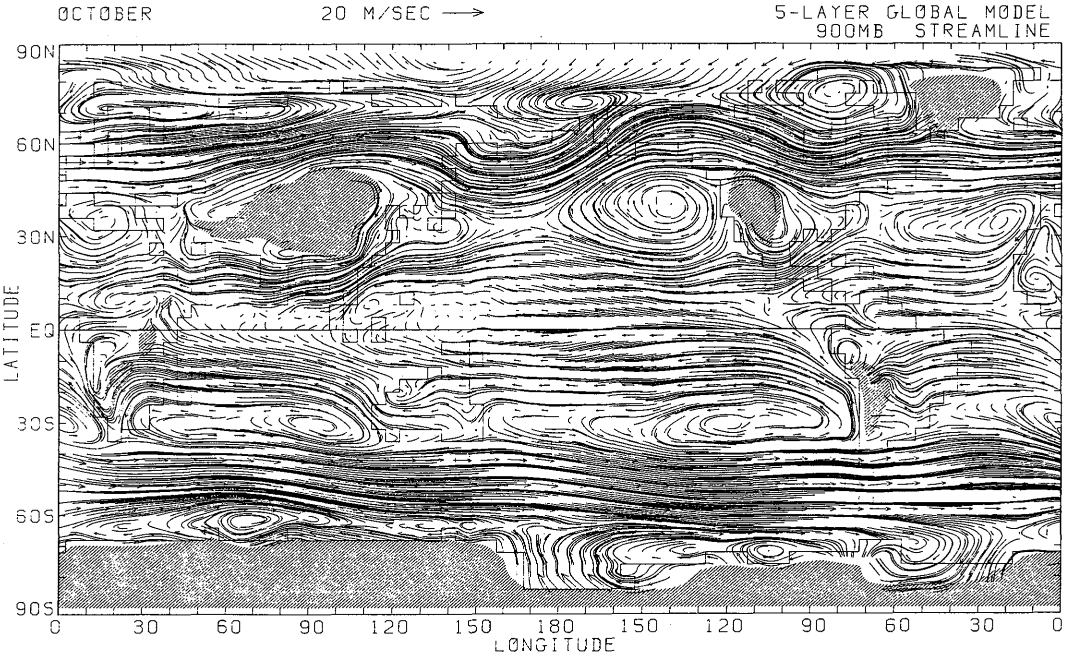

(b)

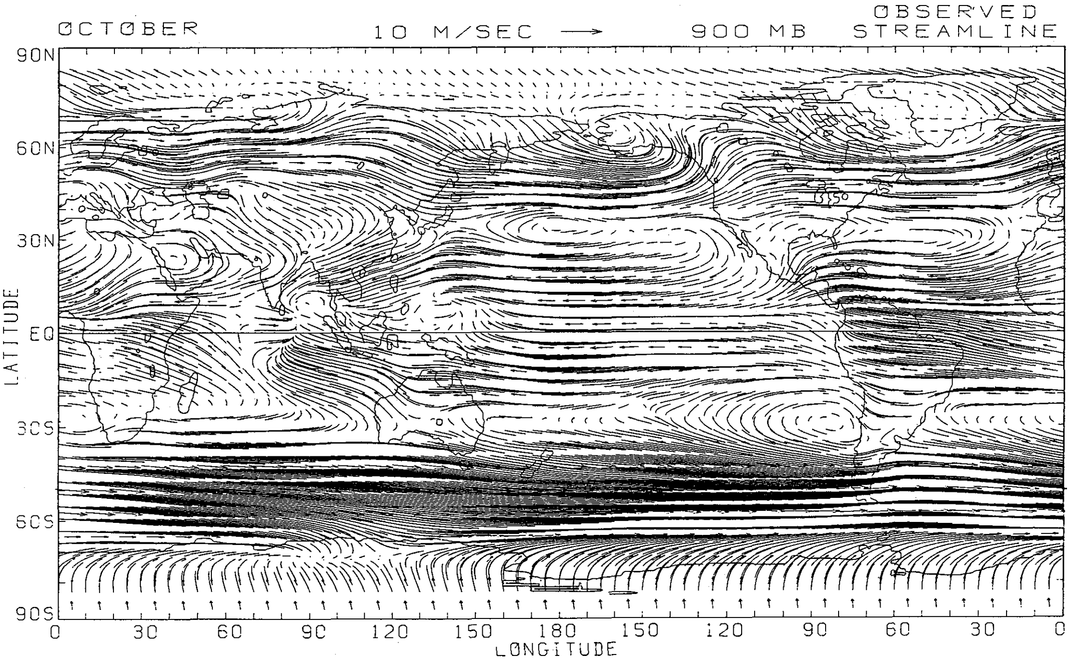

Fig. AIII.4.iii Same as in Fig. AIII.1.iii but for October.

(a)

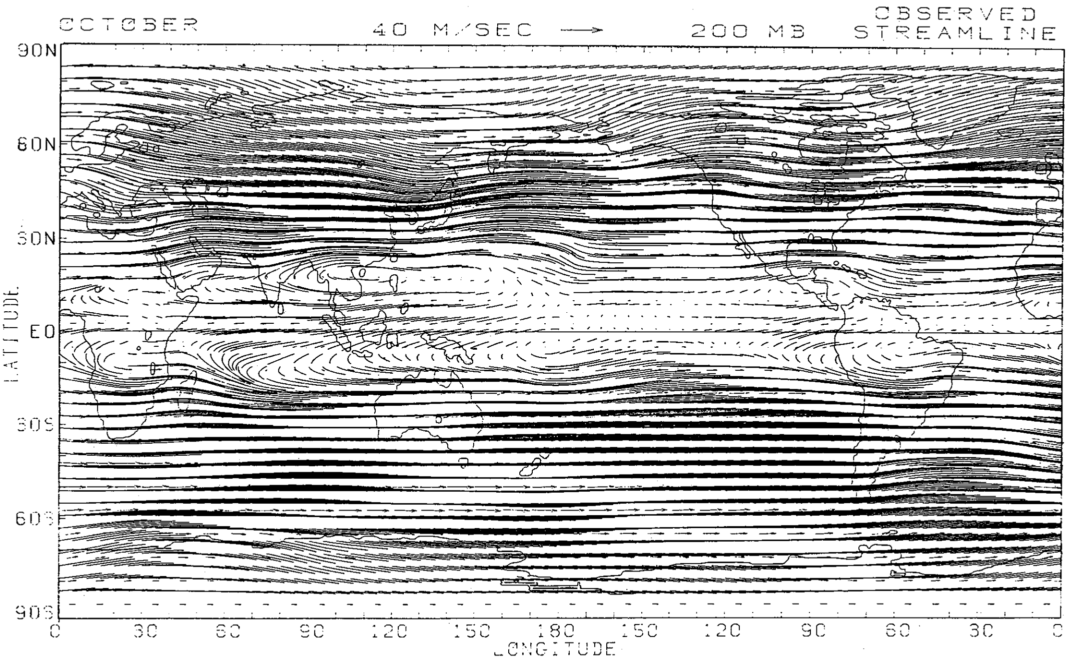

(b)

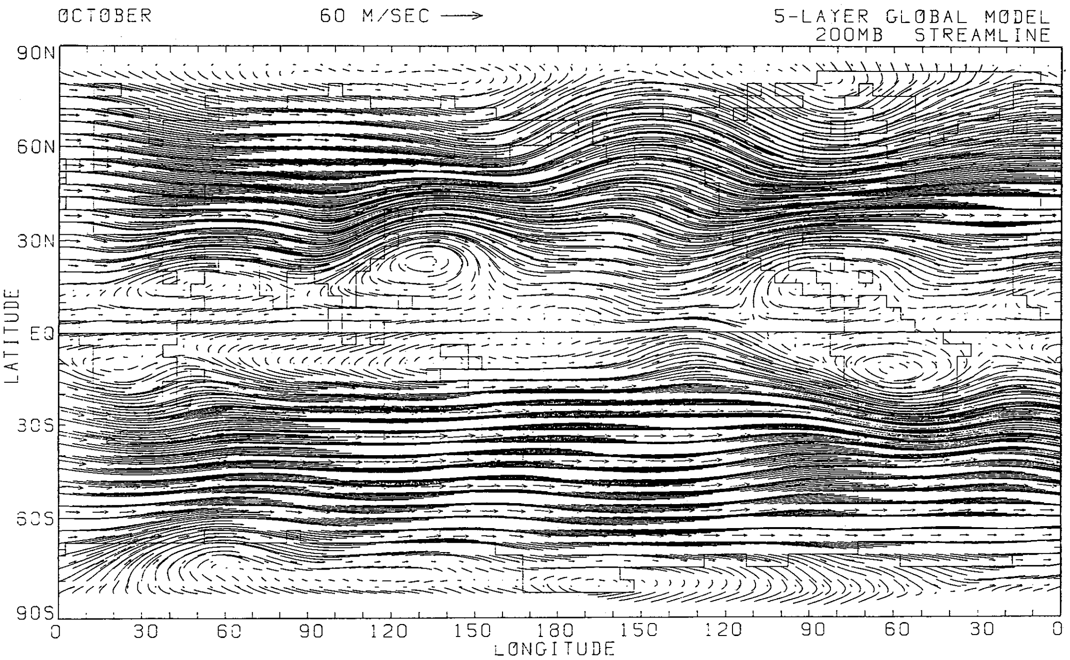

Fig. AIII.4.iv Same as in Fig. AIII.1.iv but for October.

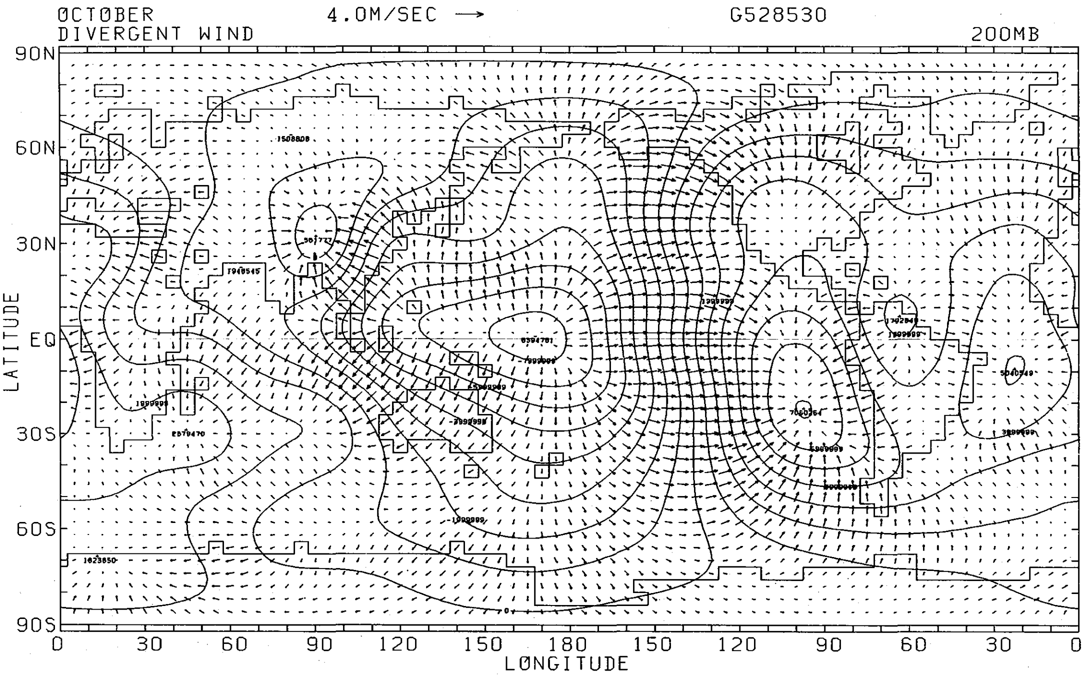

Fig. AIII.4.v Same as in Fig. AIII.1.v but for October.

(a)

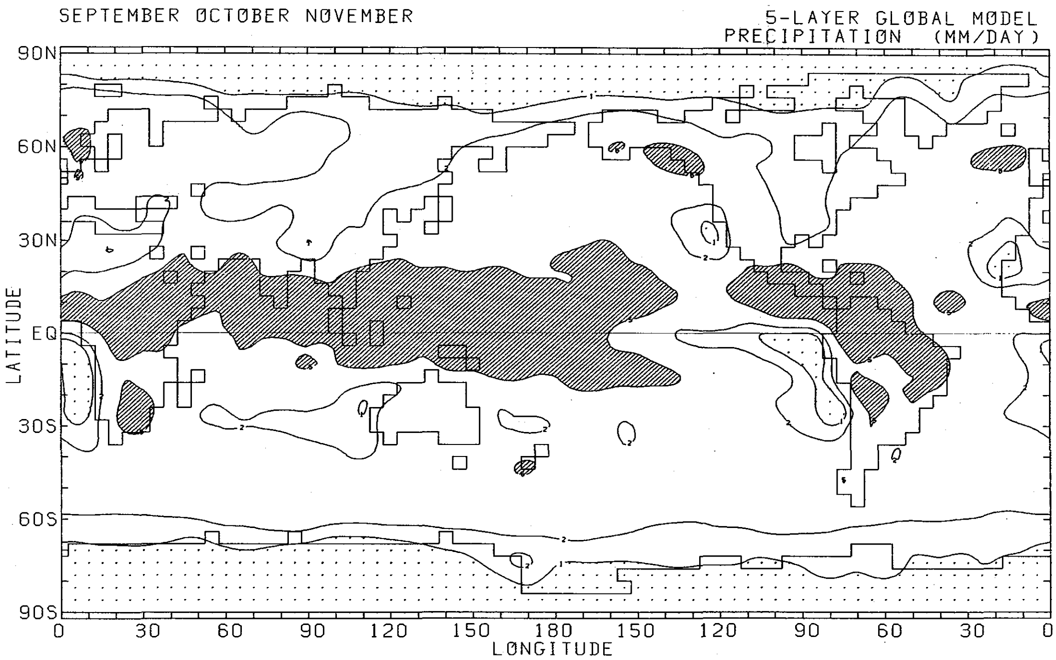

(b)

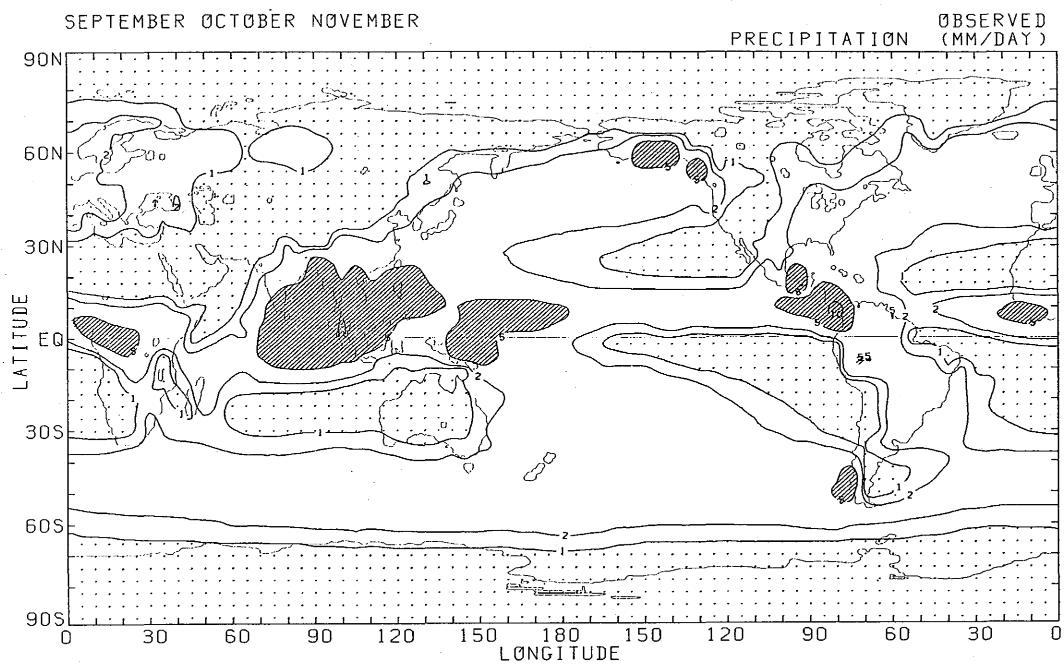

Fig. AIII.4.vi Same as in Fig. AIII.1.vi but for September, October and November.

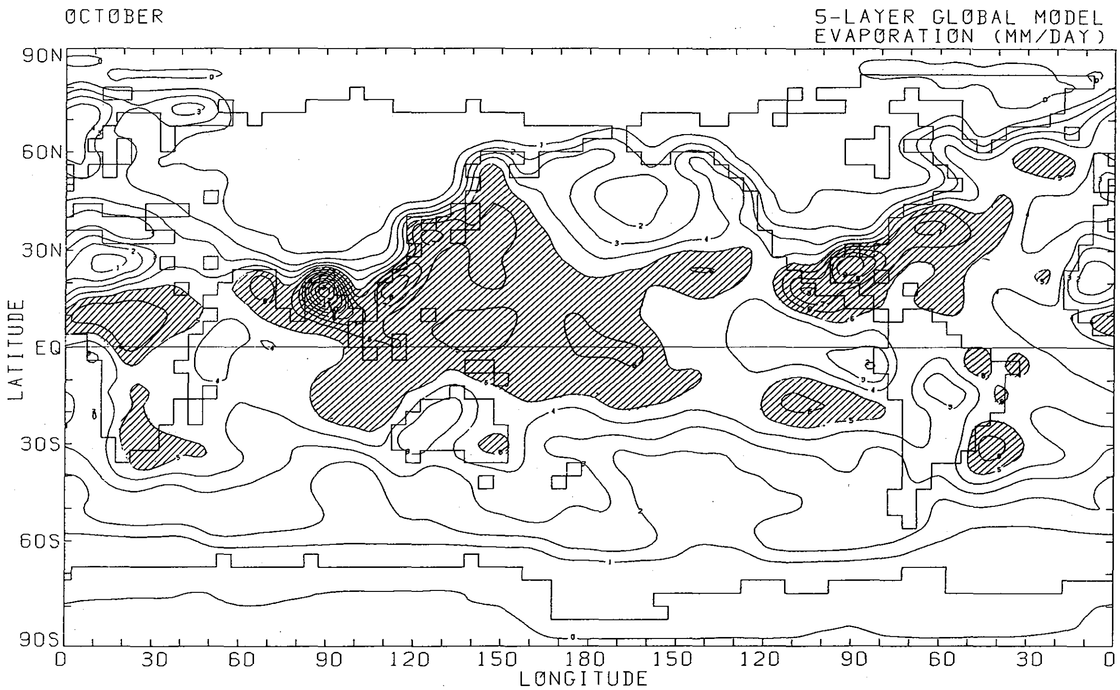

Fig. AIII.4.vii Same as in Fig. AIII.1.vii but for October.

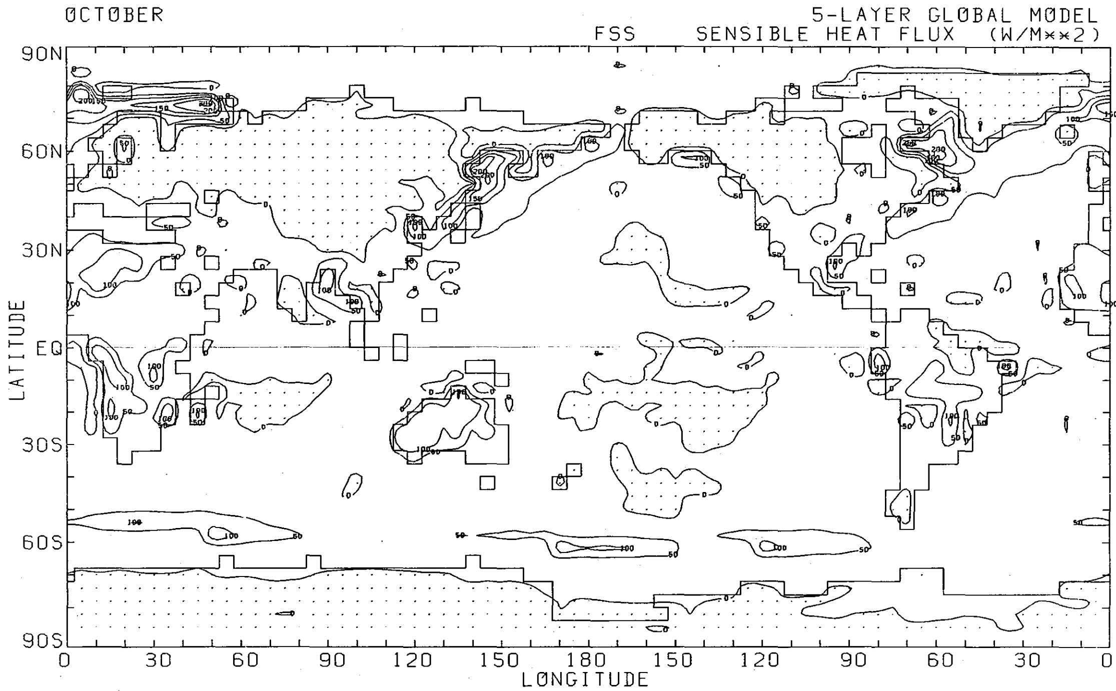

Fig. AIII.4.viii Same as in Fig. AIII.1.viii but for October.

(a)

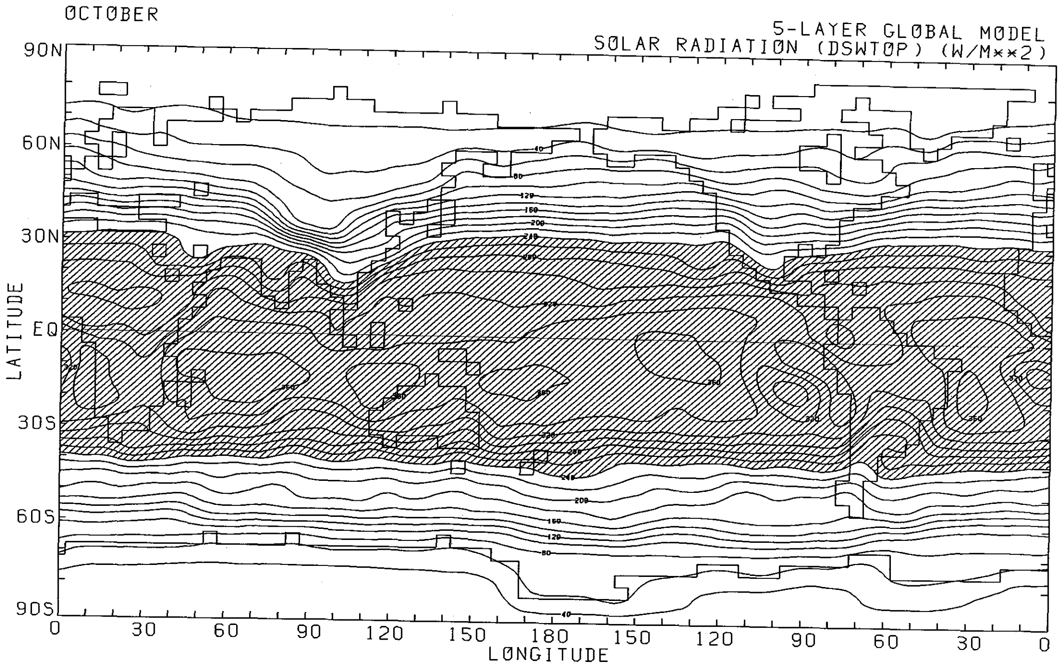

(b)

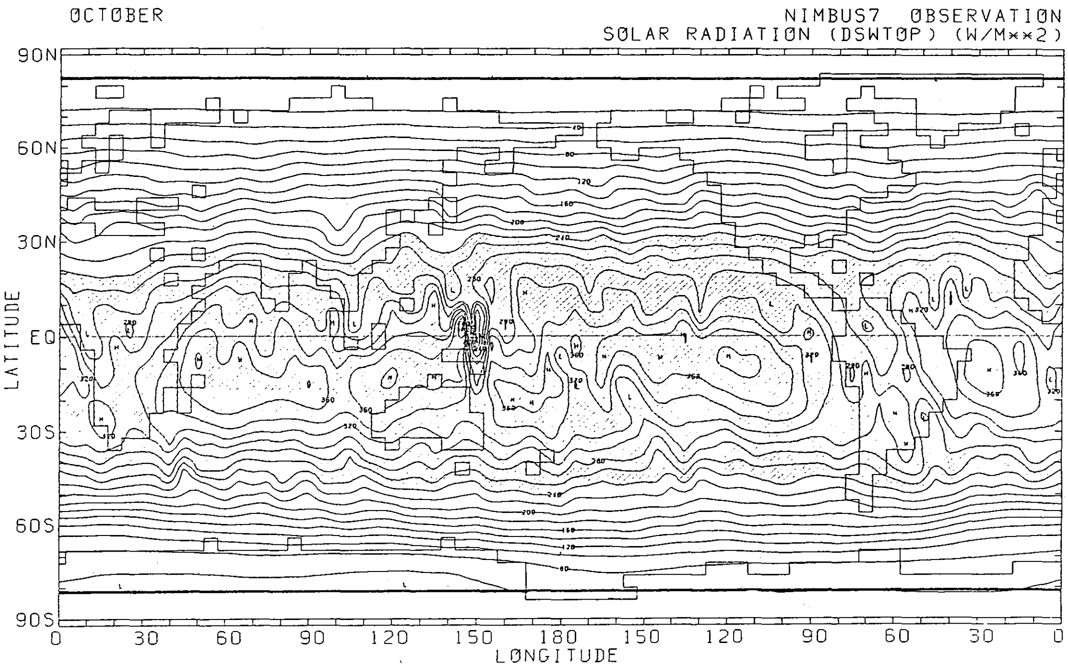

Fig. AIII.4.ix Same as in Fig. AIII.1.ix but for October.

(a)

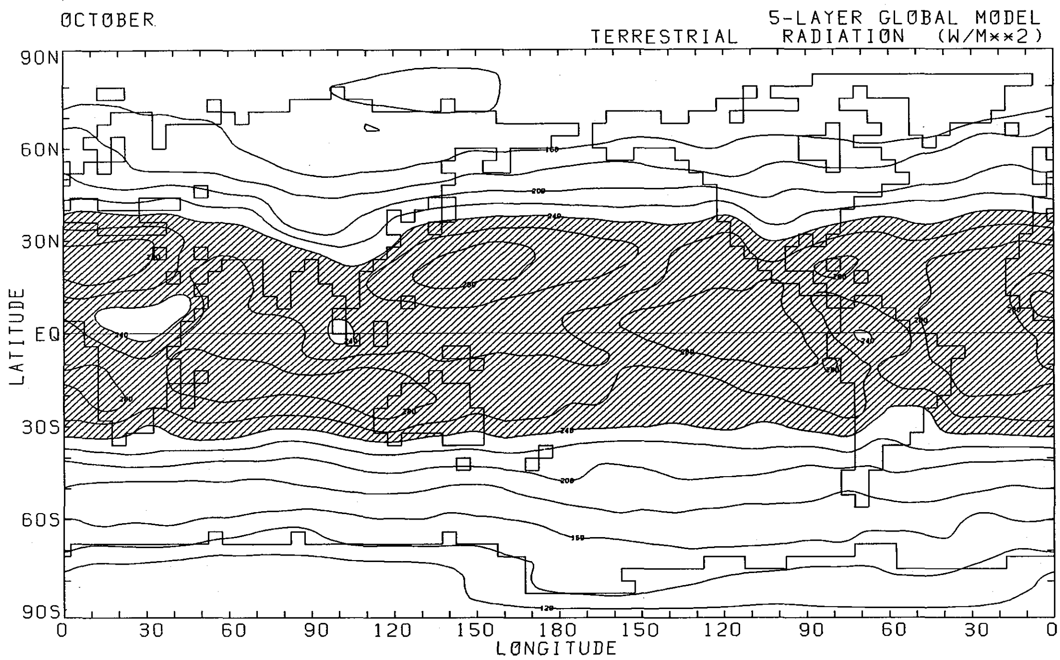

(b)

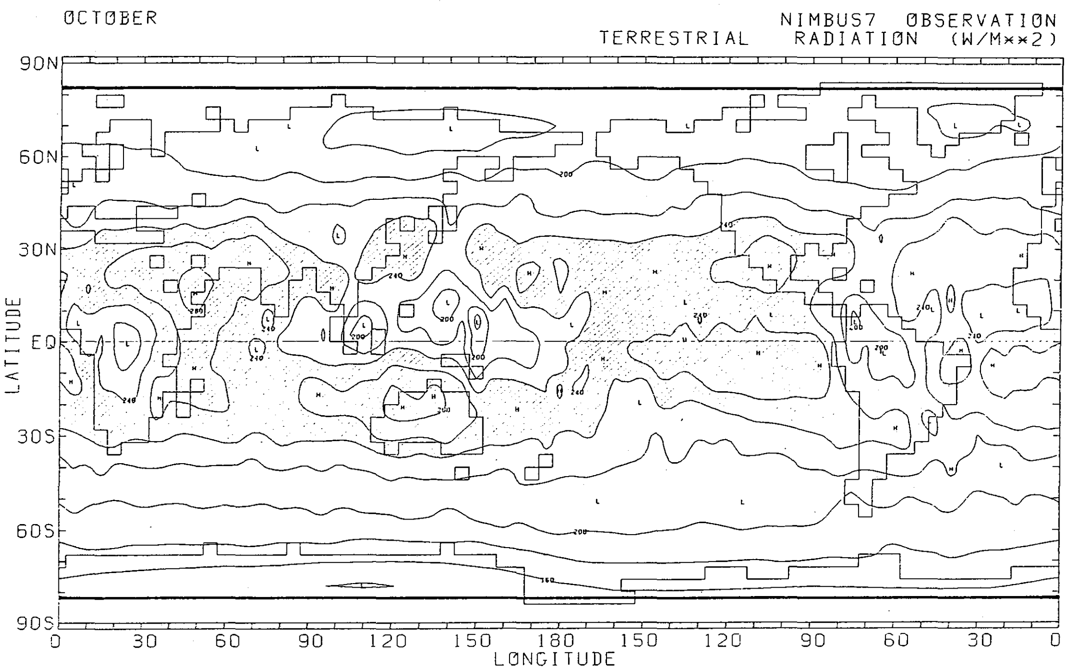

Fig. AIII.4.x Same as in Fig. AIII.1.x but for October.

(a)

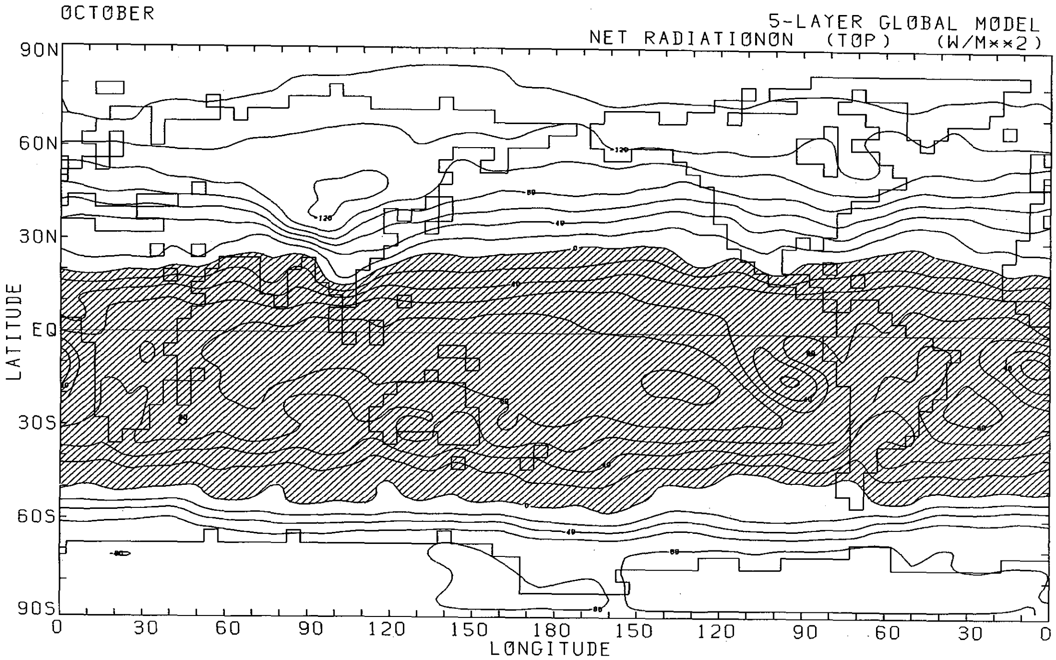

(b)

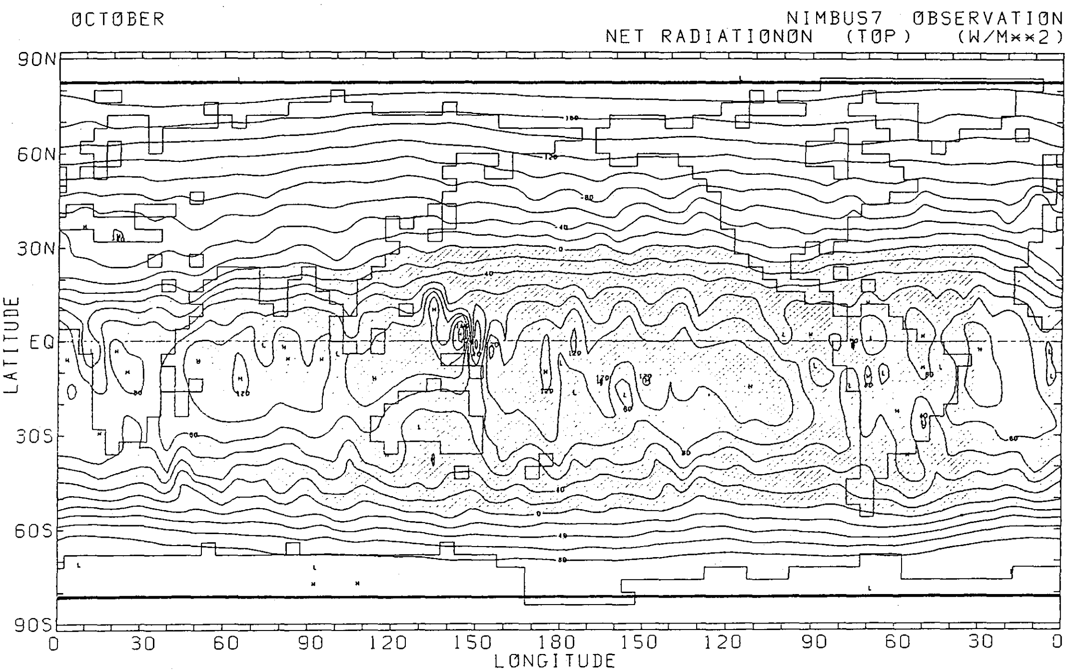

Fig. AIII.4.xi Same as in Fig. AIII.1.xi but for October.

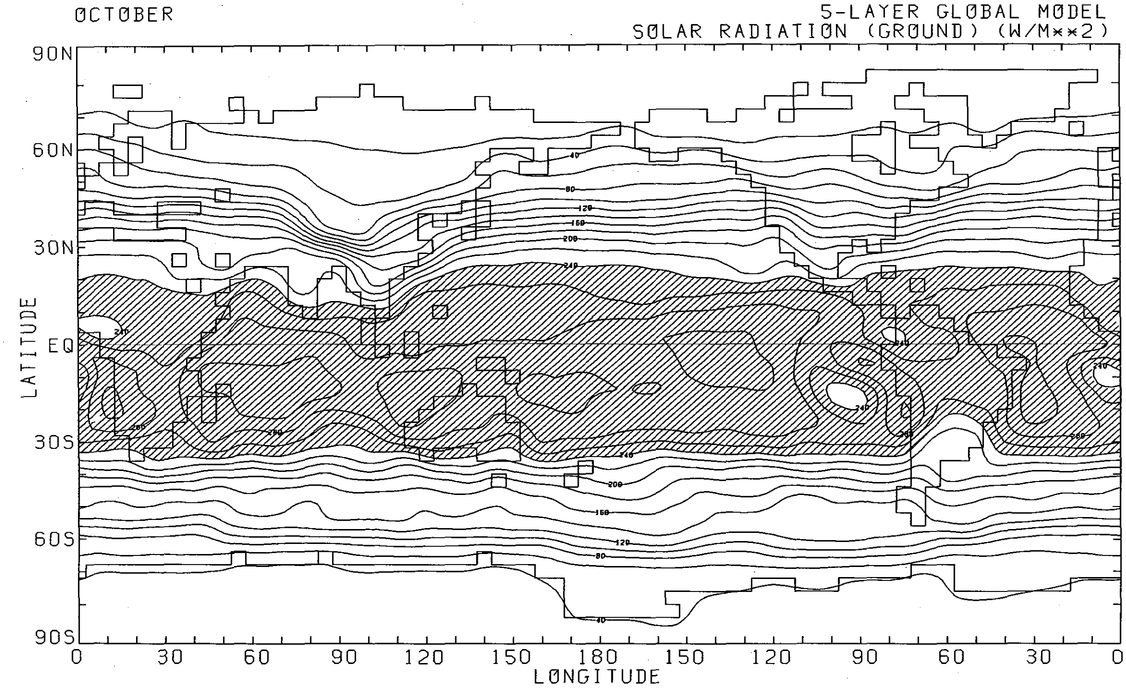

Fig. AIII.4.xii Same as in Fig. AIII.1.xii but for October.

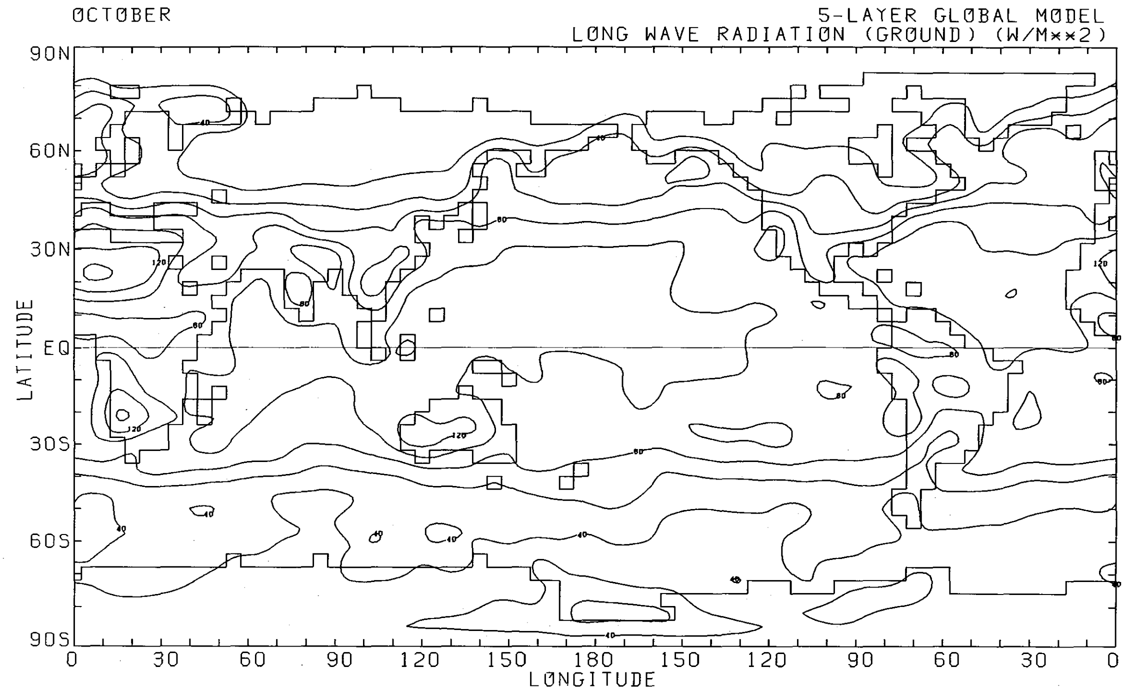

Fig. AIII.4.xiii Same as in Fig. AIII.1.xiii but for October.

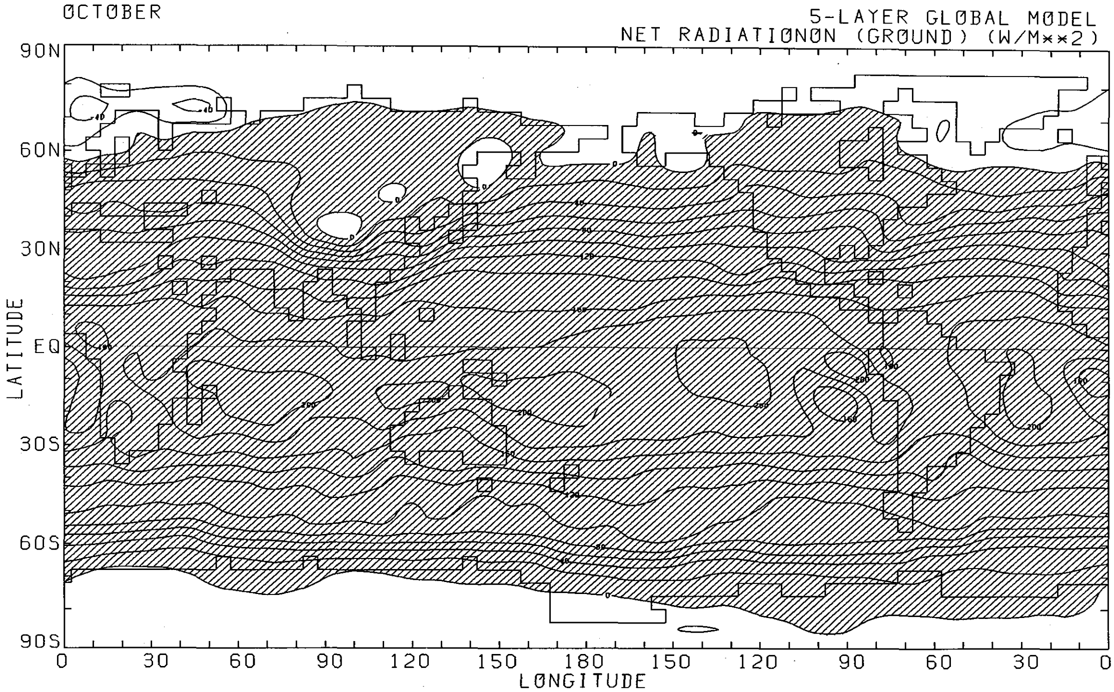

Fig. AIII.4.xiv Same as in Fig. AIII.1.xiv but for October.

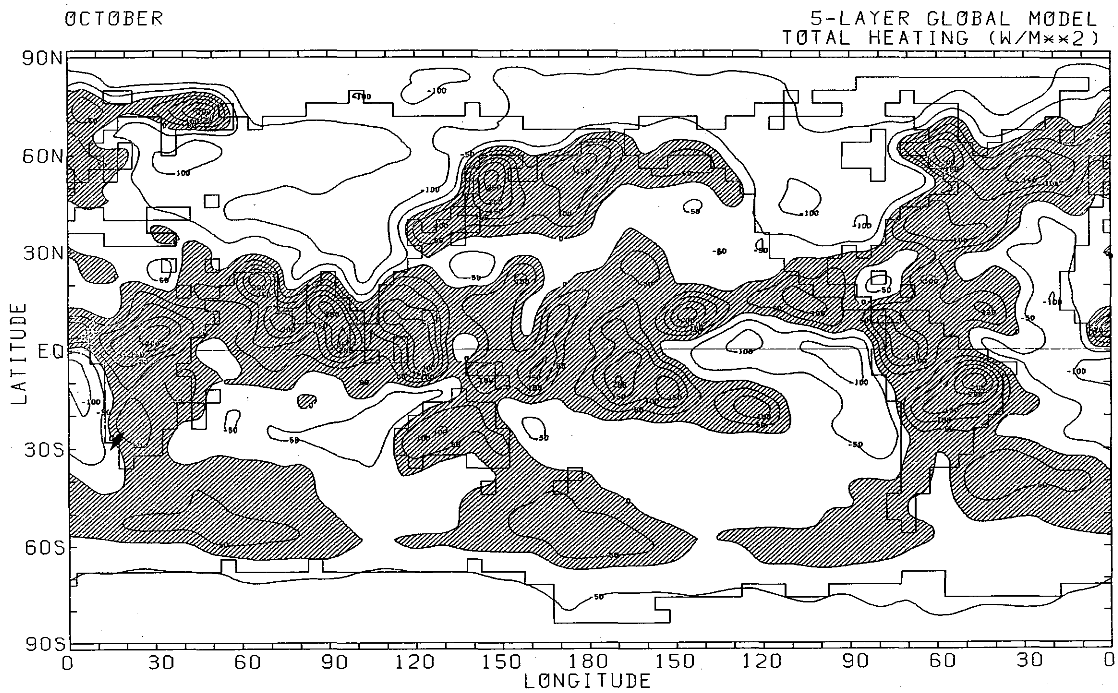

Fig. AIII.4.xv Same as in Fig. AIII.1.xv but for October.

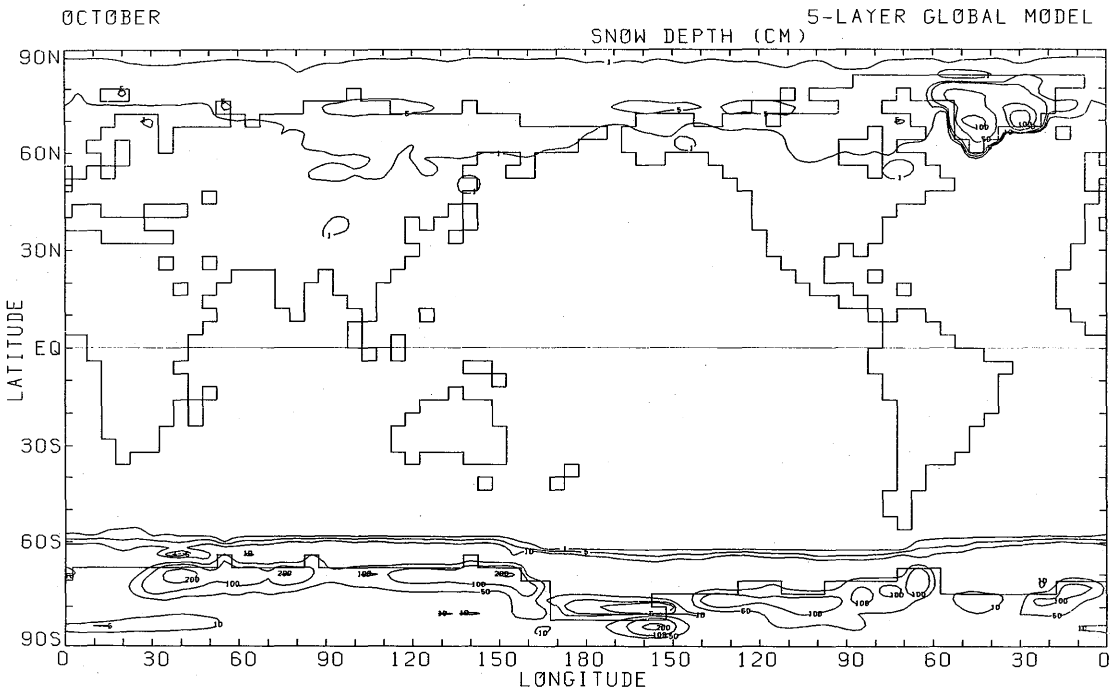

Fig. AIII.4.xvi Same as in Fig. AIII.1.xvi but for October.

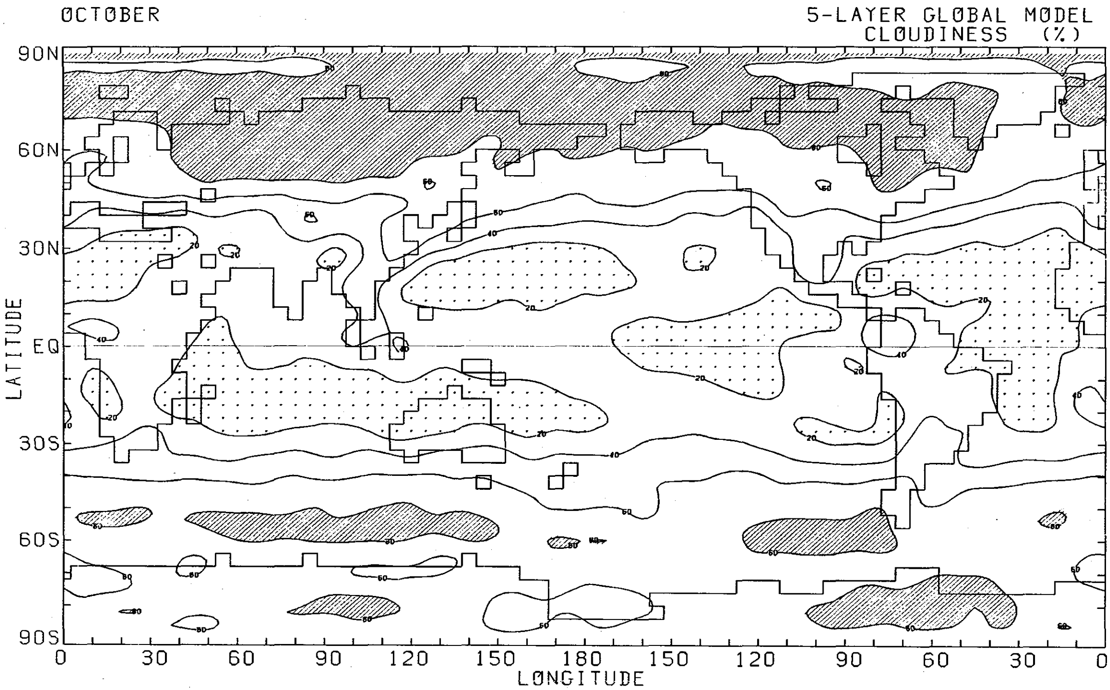

Fig. AIII.4.xvii Same as in Fig. AIII.1.xvii but for October.

(a)

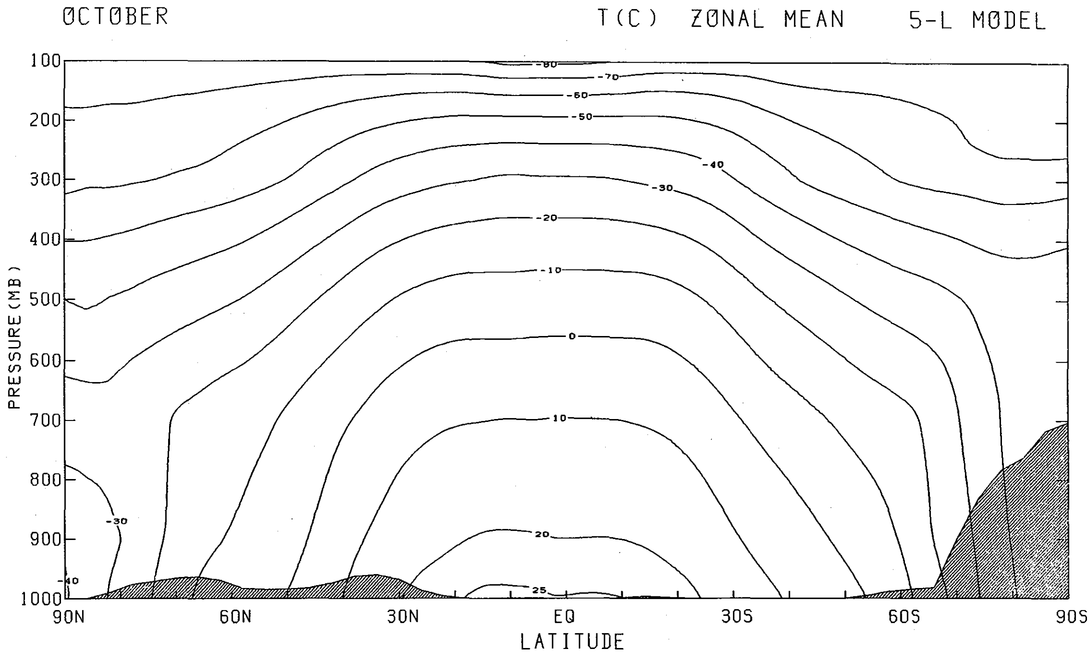

(b)

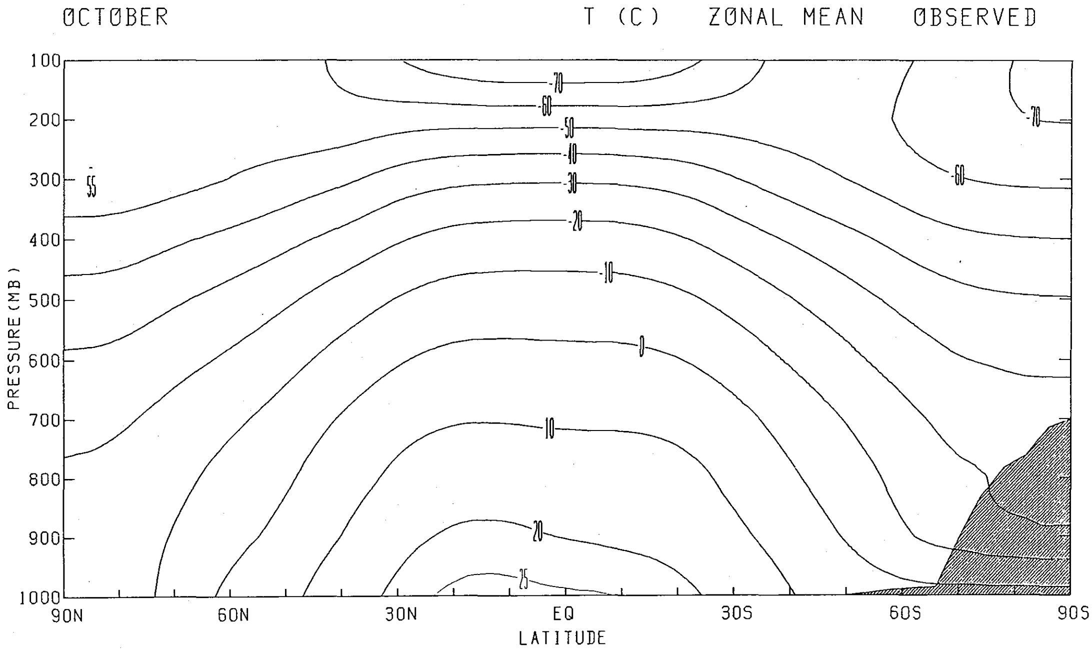

Fig. AIII.4.xviii Same as in Fig. AIII.1.xviii but for October.

(a)

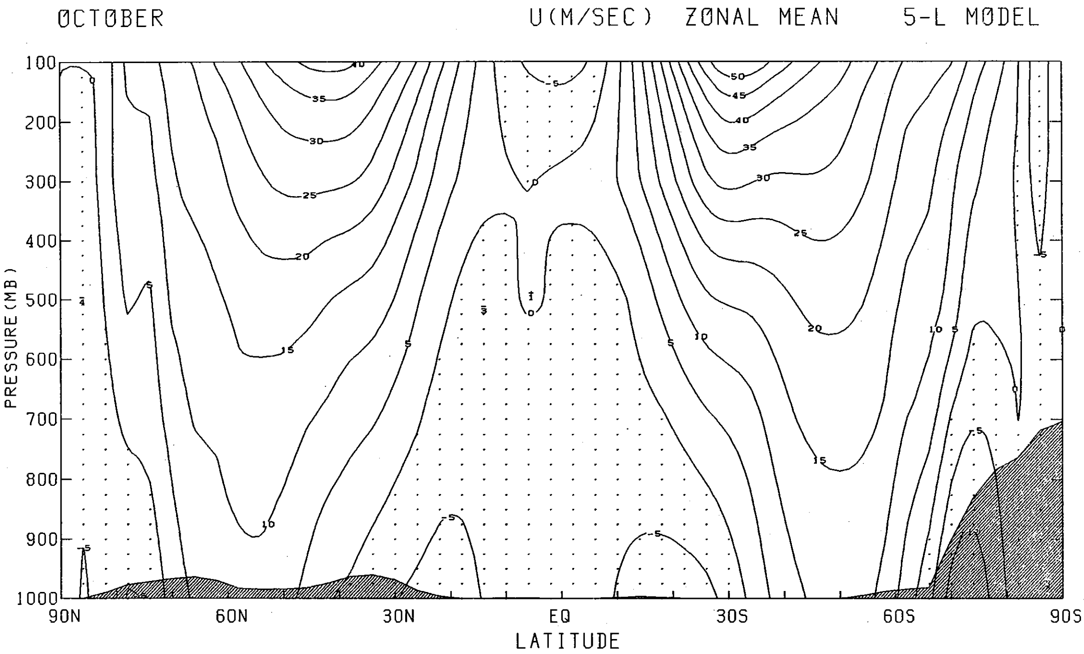

(b)

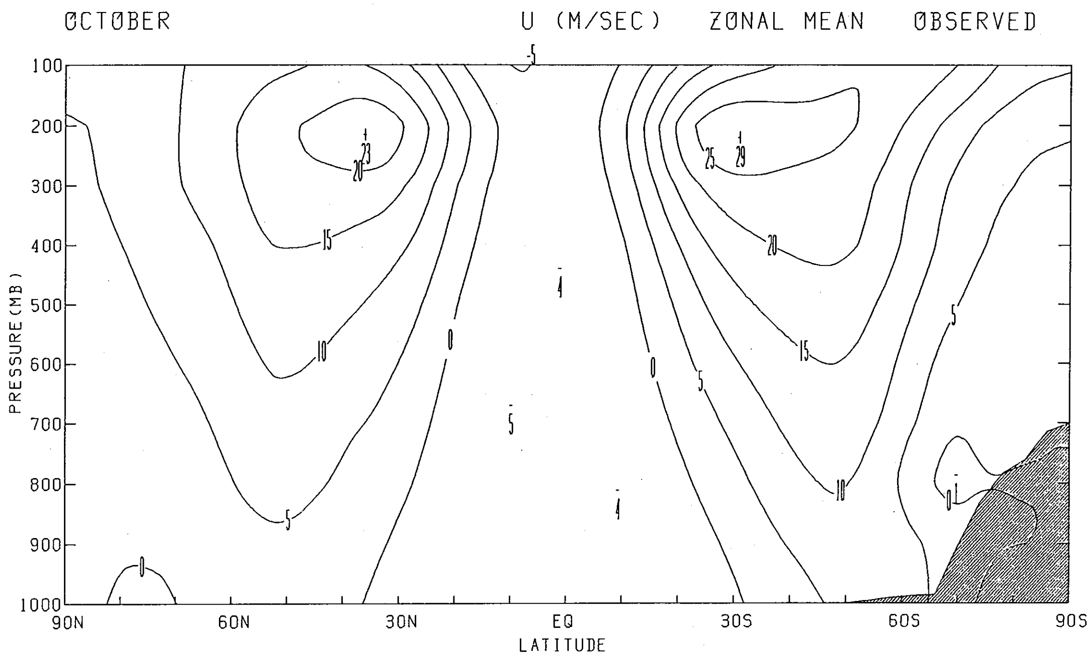

Fig. AIII.4.xix Same as in Fig. AIII.1.xix but for October.

(a)

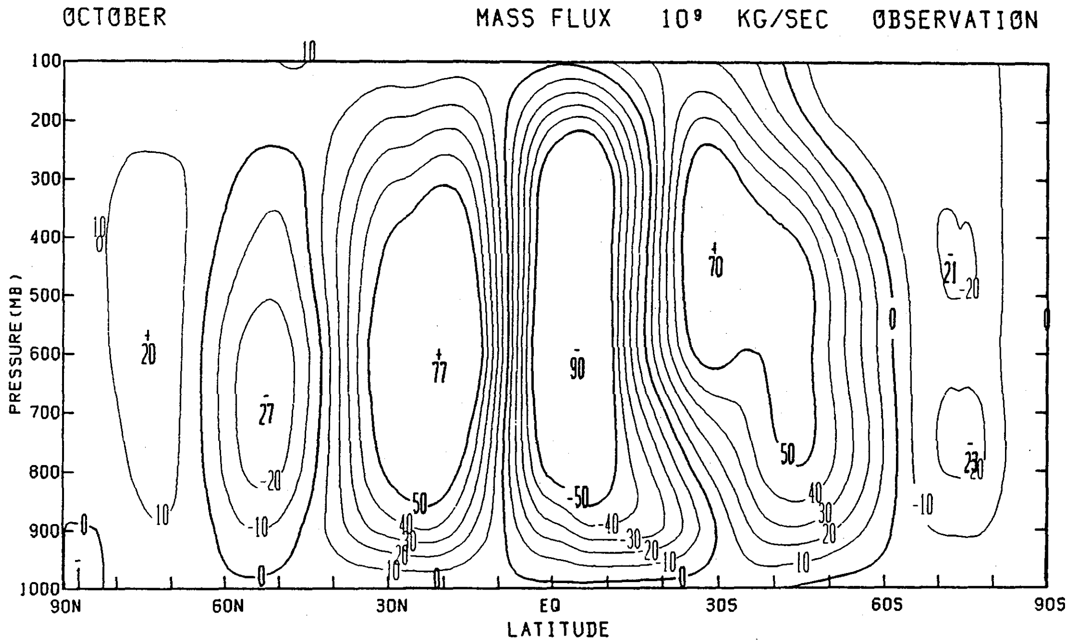

(b)

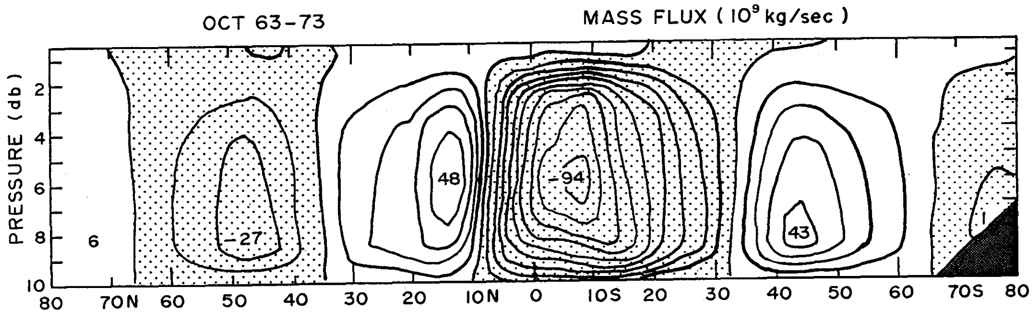

Fig. AIII.4.xx Same as in Fig. AIII.1.xx but for October.

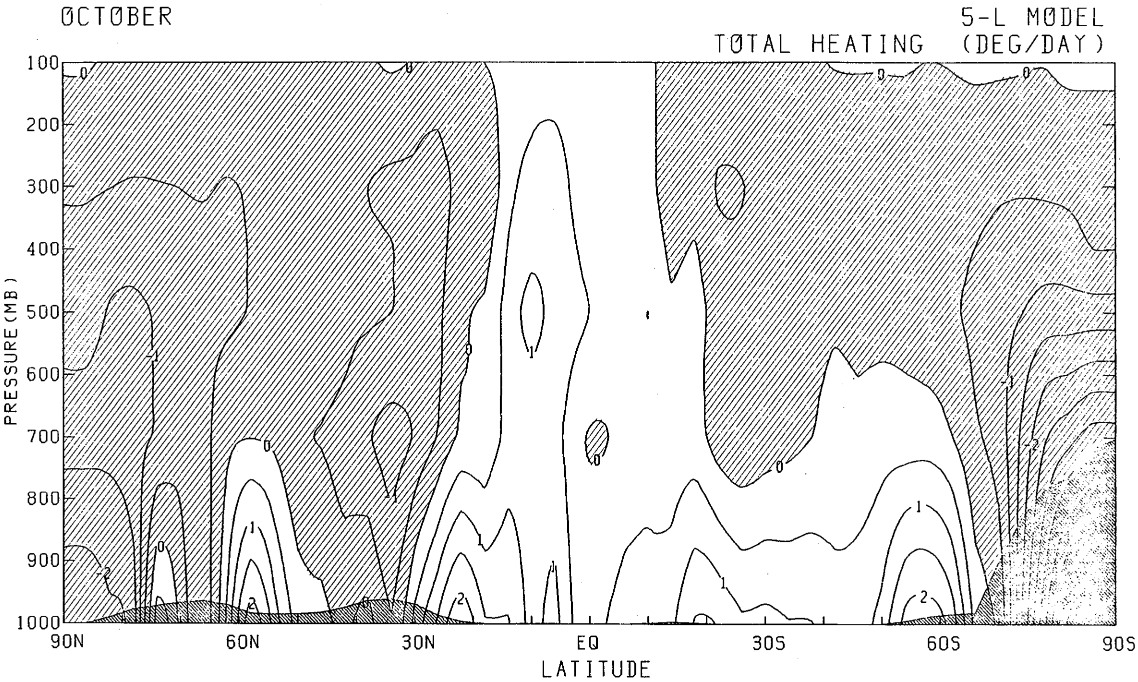

Fig. AIII.4.xxi Same as in Fig. AIII.1.xxi but for October.

References

Ackerman, B., 1963 : Some observations of water contents in huricanes. *J. Atmos. Sci.*, **20**, 238-298.

Ackerman, M., 1971 : Ultraviolet solar radiation related to mesospheric processes, *Mesospheric Models and Related Experiments*. Ed. G. Fiocco, Reidel, Dordrecht-Holland, pp. 149-159.

Arakawa, A, 1972 : Design of the UCLA general circulation model. Numerical Simulation of Weather and Climate. Tech. Rept. No. 7, Dept. of Meteorology, UCLA, 116 pp.

_______, 1975 : Modelling clouds and cloud processes for use in climate models. GARP Publ. Ser. **16**, 183-197.

_______ and V. Lamb, 1977 : Computational design of the basic dynamical processes of the UCLA general circulation model. *Methods in Computational Physics,* Advances in Research and Application, Vol. 17 : General circulation models of the atmosphere, Academic Press, Inc, 337 pp.

_______ and Y. Mintz, 1974 : The UCLA atmospheric general circulation model. Notes distributed at the workshop 25 March-4 April 1974, Dept. of Meteorology, UCLA, 404 pp.

_______ and W. H. Schubert, 1974 : Interaction of a cumulus ensemble with the large-scale environment, Part I. *J. Atmos. Sci.*, **31**, 674-701.

Beland, M. and T. Warn, 1975 : The radiation condition for transient Rossby waves. *J. Atmos. Sci.*, **32**, 1873-1880.

Betts, A. K., 1973 : Non-precipitaing cumulus convection and its parameterization. *Quart. J. Roy. Met. Soc.*, **99**, 178-196.

Businger, J. A., J. C. Wyngaard, Y. Izumi and E. F. Bradley, 1971 : Flux-profile relationships in the atmospheric surface layer. *J. Atmos. Sci.*, **28**, 181-189.

Chapman, S. and R. S. Lindzen, 1970 : Atmospheric tides. Gordon and Breach Science Publishers, New York, 200pp.

CIAP, 1974 : *The Natural Stratosphere of 1974, CIAP Monograph 1.* Ed. A. J. Grobecker, Department of Transportation, Climatic Impact Assesment Program, Washington, D. C, 1199 pp.

Coulson, K. L., 1959 : Radiative flux from the top of a Rayleigh atmosphere. Ph. D. dissertation, Department of Meteorology, Universty of California, Los Angeles, 176 pp.

Cunnold D., F. Alyea, N. Phillips and R. Prinn, 1975 : A three dimensional dynamical chemical model of atmospheric ozone. *J. Atmos. Sci.*, **32**, 170-194.

Deardorff, J. W., 1972 : Parameterization of the planetary boundary layer for use in general circulation models. *Mon. Wea. Rev.*, **100**, 93-106.

_______, 1976 : On the entrainment rate of a stratocumulus-topped mixed layer. *Quart. J. Roy. Meteor. Soc.*, **102**, 563-582.

_______, 1980 : Cloud top entrainment instability. *J. Atmos. Sci.*, **37**, 131-147.

Dickinson, R. E., 1973 : Method of parameterization for infrared cooling between the altitudes of 30 and 70 kilometers. *J. Geophys. Res.*, **78**, 4451-4457.

Dopplick, T. G., 1970 : Global radiative heating of the earth's atmosphere. Rept. No. 24, Planet. Circ. Project, Dept. of Meteorology, MIT, 128 pp. (Nuclear Science Abstracts, Cumulative Report Number Index MIT-2241-58)

_______, 1979 : Radiative heating of the global atmosphere : Corrigendum. *J. Atmos. Sci.*, **36**, 1812-1817.

Elsasser, W. M., 1960 : Atmospheric radiation tables, *Meteorological Monographs,* vol. 4, No. 23, American Meteorol. Soc., Boston, 43 pp.

Holloway, J. L. Jr., and S. Manabe, 1971 : Simulation of climate by a global circulation model : I. Hydrologic cycle and heat balance. *Mon. Wea. Rev.*, **99**, 335-370.

Jacobowitz, H., and R. J. Tighe, and the NIMBUS 7 ERB Experiment Team, 1984 : The earth radiation budget derived from the NIMBUS 7 earth radiation budget experiment. *J. Geophys. Res.*, **89**, 4997-5010.

Jordan, C. L., 1958 : Mean soundings for the West Indies area. *J. Meteor.*, **15**, 91-97.

Joseph, J. H., 1966 : Calculation of radiative heating in numerical general circulation models. Technical Report No. 1, Department of Meteorology, University of California, Los Angeles, 60 pp.

________, 1970 : On the calculation of solar radiation fluxes in the troposphere. *Solar Energy.*, **13**, 251-261.

Katayama, A., 1972 : A simplified scheme for computing radiative transfer in the troposphere. Technical Report No. 6, Department of Meteorology, University of California, Los Angeles, 77 pp.

Kato, H. and O. M. Phillips, 1969 : On the penetration of a turbulent layer into stratified fluid. *J. Fluid Mech.*, **37**, 643-655.

Kim, J.-W., 1976 : A generalized bulk model of the oceanic mixed layer. *J. Phys. Oceanogr.*, **6**, 686-695.

Kitoh, A. and T. Tokioka, 1985 : A simulation of the tropospheric general circulation with the MRI atmospheric general circulation model. Part II : July performance. (to be submitted)

Kockarts, G., 1971 : Penetration of solar radiation in the Schuman Runge bands of molecular oxygen. *Mesospheric models and Related Experiments*, Ed. G. Fiocco, Reidel, Dordrecht-Holland, 160-176.

Krueger, A. J., 1973 : The mean ozone distribution from several series of rocket soundings to 52 km at latitudes from 58°S to 64°N. *Pure and Appld. Geophys.*, **106-108**, 1254-1263.

Lacis, A. A., and J. E. Hansen, 1974 : A parameterization for the absorption of solar radiation in the earth's atmosphere. *J. Atmos. Sci.*, **31**, 118-133.

Lindzen, R. S., E. S. Batten and J.-W. Kim, 1968 : Oscillations in atmospheres with tops. *Mon. Wea. Rev.*, **96**, 133-140.

Lord, S. J., 1982 : Interaction of a cumulus ensemble with the large-scale environment. Part III : Semi-prognostic test of the Arakawa-Schubert cumulus parameterization. *J. Atmos. Sci.*, **39**, 88-103.

________ and A. Arakawa, 1980 : Interaction of a cumulus ensemble with the large-scale environment. Part II. *J. Atmos. Sci.*, **37**, 2677-2692.

________, W. C. Chao and A. Arakawa, 1982 : Interaction of a cumulus ensemble with the large-scale environment. Part IV : The discrete model. *J. Atmos. Sci.*, **39**, 104-113.

Lungren, T. S. and F. C. Wang, 1973 : Eddy viscosity models for free turbulent flows. *Phys. Fluids.*, **16**, 174-178.

Manabe, S., and F. Möller, 1861 : On the radiative equilibrium and heat balance of the atmosphere. *Mon. Wea. Rev.*, **89**, 503-532.

________ and R. T. Wetherald, 1967 : Thermal equilibrium of the atmosphere with a given distribution of relative humidity. *J. Atmos. Sci.*, **24**, 241-259.

McClatchey, R. A., R. W. Fenn, J. E. A. Selby, F. E. Volz, and J. S. Goring, 1972 : Optical properties of the atmosphere, AFCRL 72-0497, 108 pp.

Oort, A. H., 1983 : Global atmospheric circulation statistics, 1958-1973. NOAA Professional Paper 14. 180 pp.

Orlanski, I., 1976 : A simple boundary condition for unbounded hyperbolic flows. *J. Comp. Phys.*, **21**, 251-269.

Pearson, R. A., 1974 : Consistent boundary conditions for numerical models of systems that admit dispersive waves. *J. Atmos. Sci.*, **31**, 1418-1489.

Randall, D., 1976 : The interaction of the planetary boundary layer with large-scale circulations. Ph. D. dissertation, The University of California, Los Angeles, 247 pp.

_______, 1980 : Conditional instability of the first kind upside-down. *J. Atmos. Sci.,* **37**, 125-130.

Rodgers, C. D., 1967 : The radiative heat budget of the troposphere and lower stratosphere. Planetary Circulation Project, Department of Meteorology, MIT, Rep. No. 2, 99 pp.

Sasamori, T., 1968 : The radiative cooling calculation for application to general circulation experiments *J. Appl. Meteorol.,* **7**, 721-729.

Schlesinger, M. E., 1976 : A Numerical simulation of the general cirulation of atmosperic ozone. Ph. D. dissertation, University of California, Los Angels, 376 pp.

_______ and Y. Mintz, 1979 : Numerical simulation of ozone production, transport and distribution with a global atmospheric general circulation model. *J. Atmos. Sci.,* **36**, 1325-1361.

Schubert, W. H., 1973 : The interaction of a cumulus ensemble with the large-scale environment. Ph. D. Dissertation, UCLA, 168 pp.

Schutz, C. and W. L. Gates, 1972 : Global climatic data for surface, 800mb, 400mb,: :July. Advanced Research Projects Agency, Rep. R-1029-ARPA, Rand Corporation, Santa Monica, 180 pp.

Stull, R. B., 1976 : The energetics of entrainment across a density interface. *J. Atmos. Sci.,* **33**, 1260 -1267.

Suarez, M. J. and A. Arakawa, 1981 : First Conference on Climate Variation, AMS, 19-23 January 1981, San Diego, Calif..

_______, _______ and D. A. Randall, 1983 : The parameterization of the planetary boundary layer in the UCLA general circulation model : formulation and results. *Mon. Wea. Rev.,* **111**, 2224-2243.

Tokioka, T., 1978 : Some considerations on vertical differencing. *J. Meteor. Soc. Japan,* **56,** 98-111.

_______, A. Kitoh, I. Yagai and K. Yamazaki, 1985 : A simulation of the tropospheric general circulation with the MRI atmospheric general circulation model. Part I : The January performance. *J. Meteor. Soc. Japan.* (to be published)

_______ and I. Yagai, 1984 : On the January simulation of stratosheric circulations with the MRI general circulation model : Preliminary results. *Dynamics of the Middle Atmosphere,* Ed. J. R. Holton and T. Matsuno, Reidel, Dordrecht-Holland, 527-537.

Winninghoff, F. J., 1968 : On the adjustment towards a geostrophic balance in a simple primitive equation model with application to the problems of initialization and objective analysis. Ph. D. Dissertation, Dept. of Meteorology, UCLA, 161 pp.

Wurtele, M. G., J. Paegle and A. Sielecki, 1971 : The use of open boundary conditions with the storm-surge equations. *Mon. Wea. Rev.,* **99**, 537-544.

Yamada, T., 1976 : On the similarity functions A, B and C of the planetary boundary layer. *J. Atmos. Sci.,* **33**, 781-793.

Yamamoto, G., 1952 : On a radiation chart. *Sci. Rept. Tohoku Univ.,* S. 5, Geophysics, **4,** 9-23.

Yanai, M., J.-H. Chu, T. E. Stark and T. Nitta, 1976 : Response of deep and shallow tropical maritime cumuli to large-scale processes. *J. Atmos. Sci.,* **33**, 976-991.

気象研究所技術報告は、気象学、海洋学、地震学、その他関連の地球科学の分野において，気象研究所職員が得た研究成果に関し，技術報告，資料報告及び総合報告を掲載する。

気象研究所技術報告は，1978年（昭和53年）以降、必要の都度刊行される。

昭和60年３月30日発行　ＩＳＳＮ　0386—4049
編集兼発行所　気　象　研　究　所
茨城県筑波郡谷田部町長峰１—１
印　刷　所　東京都小石川１—３—７
勝美印刷株式会社